Membrane Contactors for Stripping of Ammonia from Aqueous Solutions

Sung Bin Park

Dept. of Chemical & Biological Engineering, Korea University

Scheme

- Introduction
- Mass transfer for Membrane Contactor
- Equilibrium & Henry's Constant
- Mass transfer coefficient correlation
- Application of Lee et al. model
- Extension of Lee et al. model
- Conclusion

Hollow Fiber Membrane contactor?

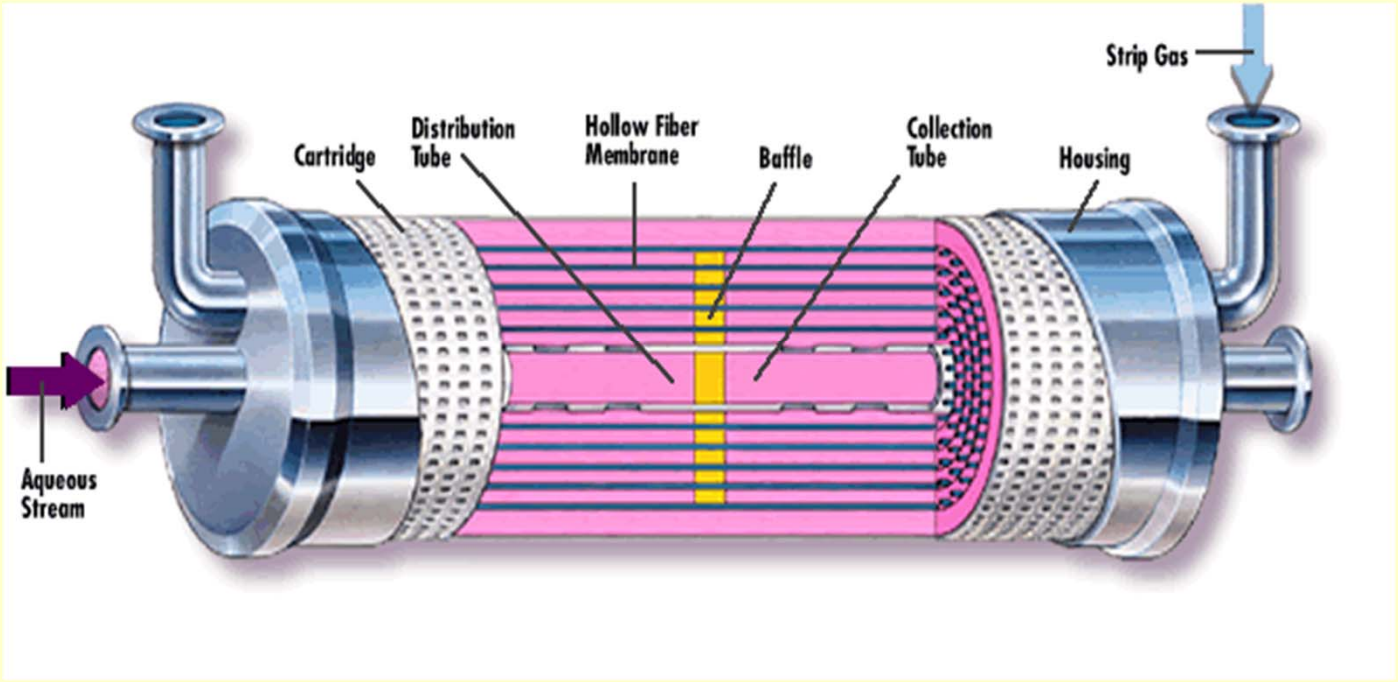

Hollow Fiber Membrane contactor?

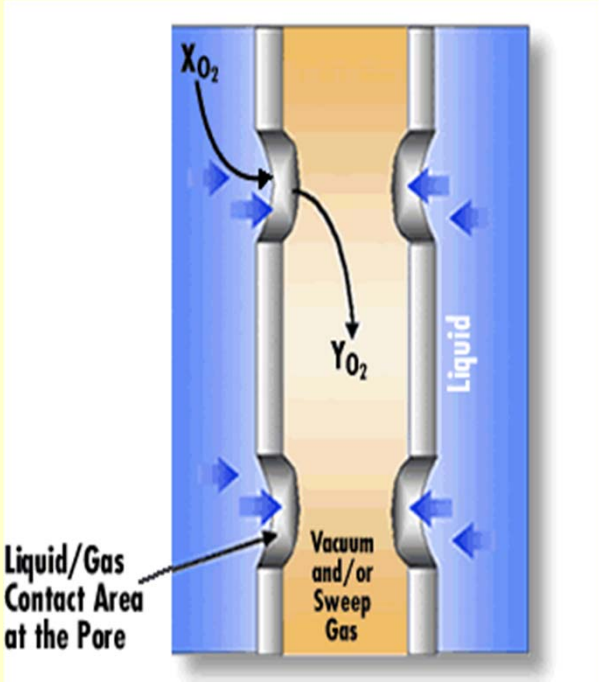

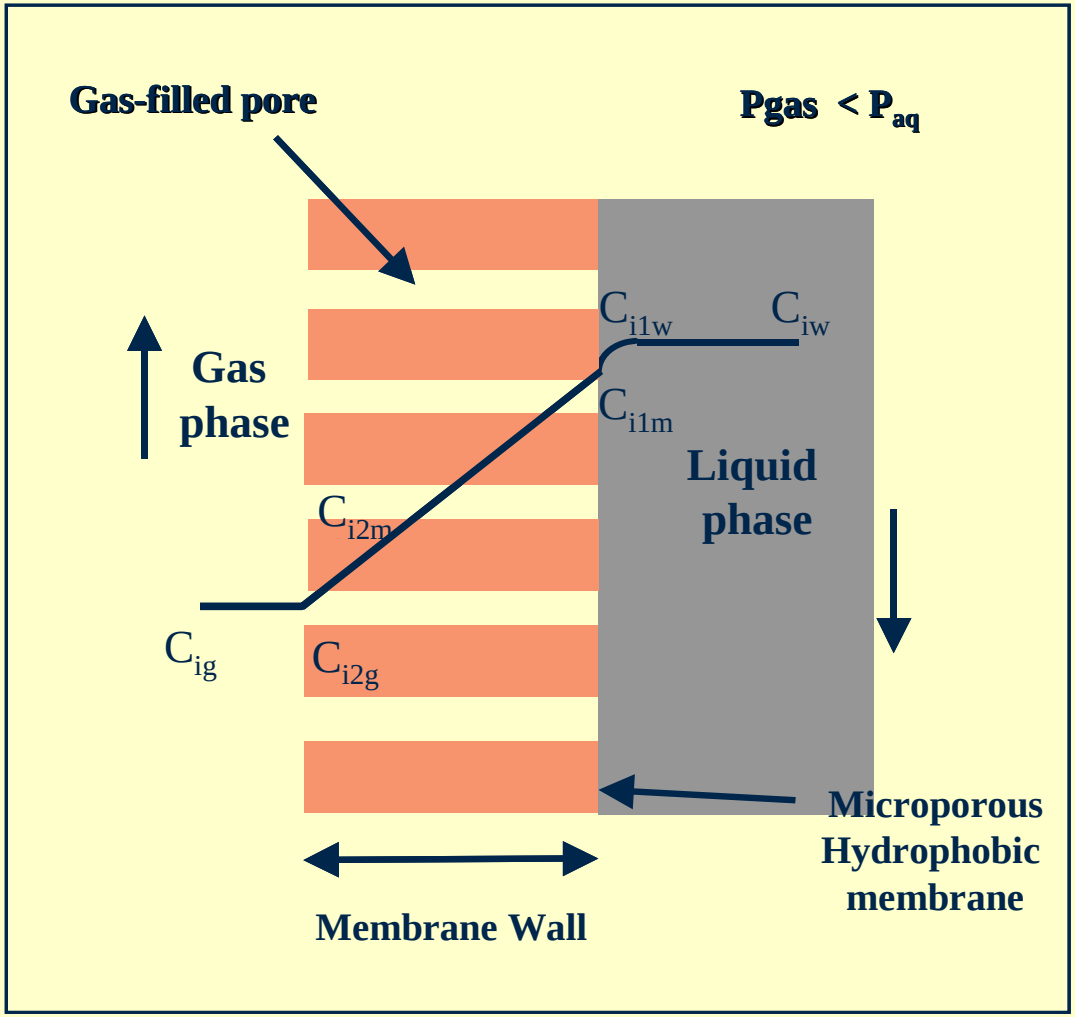

Types of Hollow Fiber Membrane

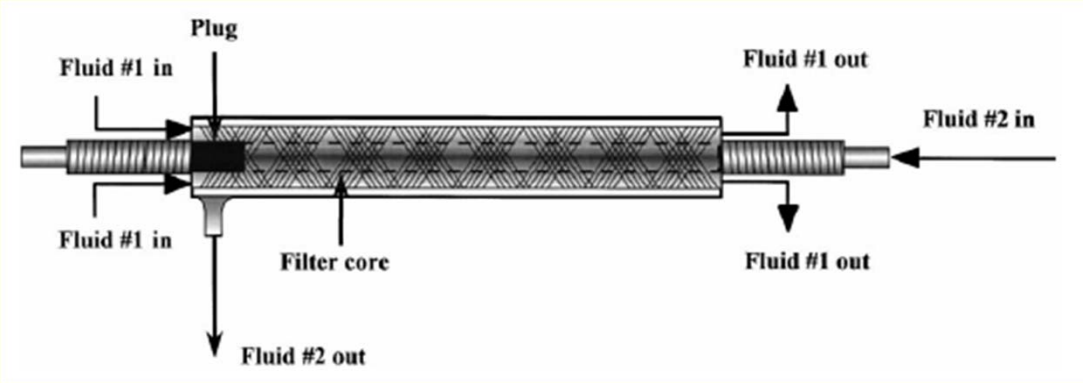

Types of Hollow Fiber Membrane

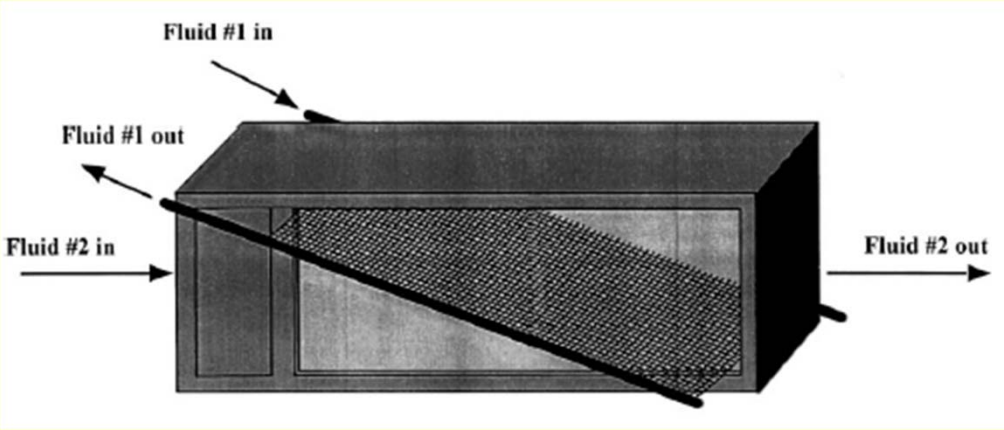

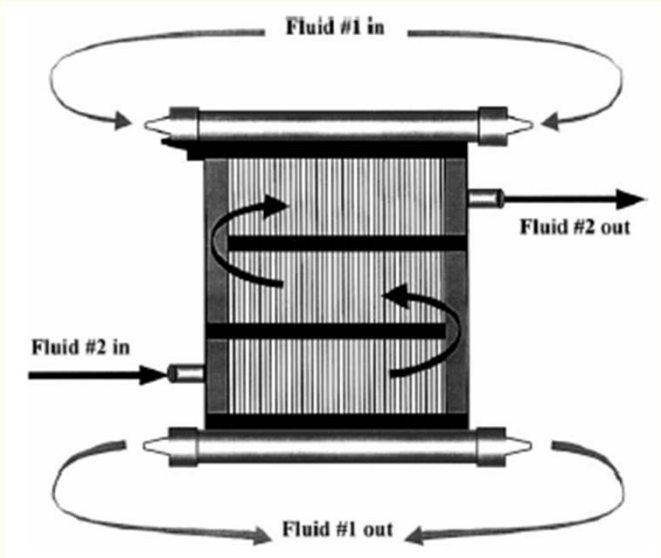

Introduction

- **Membrane Contactor Process**
  - A new way to accomplish separation process
    - Liquid/liquid extraction
    - Gas absorption/stripping
  - Applications
    - Fermentation
    - Pharmaceuticals
    - Wastewater treatment
    - Chiral separations
    - Semiconductor Manufacturing
    - Metal ion extraction
    - VOC removal from wastewater etc.

Introduction

- **Membrane Contactor Process**
  - **Advantages**
    - **Large extensive interfacial area of mass transfer**
      1/30 in gas absorber, 1/500 in L/L extraction column
    - **No flooding, no unloading**
    - **The possibility of realization of extreme phase ratios**
    - **Nondispersive phase contact avoiding entrainment**
    - **Direct scale-up**
  - **Disadvantages**
    - **Significant membrane resistances**
    - **Limited applications : weak for organic solvents, solids**
    - **Expensive**

Membrane Contactor

- **Qi and Cussler (1985a,b)**
  - Mass transfer in gas absorption
  - Mechanism
    - Mass transfer out of feed solution
    - Diffusion across the membrane
    - Mass transfer into the product solution
- **Yang and Cussler (1986)**
  - Mass transfer in aqueuos deaeration and CO_2 absorption
  - Basis for designing hollow fiber membrane module
- **Semmens et al. (1990)**
  - Experiment for ammonia removal with a parallel hollow fiber module
  - Correlation for mass transfer coefficients

Membrane Contactor

- **Dahuron and Cussler (1988)**
  - **Protein extraction with hollow fiber contactors**
  - **Faster than conventional extraction equipment**
- **Prasad and Sirkir (1988)**
  - **Dispersion-free solvent extraction with hydrophobic and hydrophilic micoporous hollow fiber membrane module**
  - **Overall mass transfer coefficient charactrerized with distribution coefficients and interfacial tensions**
- **Wang and Cussler (1993)**
  - **Performance of baffled hollow fiber fabric module**
  - **Better performance than most conventional module geometries**

Membrane Contactor

- **Sengupta et al.(1998)**
  - Empirical correlation of mass transfer for transverse flow
  - Removal of dissolved oxygen from water with excess sweep gas
- **Schöner et al.(1998)**
  - Correlation for calculation the shell side mass transfer coefficient in cross flow
  - Application to extraction
- **Gabelman and Hwang (1999)**
  - General review of membrane contactors
  - Summary for mass transfer coefficient correlation
    - In tube side : reasonable accuracy
    - In shell side : more difficult to determine

Membrane Contactor

Analysis of Membrane Contator

Key information : Mass Transfer, Equilibrium, Breakthrough pressure

- **Mass transfer : mass balance**
  - **Mass transfer coefficient from experimental data**
  - **Parallel hollow fiber**
    - **Countercurrent : Qi and Cussler (1985a), Sirkar (1992)**
    - **Cocurrent : Qi and Cussler (1985b)**
  - **Baffled hollow fiber : cross flow**
    - **Sengupta et al. (1998), Schöner et al.(1998)**

Membrane Contactor

- **Correlation for mass transfer coefficients**
  - **Dimensionless group : Re, Sc, Sh**
- **Equilibrium at the gas-liquid interface**
  - **Henry's law**
    - **From vapor-liquid equilibrium data**
    - **Henry's constant estimated for processes involving stripping fluids**

In present work

- **Application to ammonia stripping**
  - **One baffled commercial hollow fiber membrnae contactor from Liqui-Cel®**
- **Analysis of mass transfer in shell side according to the flow pattern**
  - **Parallel flow and cross flow**
- **Equilibrium : Henry's constant**
  - **Ammonia stripping process**
    - **NaOH added : Ammonia molecule in pH>11**
    - **NH_3-H_2O-NaOH VLE data needed**
- **Experiment : NH_3-H_2O-NaOH VLE**
  - **A modified static measurement**

In present work

- **Lee et al. model (1996)**
  - **Applied to NH_3-H_2O-NaOH**
  - **Assuming ammonia as a solvent species**
- **Application to mixed solvent systems with Lee et al. model**
- **Extension of Lee et al. model based on solvation**

Mass Transfer

- **Steady state mass balance for shell side flow**

1. Counter-current flow

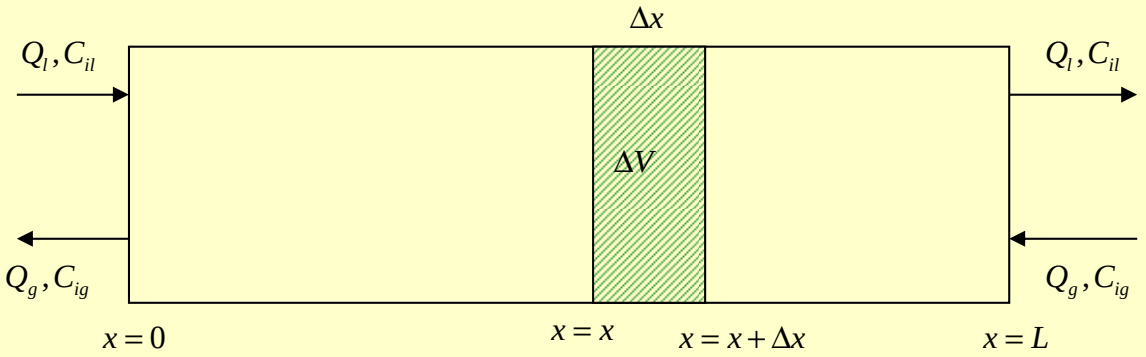

$$\frac{dC_{il}}{dx} + K_Q(1-R)C_{il} = -K_Q\left(RC_{il}^{L} - C_{ig}^{L}/H_i\right) \qquad K_Q = K_{il}A/Q_l \qquad R_Q = Q_l/Q_gH_i$$

$$\frac{C_{il}^{L}}{C_{il}^{0}} = \frac{1-R}{\exp\left[K_Q(1-R)L\right]-R} + \frac{C_{ig}^{L}}{C_{il}^{0}H_i}\,\frac{\exp\left[K_Q(1-R_Q)L\right]-1}{\exp\left[K_Q(1-R_Q)L\right]-R_Q}$$

Mass Transfer

2. Cross flow

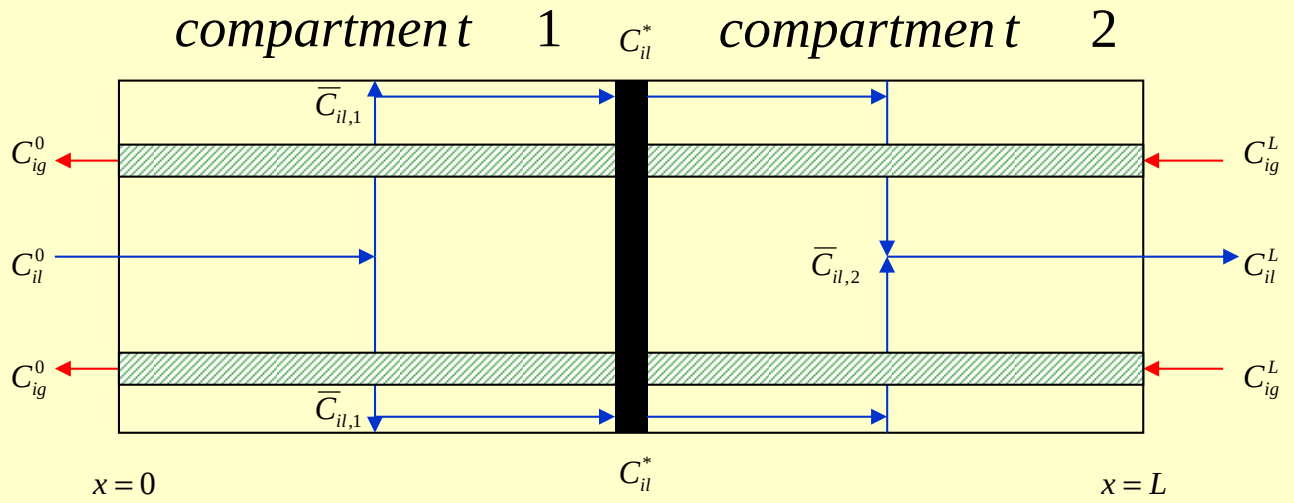

- **Gas phase : Tube side**
  - **Concentration : Only dependent on *x***
- **Liquid phase : Shell side**
  - **Concentration : dependent on *x*, *r***

Mass Transfer

- Mass Balance

$$\frac{2Q_g}{\left(R^2 - R_o^2\right)}\frac{dC_{ig}(x)}{dx} = \frac{Q_l}{rL}\frac{\partial C_{il}(x,r)}{\partial r} \qquad Q_g\frac{dC_{ig}}{dx} = -k_{il}A\left(C_{il,2} - \frac{C_{ig}}{H_i}\right)$$

$$Q_g\left(C_{ig}^{L} - C_{ig}^{0}\right) = Q_l\left(C_{il}^{L} - C_{il}^{0}\right)$$

$$\frac{C_{ig}^{0}}{C_{il}^{R_0}H_i} = 1 - \exp\left[-R_Q(1-E)\right] + \frac{C_{ig}^{L}}{C_{il}^{R_0}H_i}\exp\left[-R_Q(1-E)\right] \qquad E = \exp\left(-K_Q L\right)$$

- Removal efficiency

$$1 - \frac{C_{il}^{L}}{C_{il}^{R_0}} = \frac{(1-F)\left\{R_Q(1+F) - (1-F)\right\}}{R_Q\left\{R_Q - (1-F)^2\right\}} - \frac{C_{ig}^{L}}{C_{il}^{R_0}H_i}\frac{R_Q\left(1-F^2\right) - (1-F)^2}{R_Q\left\{R_Q - (1-F)^2\right\}}$$

$$F = \exp\left[-R_Q\left(1 - E^{1/2}\right)\right]$$

Experiment

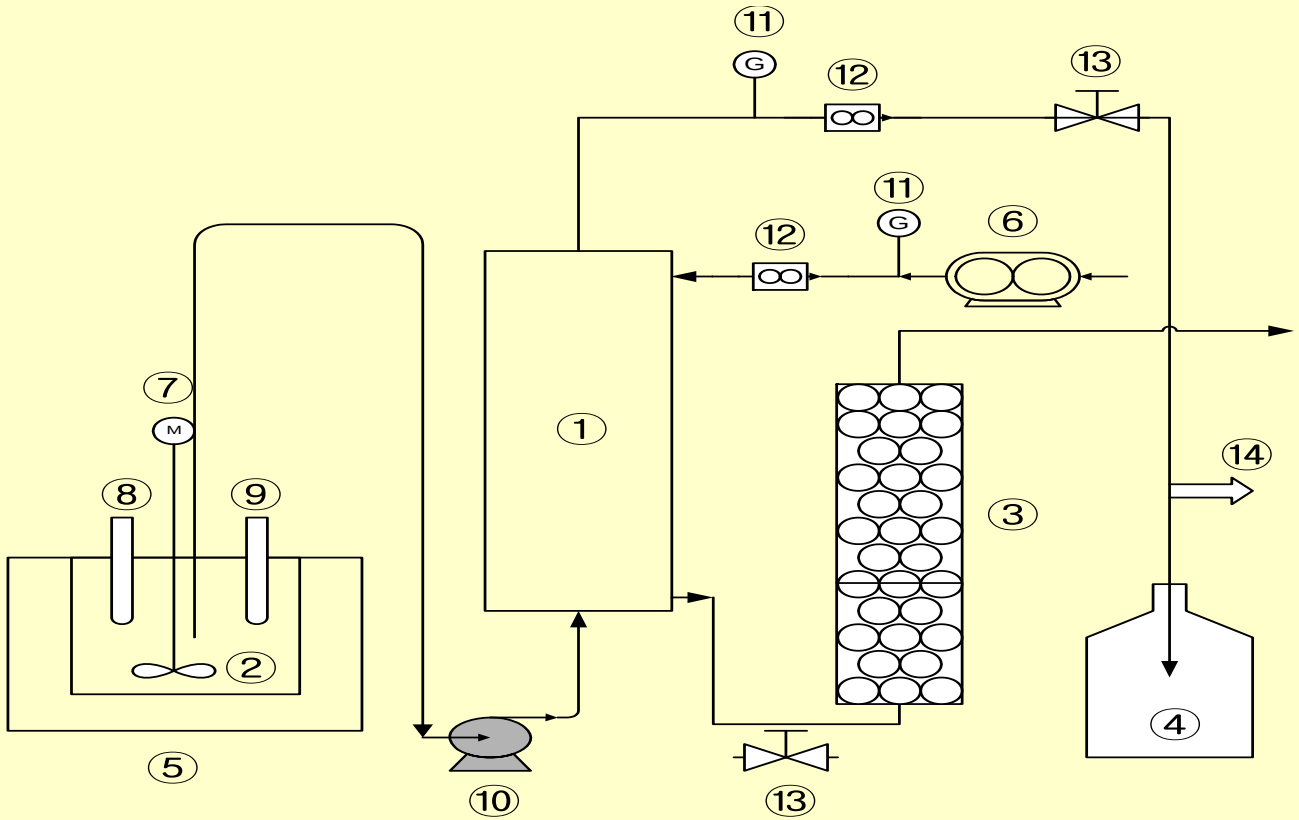

Fig. 1 Schematic diagram of experimental apparatus

① Hollow fiber membrane contactor ② Ammonia solution reservoir ③ Packed column
④ Storage tank ⑤ Water bath ⑥ Air blower ⑦ Stirrer ⑧ pH electrode ⑨ ATC probe
⑩ water pump ⑪ Pressure gauge ⑫ Flow meter ⑬ Needle valve ⑭ Sampling valve

Characteristics of HFMC

Hollow fiber Membrane modules		2.5”x8”	4”x28”
Membrane fiber material		Polypropylene	Polypropylene
Potting material		Polyethylene	Polyethylene
Priming volume (dm3)[a]	Shell side	0.4 liters	4.2 liters
	Lumen side	0.15 liters	1.1 liters
Equivalent diameter of shell side[c]		4.10 cm	6.94 cm
Shell side cross section area[c]		13.2 cm2	37.8 cm2
Lumen side cross section area[c]		2.92 cm2	10.2 cm2
Pore diameter[a]		0.03 micron	0.03 micron
Membrane module inside diameter[a]		2.5 in	4 in
Membrane Porosity[a]		25%	25%
Shell side geometric void fraction[b]		0.40	0.04
Fiber OD/ID[a]		300/200 micron	300/200 micron
Fiber wall thickness[a]		50 micro	50 micro
Maximum allowable working temperature/pressure[a]		60°C/7.4 kg/cm^2	60°C/7.4 kg/cm^2
Effective fiber length[c]		16 cm	62 cm
Effective membrane surface area based on fiber outside diameter[a]		1.40 m2	19 cm2
Fiber number (EA)[c]		10200	31800

[a]Given by Hoechest Celanese.
[b]Estimated by Pierre et al. (2000)
[c]Estimated by Sengupta et al.(1998)

Results

Table 2-1. Comparison of mass transfer coefficients of stripped gases in 2.5”x8” module

	Q_l (ml/min)	Parallel flow	Cross flow	Infinite gas phase
NH_3	10	8.167×10^{-6}	8.501×10^{-6}	4.677×10^{-6}
	20	9.696×10^{-6}	9.983×10^{-6}	4.825×10^{-6}
	30	1.403×10^{-5}	1.465×10^{-5}	5.349×10^{-6}
	100	2.121×10^{-5}	2.135×10^{-5}	1.449×10^{-5}
	200	2.389×10^{-5}	2.398×10^{-5}	1.548 x10-5
	300	2.710×10^{-5}	2.719×10^{-5}	1.661 x10-5
	500	2.603×10^{-5}	2.608×10^{-5}	1.618 x10-5
O_2	1920	6.970×10^{-3}	7.065×10^{-3}	6.943 x10-3
	3780	9.457×10^{-3}	9.473×10^{-3}	9.395 x10-3
	7560	1.330×10^{-2}	1.333×10^{-2}	1.316 x10-2
	11340	1.556×10^{-2}	1.559×10^{-2}	1.535 x10-2

Results

Table 2-2. Comparison of mass transfer coefficients of stripped gases in 4”x28”

	Q_l (ml/min)	Parallel flow	Cross flow	Infinite gas phase
NH_3	100	9.856×10^{-6}	1.023×10^{-5}	7.243×10^{-6}
	150	1.259×10^{-5}	1.309×10^{-5}	8.468×10^{-6}
	200	1.509×10^{-5}	1.573×10^{-5}	9.241×10^{-6}
	250	1.631×10^{-5}	1.694×10^{-5}	9.508×10^{-6}
O_2	15138	7.900×10^{-3}	7.914×10^{-3}	7.792×10^{-3}
	18924	8.850×10^{-3}	9.162×10^{-3}	8.704×10^{-3}
	30282	1.124×10^{-2}	1.158×10^{-2}	1.096×10^{-2}
	37848	1.248×10^{-2}	1.283×10^{-2}	1.210×10^{-2}
	45420	1.353×10^{-2}	1.389×10^{-2}	1.306×10^{-2}
	56778	1.483×10^{-2}	1.520×10^{-2}	1.422×10^{-2}
	60558	1.520×10^{-2}	1.557×10^{-2}	1.455×10^{-2}
	75702	1.652×10^{-2}	1.689×10^{-2}	1.569×10^{-2}
	90840	1.765×10^{-2}	1.802×10^{-2}	1.664×10^{-2}
	94626	1.793×10^{-2}	1.829×10^{-2}	1.687×10^{-2}
	105978	1.875×10^{-2}	1.912×10^{-2}	1.756×10^{-2}
	121122	1.998×10^{-2}	2.037×10^{-2}	1.859×10^{-2}

Results

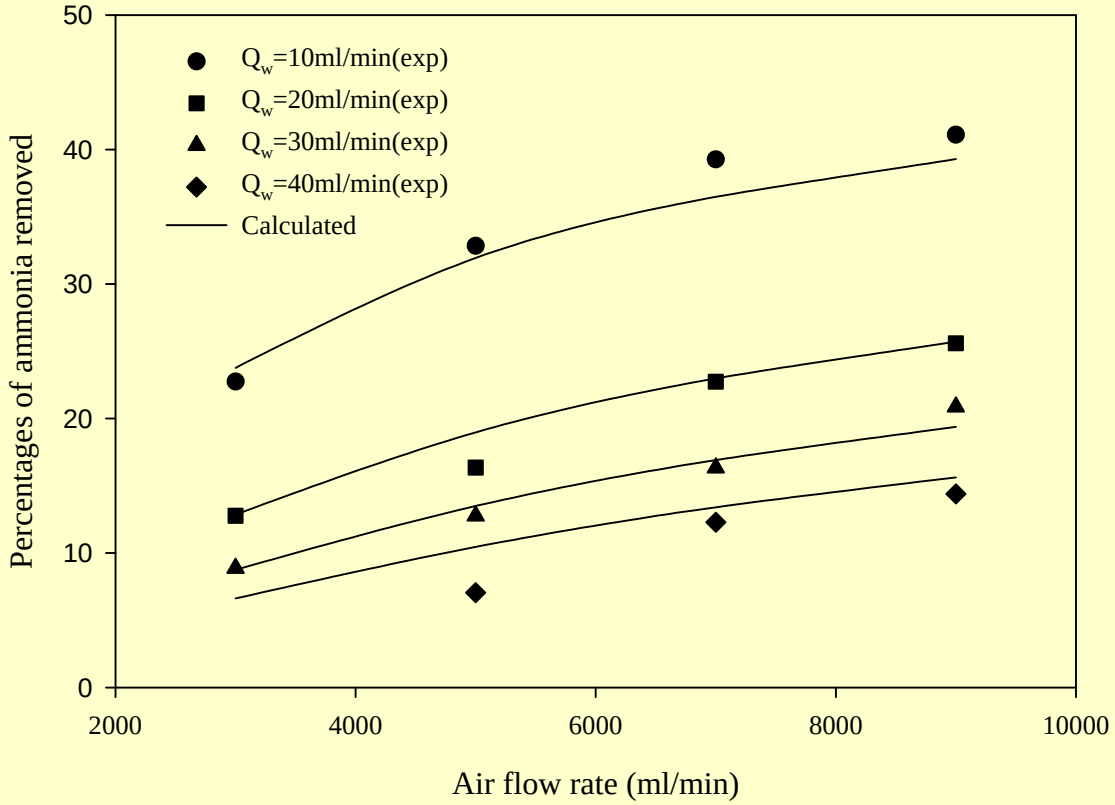

Fig.2-3 Comparison of experimental percentage of ammonia removed with calculated values using 2.5"x8" hollow fiber membrane module with aqueous ammonia solutions

Results

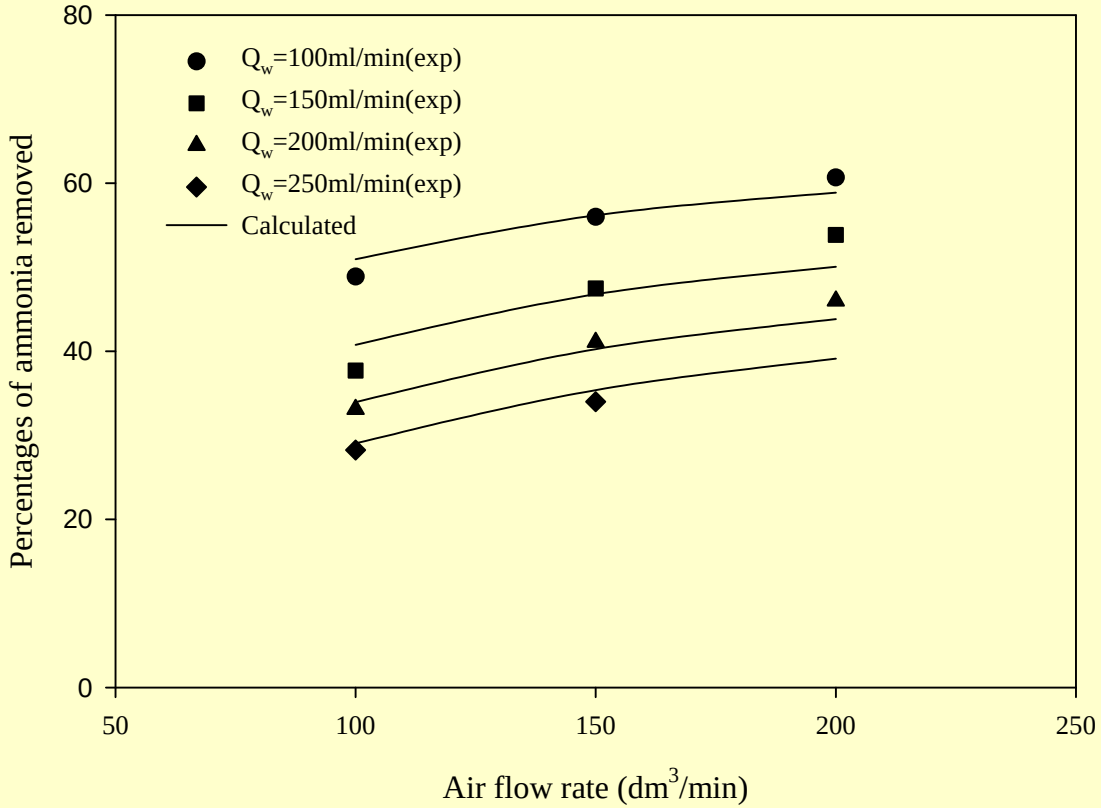

Fig.2-4 Comparison of experimental percentage of ammonia removed with calculated values using 4"x28" hollow fiber membrane module with aqueous ammonia solution

Results

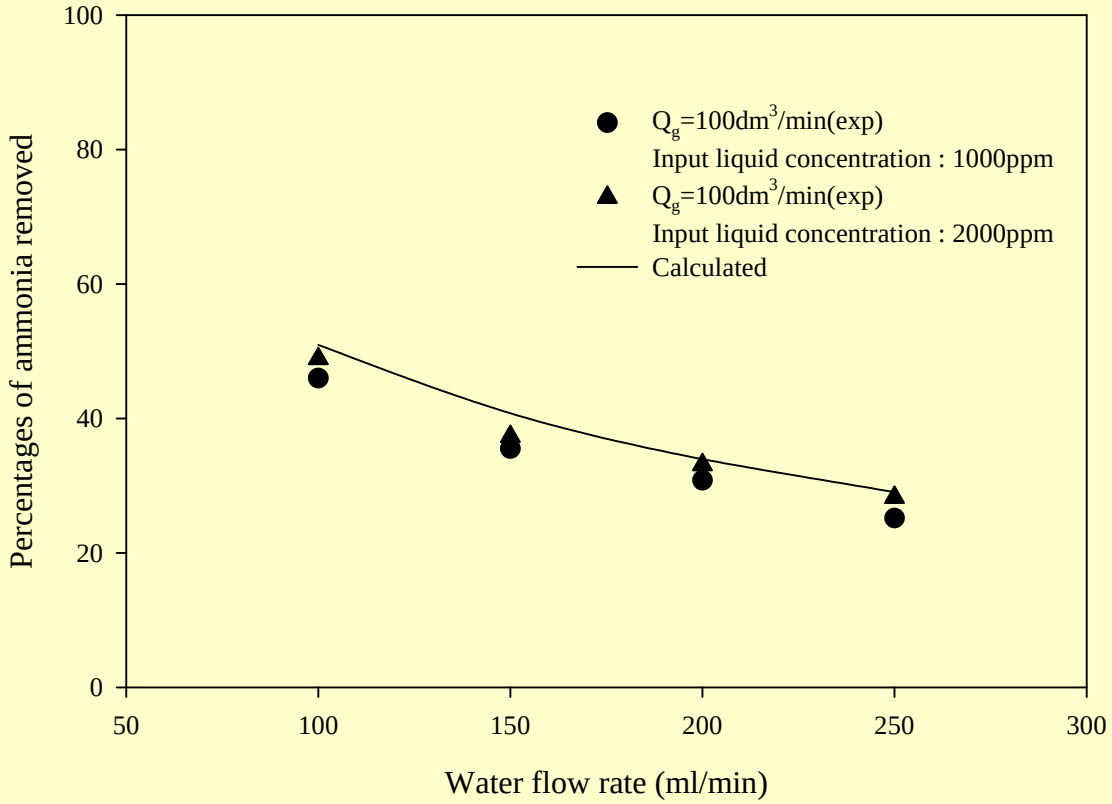

Fig.2-5 Comparison of experimental percentages of ammonia removed with calculated values using 4"x28" hollow fiber membrane module for different input concentrations

Henry's Law

- **Henry's Constant**

$$H_i = \lim_{C_{il} \to 0} \frac{C_{ig}}{C_{il}} = \frac{V_l}{RT} \lim_{x_i \to 0} \frac{p_i}{x_i}$$

  - **Assuming ideal gas phase**
  - **From ammonia-water vapor-liquid equilibrium data at several temperatures, (x>0.05)**
  - **From ammonia-water-NaOH VLE (pH>11)**

Experiment

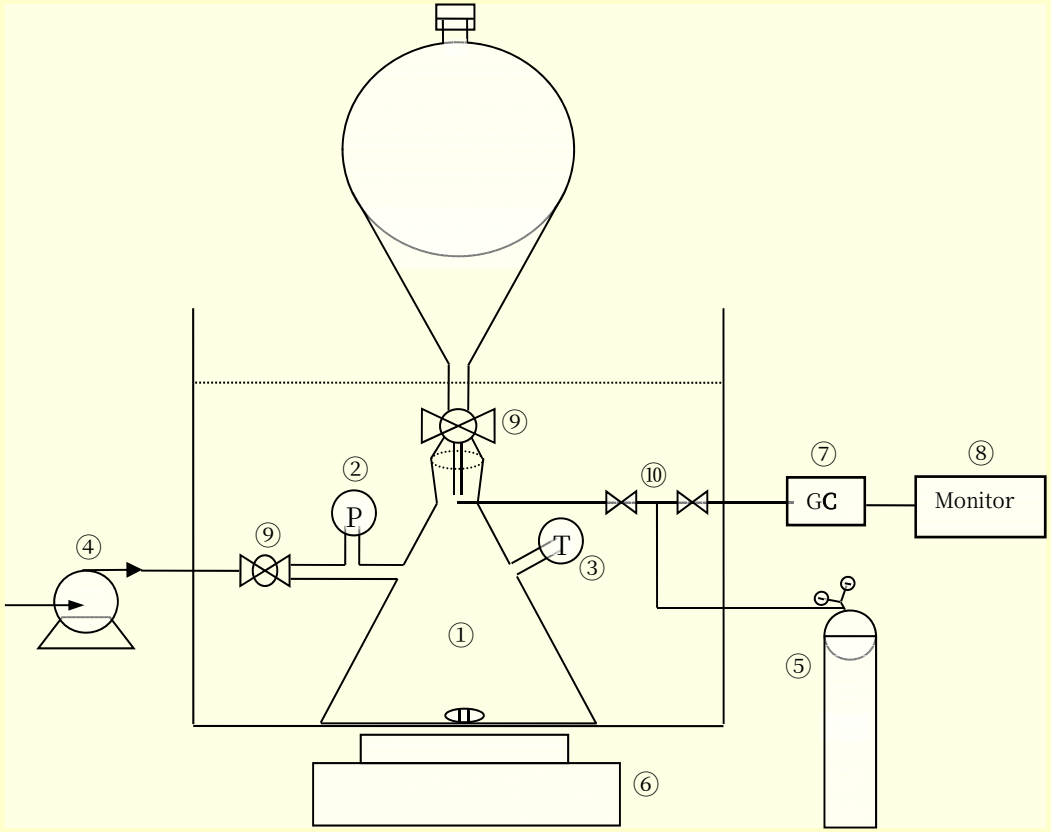

Fig.3.3 Schematic diagram of a modified static measurement

① Equilibrium Cell ② Pressure Transduser ③ Thermometer ④ Vacuum Pump
⑤ Helium Gas ⑥ Magnetic Stirrer ⑦ Gas Chromatograph ⑧ A/D Converter
⑨ Cork ⑩ Sampling loop

Results

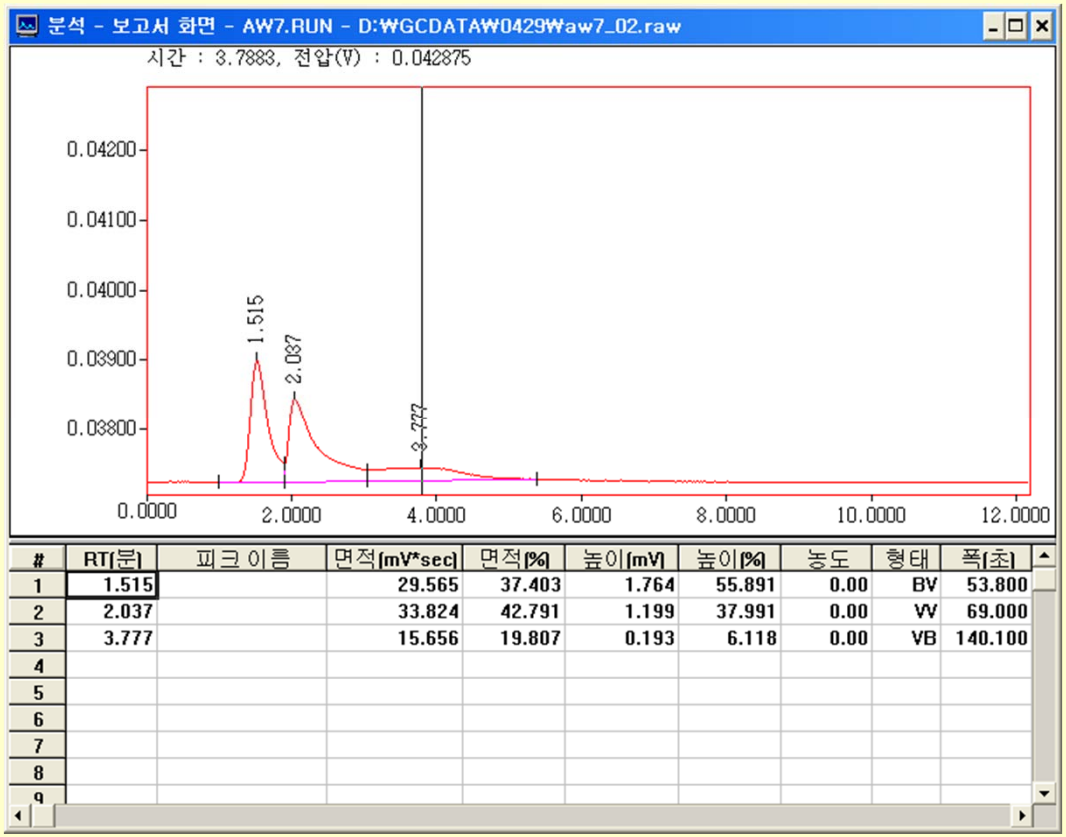

#	RT[분]	피크 이름	면적[mV*sec]	면적[%]	높이[mV]	높이[%]	농도	형태	폭[초]
1	1.515		29.565	37.403	1.764	55.891	0.00	BV	53.800
2	2.037		33.824	42.791	1.199	37.991	0.00	VV	69.000
3	3.777		15.656	19.807	0.193	6.118	0.00	VB	140.100
4									
5									
6									
7									
8									
9									

Fig.3-6 The diagram of analysis for vapor phase composition of 7.4% ammonia solution with GC.

Results

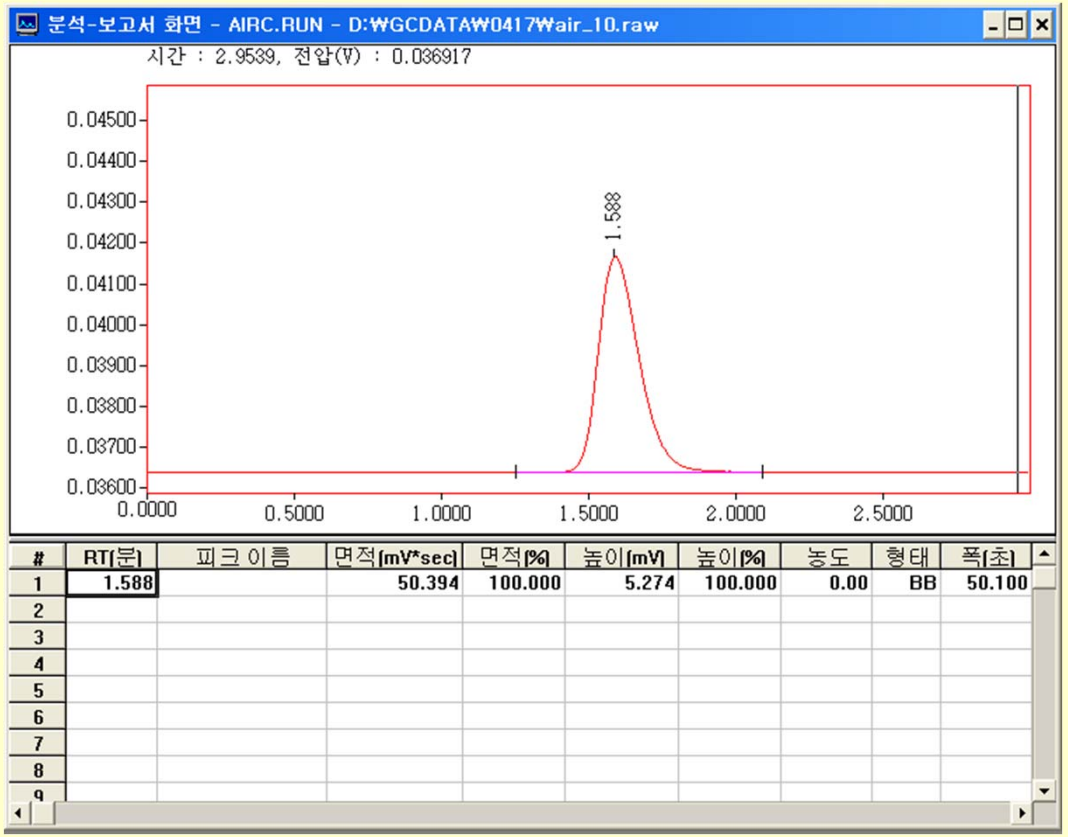

#	RT[분]	피크 이름	면적[mV*sec]	면적[%]	높이[mV]	높이[%]	농도	형태	폭[초]
1	1.588		50.394	100.000	5.274	100.000	0.00	BB	50.100
2									
3									
4									
5									
6									
7									
8									
9									

Fig.3-7 The diagram of analysis for air with GC

Results

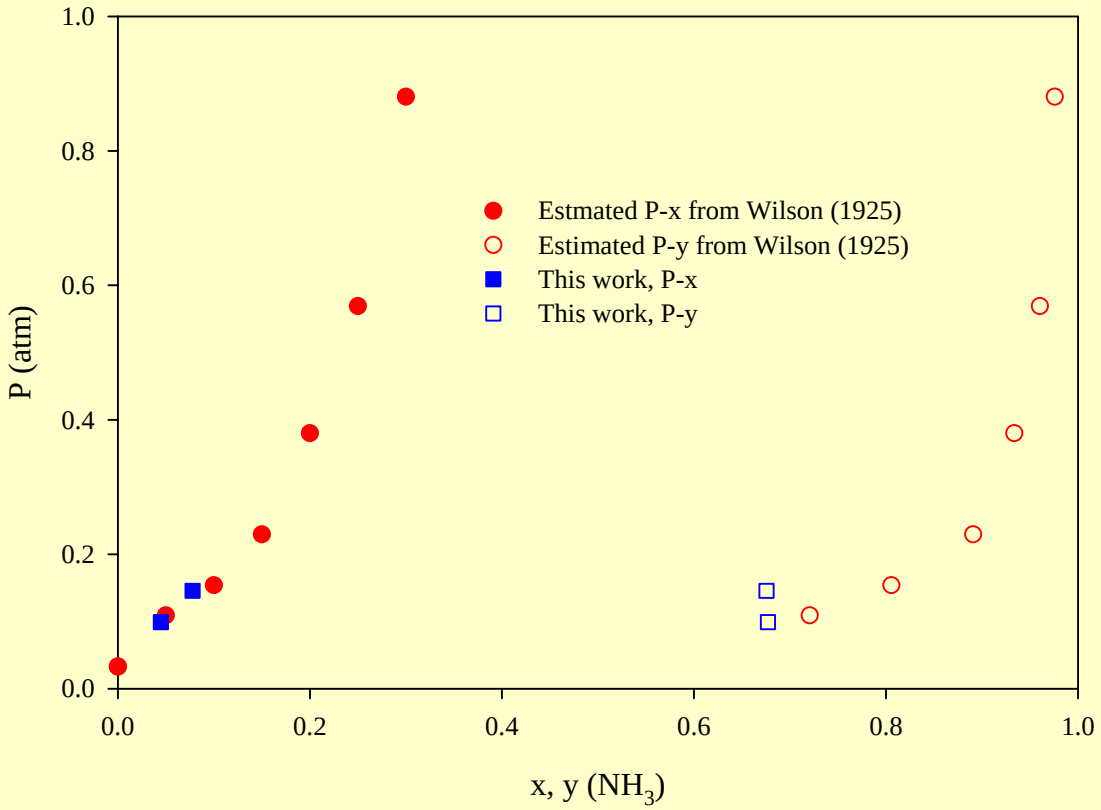

Fig.3-5 Comparison of interpolated data from Wilson (1925) with this work for ammonia-water vapor-liquid equilbria at 298.15K

Results

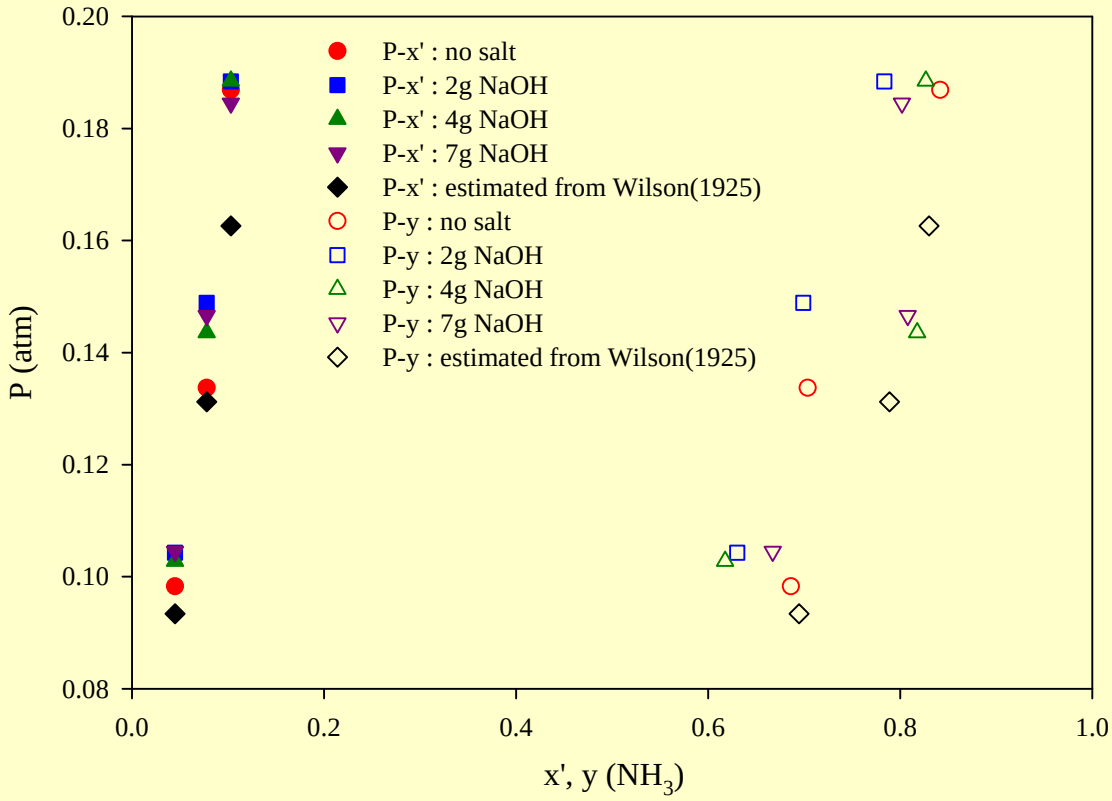

Fig.3-8 P-x'-y diagram for NH_3(1)-H_2O(2)-NaOH(3) VLE at 298.15K.

Results

Table 3-1. Henry's constants of ammonia in NH_3-H_2O-NaOH systems at 298.15K

Weight of NaOH (g)	Henry's constant
-	1.040×10^{-3}
2	1.077×10^{-3}
4	9.909×10^{-4}
7	1.217×10^{-3}

cf) H_i=8.903x10^{-4} at 298.15K : estimated from NH3-H2O VLE at several tempartures

Correlations for mass transfer coeff.

- **Mass transfer**
  - mass tranfer of liquid in shell side
  - mass transfer of vapor in membrane pore
  - mass transfer of vapor in tube side
- **Overall mass transfer coefficient**

$$\frac{1}{K_{il}} = \frac{1}{k_{il}^{l}} + \frac{1}{k_{ig}^{p} H_i} + \frac{1}{k_{ig}^{g} H_i}$$

$$k_{ig}^{g} = 1.62 \frac{D_{ig}}{d} \left(\frac{d^2 v_g}{L D_{ig}} \right)^{1/3} \qquad k_{ig}^{p} = \frac{2 r_p}{3} \left(\frac{8RT}{\pi M_i} \right)^{1/2} \frac{\varepsilon}{l\tau} \qquad \left(\frac{k_{il}^{l} d_e}{D_{il}} \right) = a \left(\frac{d_e \nu_l}{\nu_l} \right)^{b} \left(\frac{\nu_l}{D_{il}} \right)^{c}$$

  - Yang and Cussler (1986), Sengupta et al.(1998)

$$K_{il} \approx k_{il}^{l} \qquad \left(\because \; k_{il}^{l} \le k_{ig}^{p}, k_{ig}^{g} \right)$$

Hollow Fiber Membrane contactor?

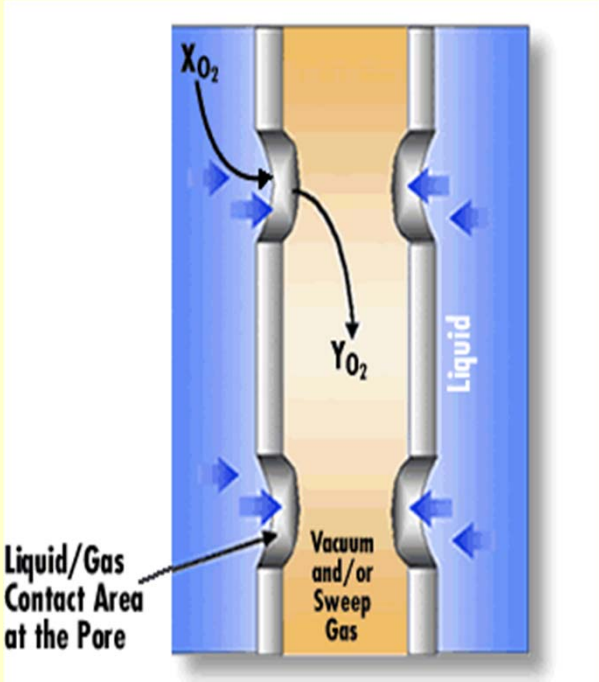

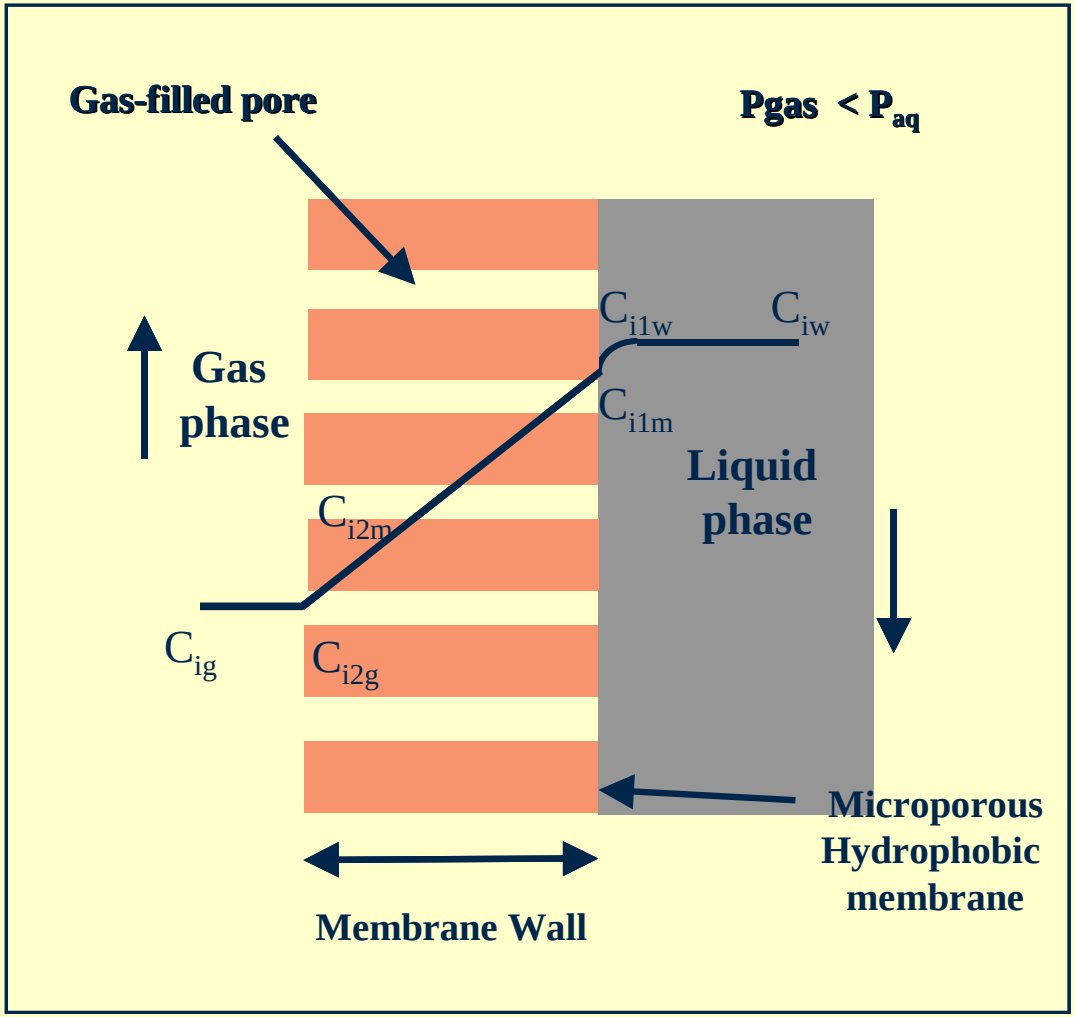

Results

Table 4-2. Comparison with individual mass transfer coefficients in 4”x28” module

Q_g (dm^3/min)	Individual mass transfer coefficients (cm/sec)	Q_l (ml/min)			
		100	150	200	250
100	k_{il}	9.11×10^{-6}	1.05×10^{-5}	1.38×10^{-5}	1.54×10^{-5}
	$k_{ig}{}^{p}H_i$	1.34×10^{-3}	1.34×10^{-3}	1.34×10^{-3}	1.34×10^{-3}
	$k_{ig}{}^{g}H_i$	9.33×10^{-3}	9.33×10^{-3}	9.33×10^{-3}	9.33×10^{-3}
150	k_{il}	9.90×10^{-6}	1.29×10^{-5}	1.54×10^{-5}	1.53×10^{-5}
	$k_{ig}{}^{p}H_i$	1.34×10^{-3}	1.34×10^{-3}	1.34×10^{-3}	1.34×10^{-3}
	$k_{ig}{}^{g}H_i$	1.18×10^{-2}	1.18×10^{-2}	1.18×10^{-2}	1.18×10^{-2}
200	k_{il}	1.06×10^{-5}	1.44×10^{-5}	1.61×10^{-5}	1.82×10^{-5}
	$k_{ig}{}^{p}H_i$	1.34×10^{-3}	1.34×10^{-3}	1.34×10^{-3}	1.34×10^{-3}
	$k_{ig}{}^{g}H_i$	1.35×10^{-2}	1.35×10^{-2}	1.35×10^{-2}	1.35×10^{-2}

Results

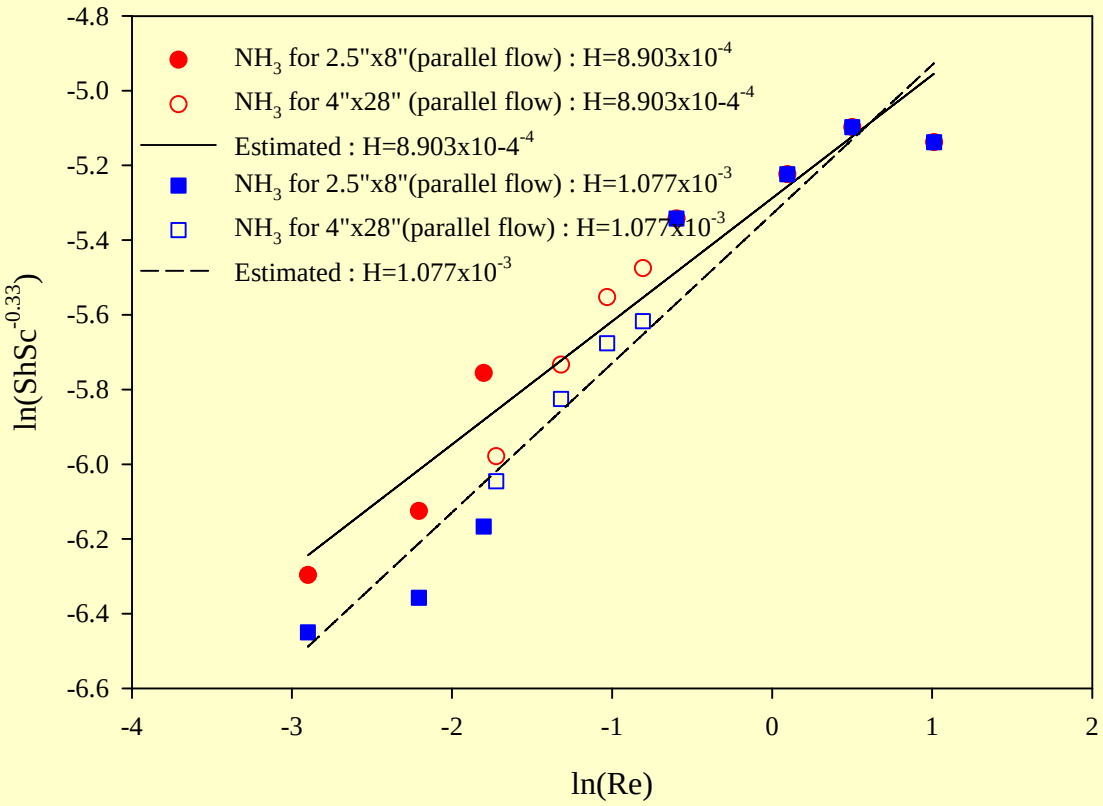

Fig.4-4 The correlation of shell side mass transfer coefficient of NH_3 with 2.5"x8" and 4"x28" membrane contactor modules

Results

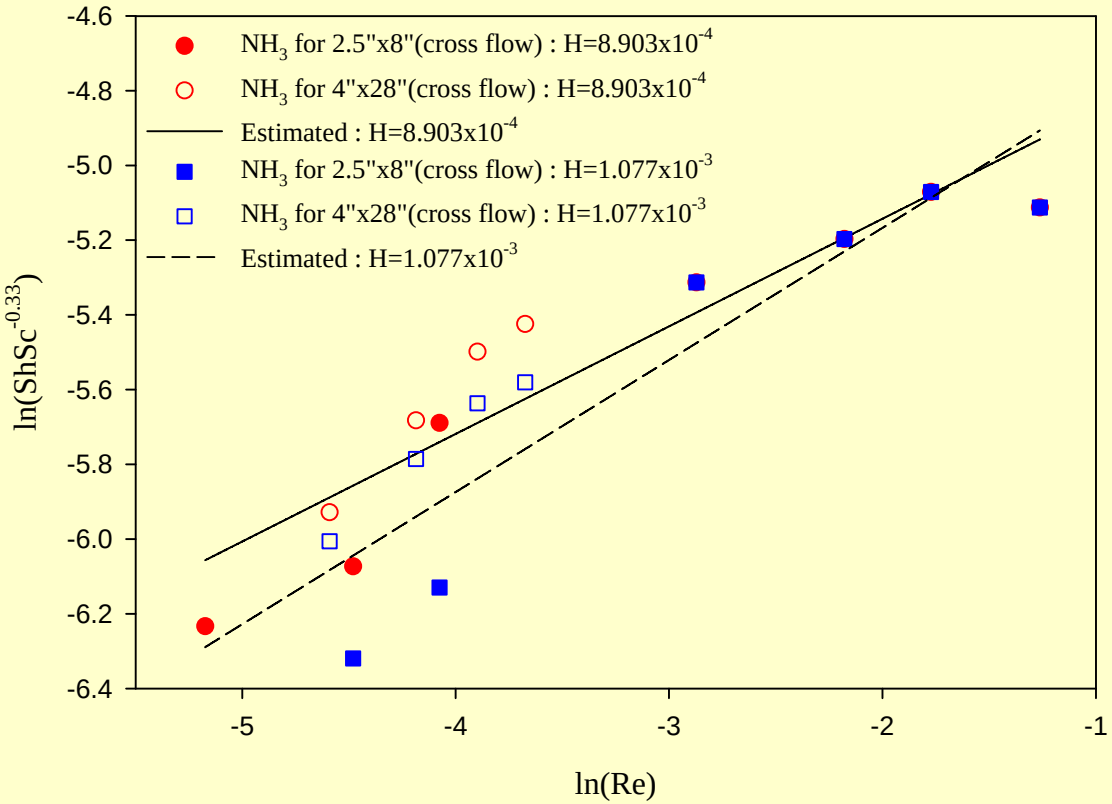

Fig.4-5 The correlation of shell side mass transfer coefficient of NH_3 with 2.5"x8" and 4"x28" membrane contactor modules

Results

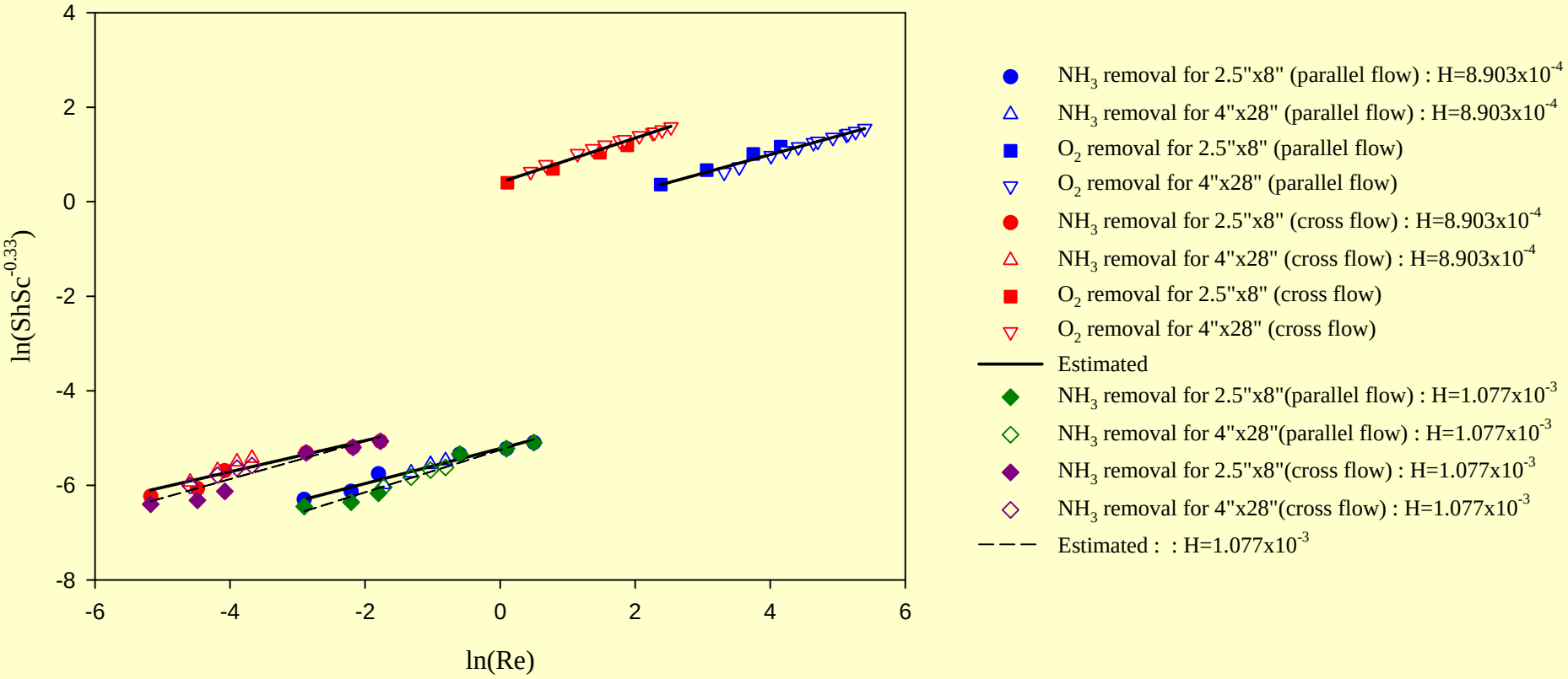

Fig.4-6 The comparison of mass transfer coefficients for ammonia removal and oxygen removal.

Results

Table 4-3. The fitted parameter a and b for the correlation of mass transfer coefficients

	Parallel flow		Cross flow	
	a	b	a	b
NH_3 [1)]	0.0055	0.37	0.012	0.33
NH_3 [2)]	0.0052	0.45	0.014	0.40
O_2	0.57	0.39	1.51	0.47

[1)] H_i=8.903x10^{-4}
[2)] H_i=1.077x10-3

Application to NH_3-H_2O VLE

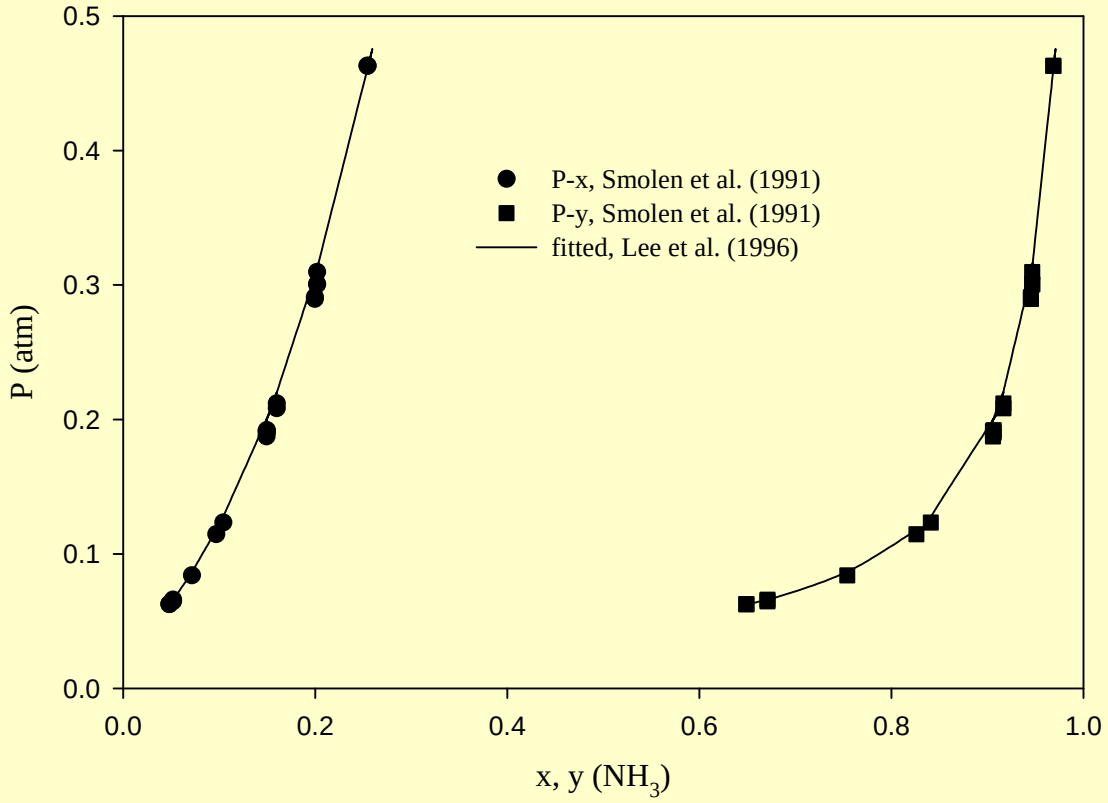

Fig.5-1 P-x, P-y diagram of ammoni-water vapor-liquid equilibrium at 293.15K

Application to NH_3-H_2O VLE

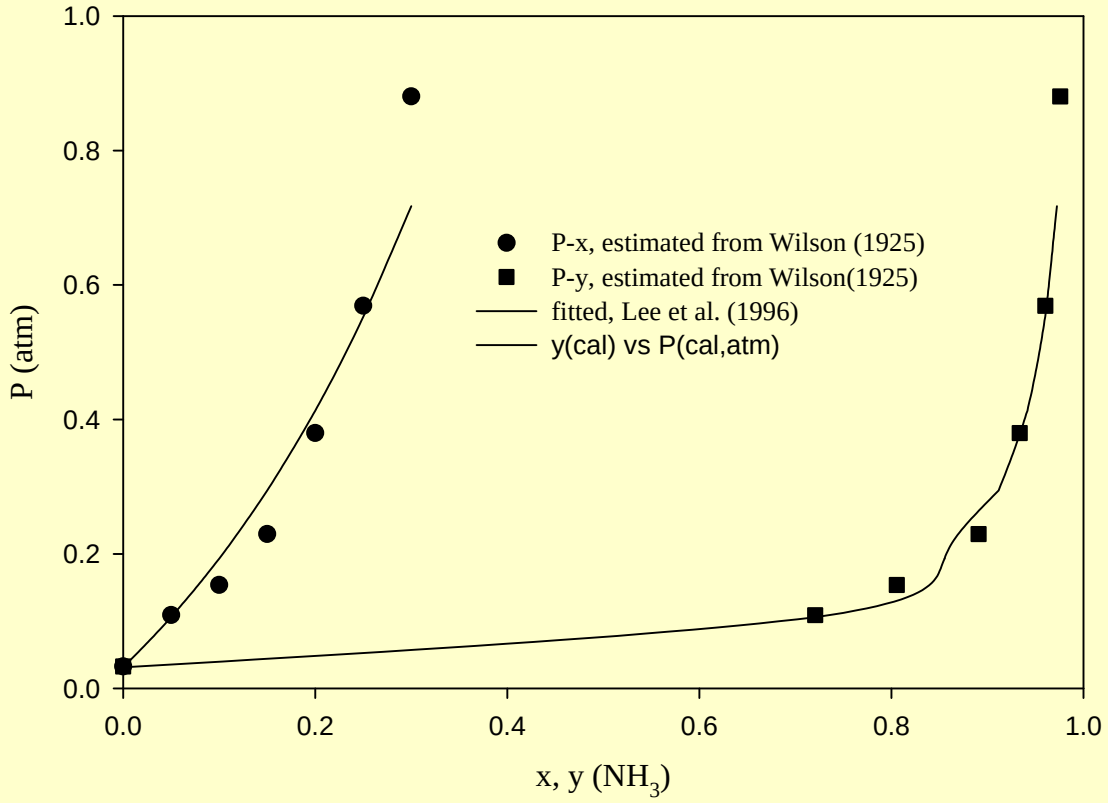

Fig.5-2 P-x-y diagram of ammonia-water vapor-liquid equilibria at 298.15K

Application to NH_3-H_2O-NaOH VLE

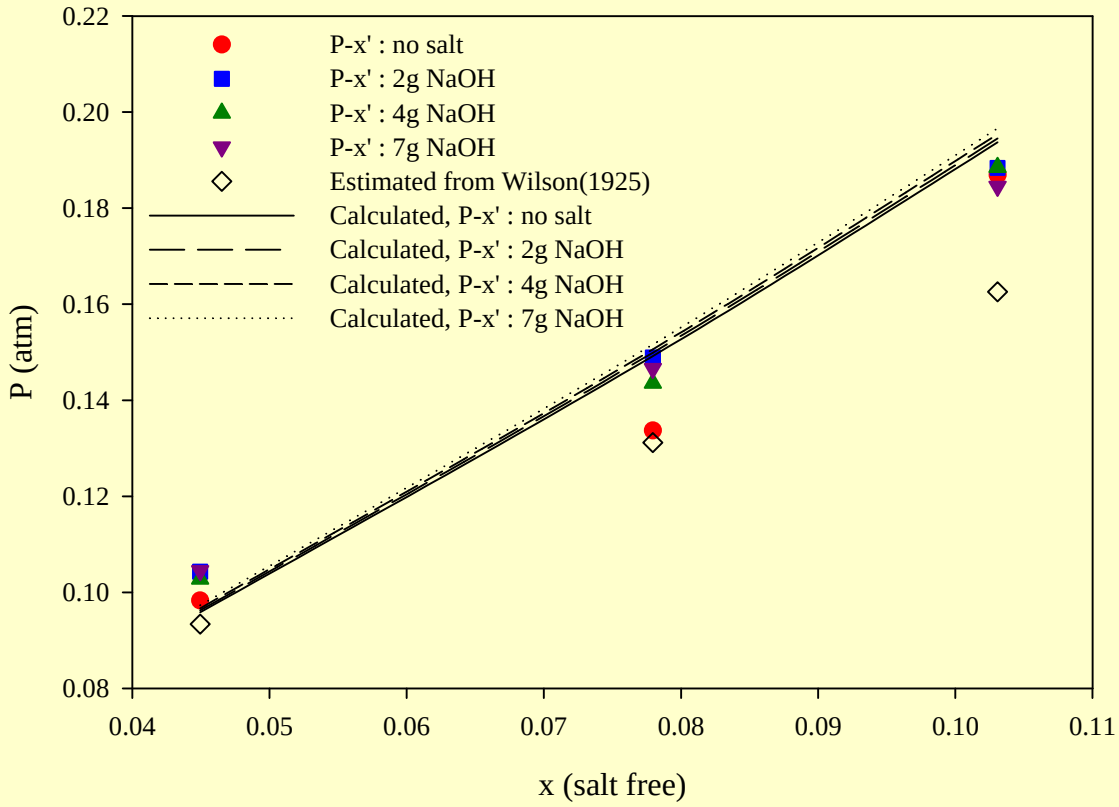

Fig.5-3 P-x' diagram of NH_3(1)-H_2O(2)-NaOH(3) at 298.15K.

Application to NH_3-H_2O-NaOH VLE

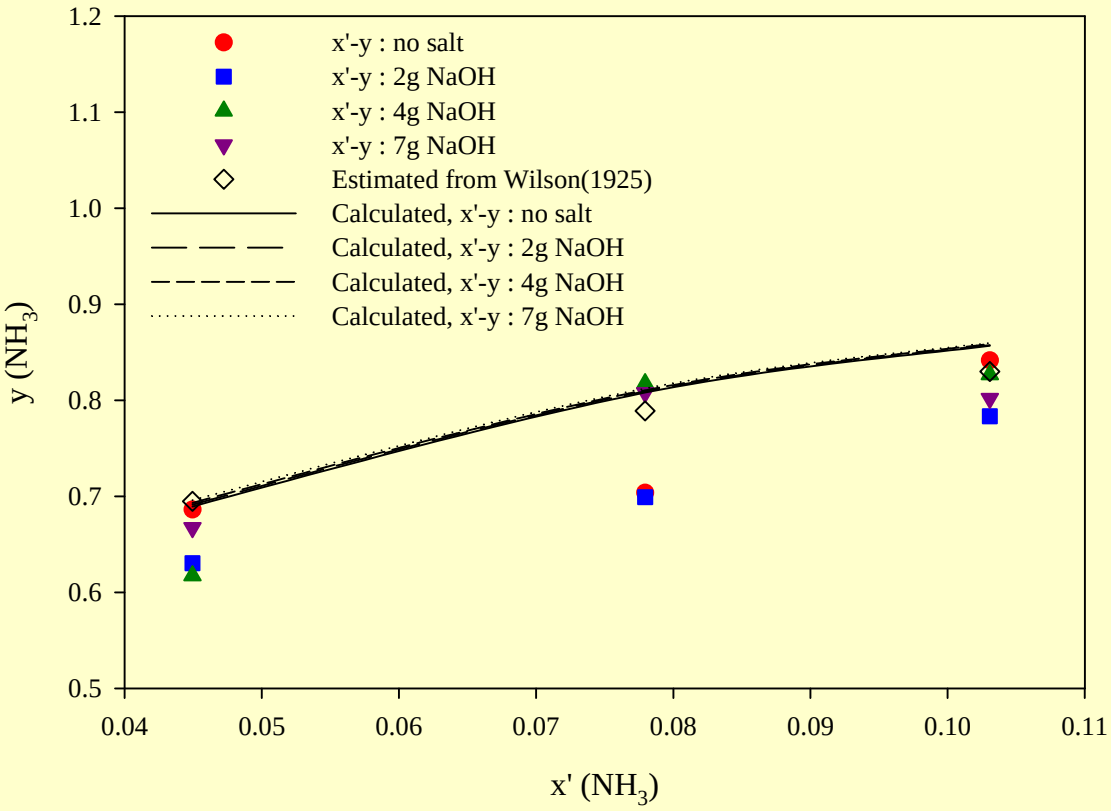

Fig.5-4 x'-y diagram of NH_3(1)-H_2O(2)-NaOH(3) at 298.15K

Mixed Solvent Systems

- Increasing interest in the effects of salts on the VLE of solvent mixtures.
  - A wide variety of important chemical processes
    - Wastewater treatment, extractive distillation, solution crystallization, desalination, gas scrubbing etc.
- The effect of salt out and salt in : shifting and eliminating azeotrpe of solvent mixtures
- Little is known about the effect of electrolyte on VLE of alcohol-water-systems because of complex interaction between mixed solvents

Mixed Solvent Systems

- **Mock et al. (1986)**
  - Extended Chen's NRTL model to mixed solvent solution
  - Ignore long-range interaction term
- **Sander et al. (1986)**
  - Extended UNIQUAC equation for the representation of salt effect on VLE
  - Concentration-dependent interaction parameter
- **Macedo et al. (1990)**
  - Modified Debye-Hückel term from Cardoso and O'Connell (1987)
- **Li et al. (1994), Polka et al. (1994)**
  - 4 ion-ion parameters
  - 2 solvent-solvent parameters
  - Applicable up to high concentration

Mixed Solvent Systems

- **Excess Gibbs Energy : Lee et al. (1996)**
  - **Long-range + Physical** $G^E = G^E_{DH} + G^E_A + G^E_R$
  - **Debye-Hückel term**

$$G^{E*}_{DH} = -\frac{RTV}{4\pi a^3 N_a}\left[\ln(1+aK) - aK + \frac{(aK)^2}{2}\right] \qquad K = \left(\frac{8\pi e^2 N_a I}{D_s kT}\right)^{1/2}$$

  - **In high pressure limit, holes are vanished**

$$A^E(T, P=\infty, x_i) = A^E(T, low\ P, x_i) = G^E(T, low\ P, x_i)$$

  - **Physical interaction : Athermal + Residual**

$$\beta G^E_A = \sum N_i \ln\frac{\theta_i}{x_i} + \left(1-\frac{z}{2}\right)\sum N_i q_i \ln\frac{q_M r_i}{r_M q_i} \qquad \beta G^E_R = -\frac{zN_q}{2}\sum \theta_i \ln\left(\sum \theta_j \tau_{ji}\right)$$

Mixed Solvent Systems

- **For solvent activity coefficient**

$$\ln\gamma_j = \ln\gamma_{DH,j} + \ln\gamma_{A,j} + \ln\gamma_{R,j}$$

- **For solute activity coefficient**

$$\ln\gamma_j^* = \ln\gamma_j - \lim_{x_i \to 0} \ln\gamma_j$$

$$\ln\gamma_{\pm j}^* = \ln\gamma_{DH,\pm j}^* + \ln\gamma_{A,\pm j}^* + \ln\gamma_{R,\pm j}^*$$

- **Interaction between ion** $\varepsilon_{ij} = \varepsilon_{ij}^{(e)} + \varepsilon_{ij}^{(n)}$
- **Interaction with uncharged species** $\varepsilon_{ij} = \varepsilon_{ij}^{(n)}$
- **Interaction between unlike species**

$$\varepsilon_{ij}^{(n)} = (\varepsilon_{ii}^{(n)}\varepsilon_{jj}^{(n)})^{1/2}(1-k_{ij})$$

Parameters for Mixed Solvent Systems

- **Parameters for Salt & Water**
  - **From Lee et al. (1996)**
- **Only parameters for pure solvent & parameters for solvent-water interaction**

$$r_i, \varepsilon_{ii}, k_{ij}$$

- **Determination**
  - **Data for alcohol-water VLE (Gmehling et al.,1977)**
  - **Data for alcohol-water mixture volume and dielectric constant (Sandler, 1989; Conway, 1952)**

Temperature-dependent parameters

$$r_i = r_a + r_b (T_0 / T) + r_c \ln(T_0 / T)$$

$$\varepsilon_{ii} = \varepsilon_a + \varepsilon_b (T_0 / T) + \varepsilon_c \ln(T_0 / T)$$

$$k_{ij} = k_a + k_b (T_0 / T) + k_c \ln(T_0 / T)$$

$$T_0 = 298.15K$$

Results

Table 5-1. Temperature coefficients of eqns (5-16) and (5-17) for methanol, ethanol, 1-propanol and 2-propanol

	r_a	r_b	r_c	ε_a	ε_b	ε_c
Methanol	281.80	-270.03	251.12	86.42	-85.13	76.65
Ethanol	16.50	-11.25	8.82	40.88	-40.00	33.16
1-Propanol	-15.20	22.05	-16.21	114.46	-113.83	98.34
2-Propanol	141.49	-136.40	117.42	-4.94	6.11	-9.30

Results

Table 5-2. Temperature coefficients of eqns (5-18) for methanol-, ethanol-, 1-propanol- and 2-propanol-water

	k_a	k_b	k_c
Methanol-water	281.80	-270.03	251.12
Ethanol-water	16.50	-11.25	8.82
1-Propanol-water	-15.20	22.05	-16.21
2-Propanol-water	141.49	-136.40	117.42

Results : Isothermal VLE

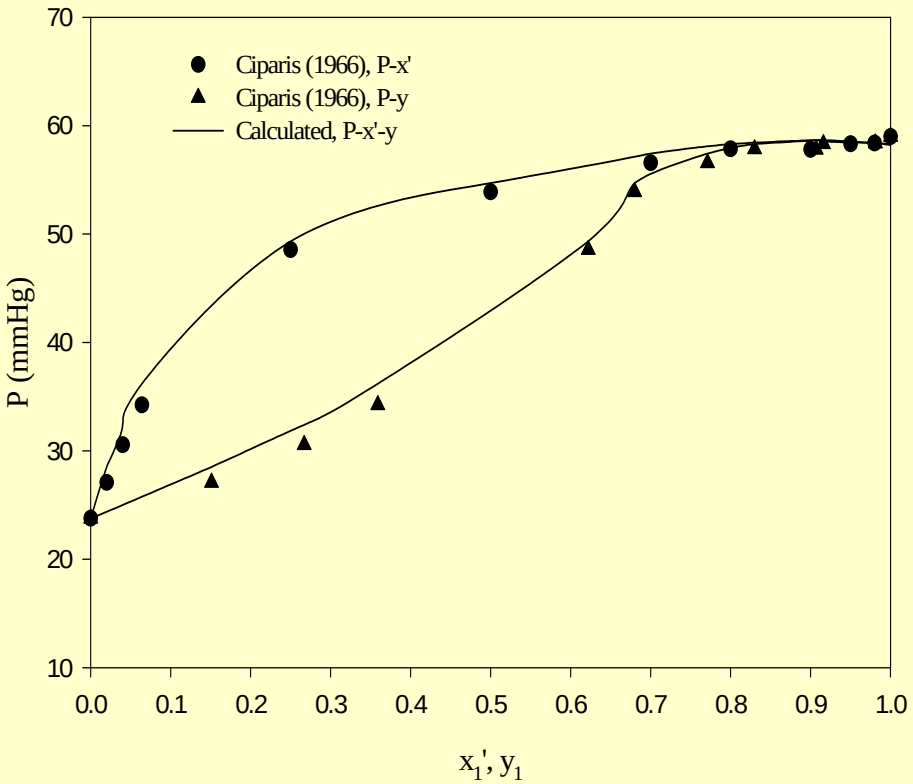

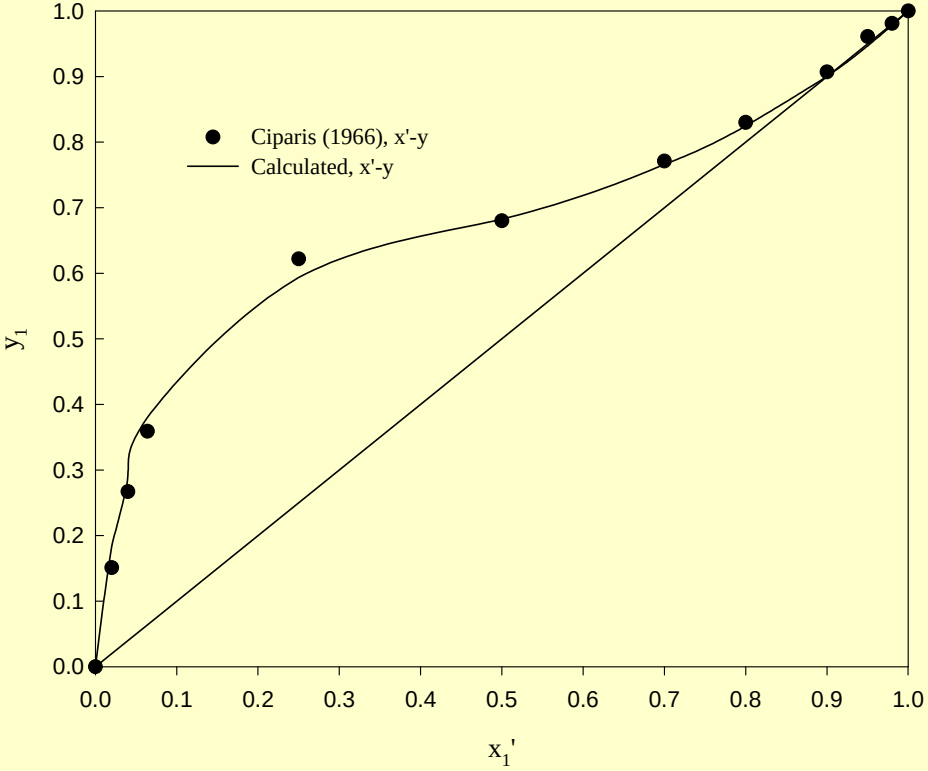

Fig.5-5 P-x'-y for EtOH(1)-H_2O(2)-LiCl(3) VLE at 298.15K.
m(LiCl)=0.0 mol/kg.

Results : Isothermal VLE

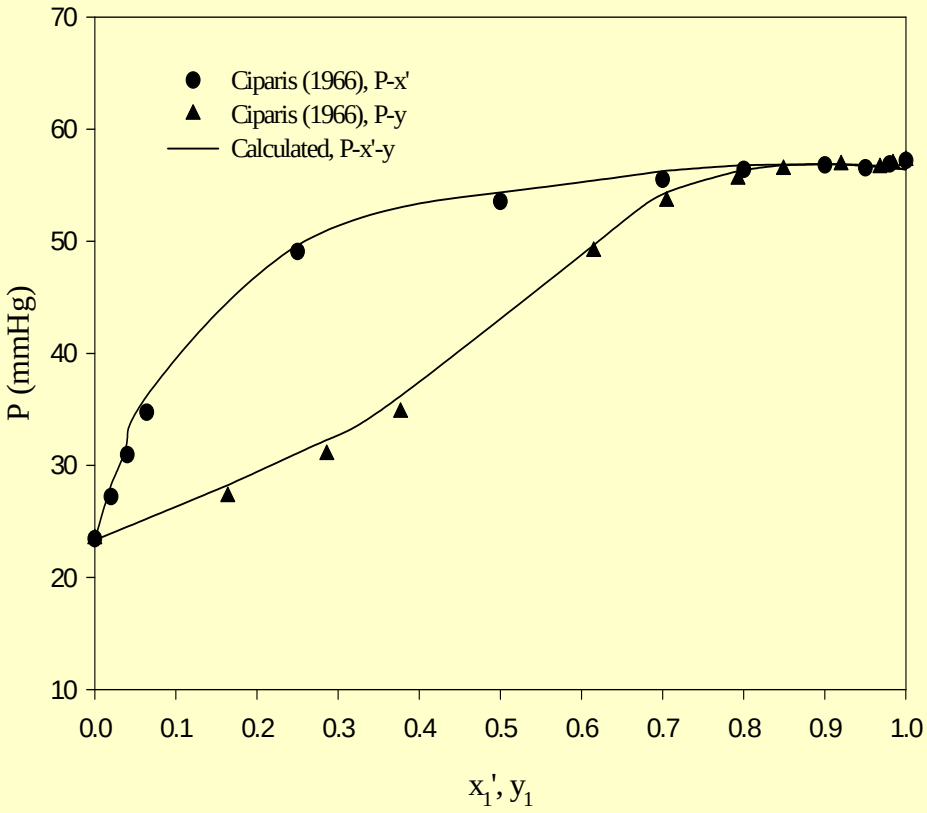

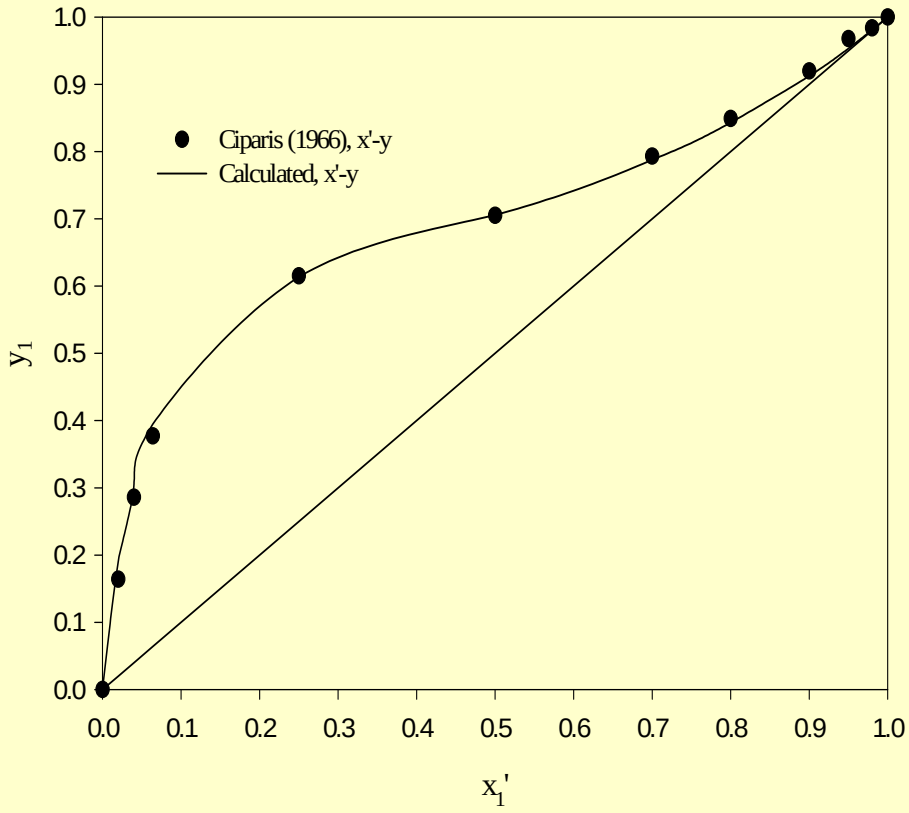

Fig.5-6 P-x'-y for EtOH(1)-H_2O(2)-LiCl(3) VLE at 298.15K.
m(LiCl)=0.5 mol/kg.

Results : Isothermal VLE

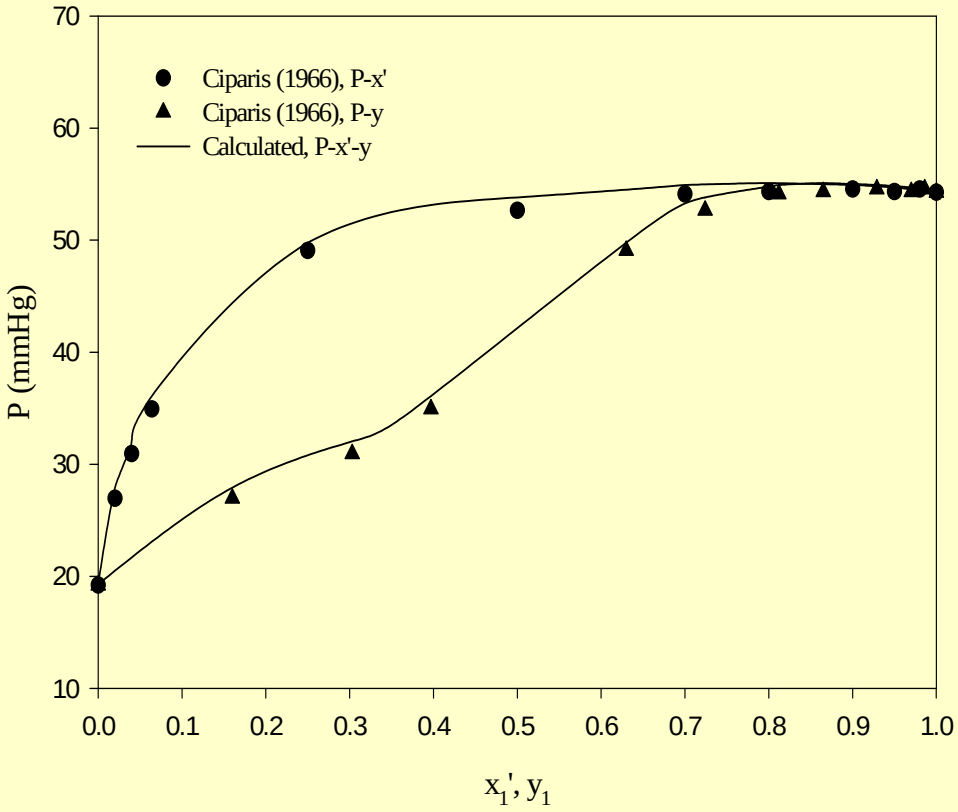

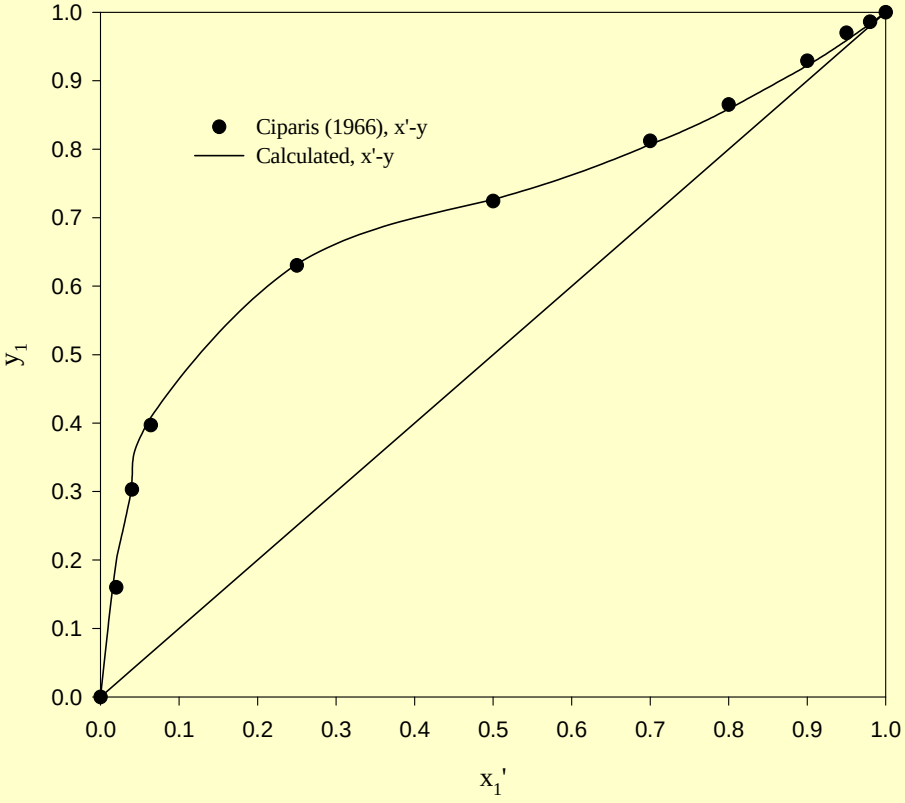

Fig.5-7 P-x'-y for EtOH(1)-H_2O(2)-LiCl(3) VLE at 298.15K.
m(LiCl)=1.0 mol/kg.

Results : Isothermal VLE

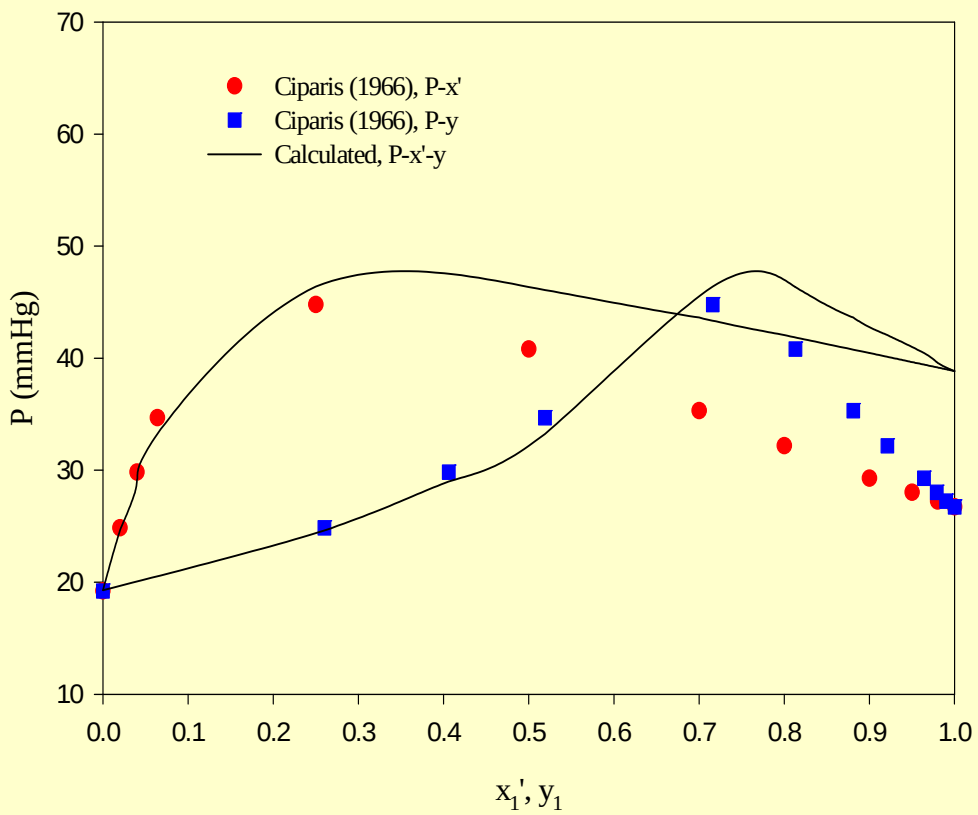

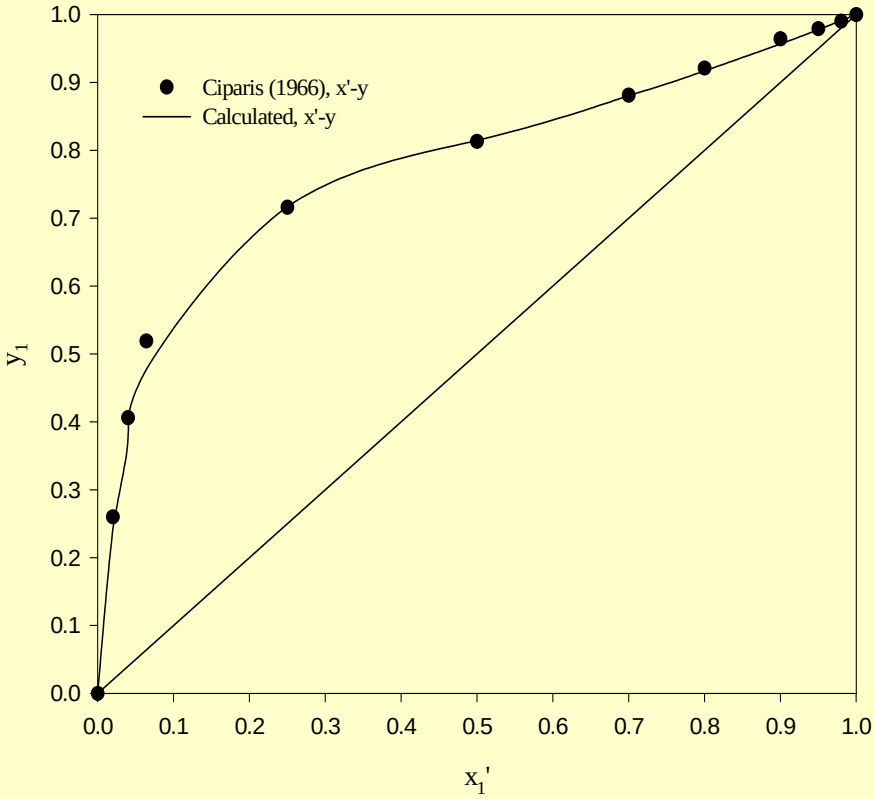

Fig.5-8 P-x'-y for EtOH(1)-H_2O(2)-LiCl(3) VLE at 298.15K.
m(LiCl)=4.0 mol/kg

Results : Isothermal VLE

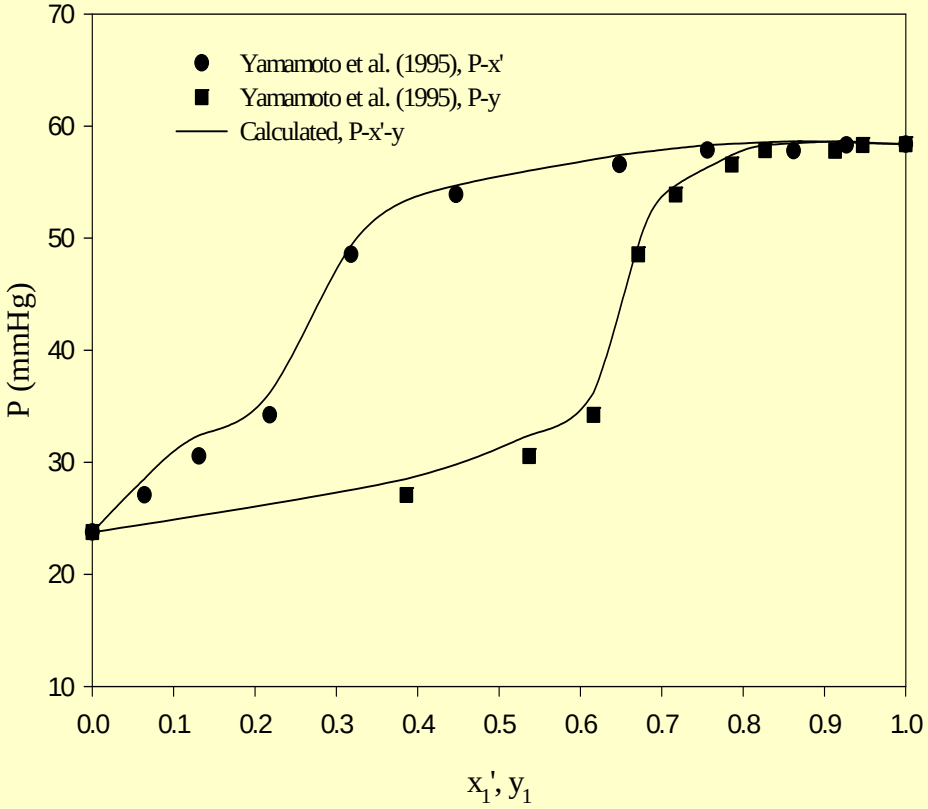

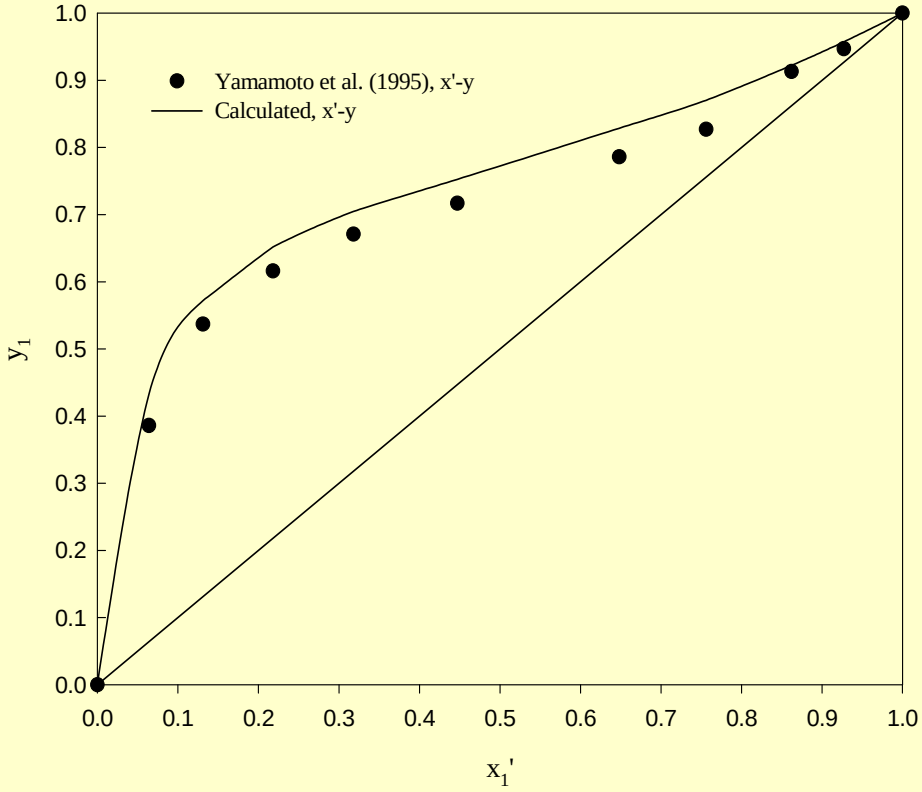

Fig.5-9 P-x'-y for EtOH(1)-H_2O(2)-$CaCl_2$(3) VLE at 298.15K.

Results : Isothermal VLE

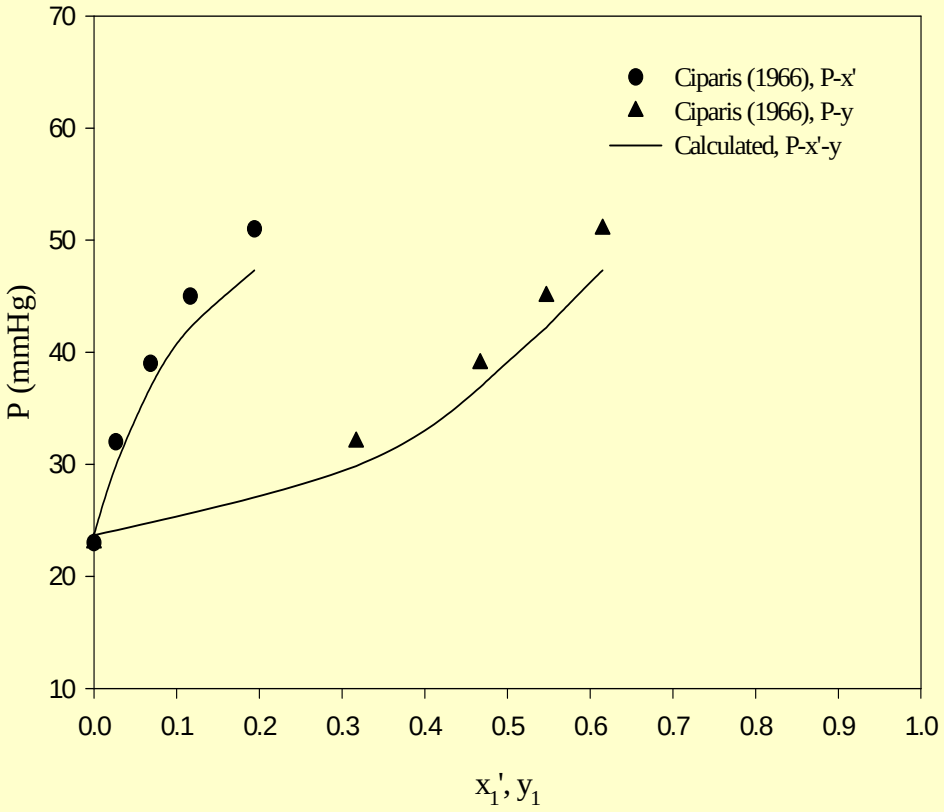

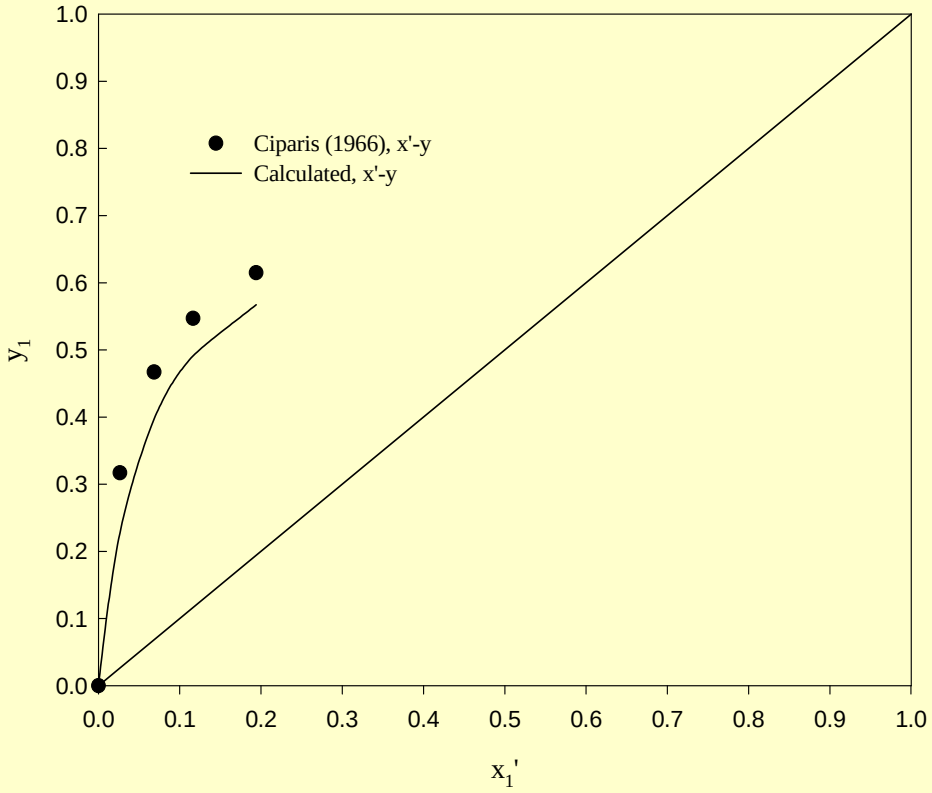

Fig.5-10 P-x'-y for EtOH(1)-H_2O(2)-Na_2SO_4(3) VLE at 298.15K.

Results : Isothermal VLE

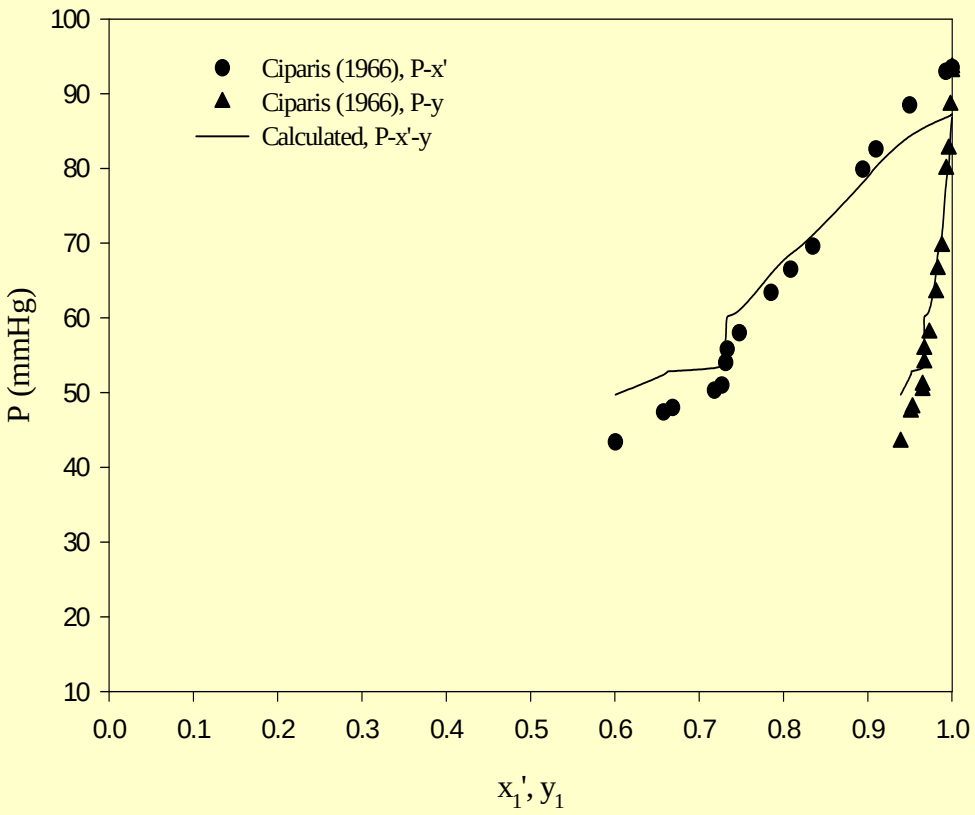

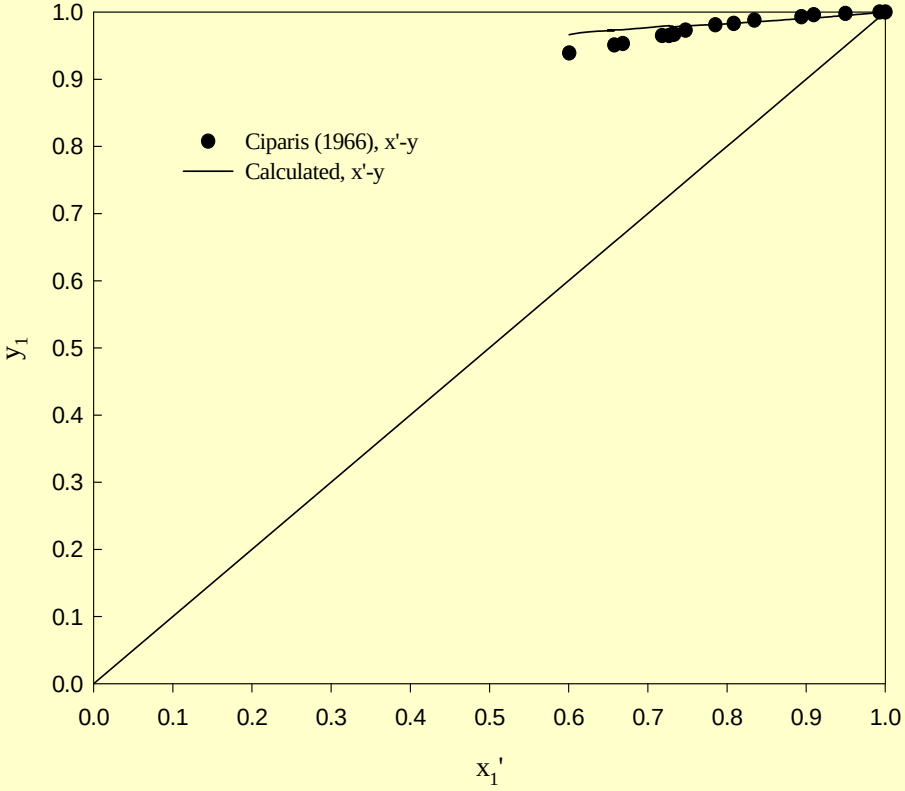

Fig.5-11 P-x'-y for MeOH(1)-H_2O(2)-$CaCl_2$(3) VLE at 298.15K.

Results : Isothermal VLE

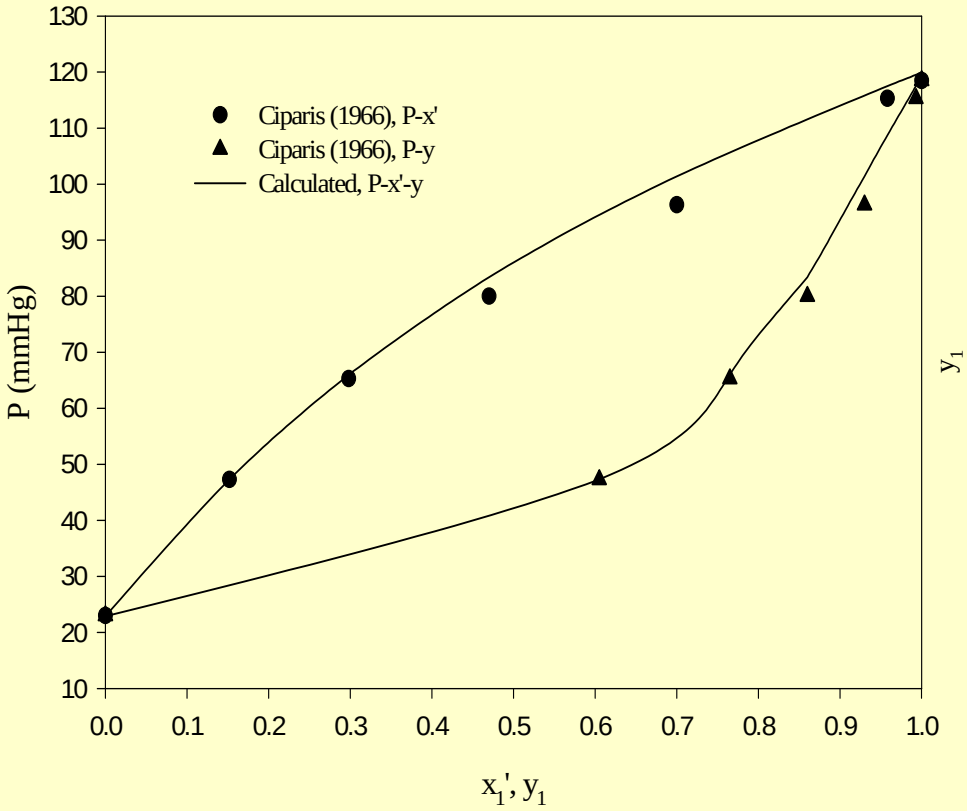

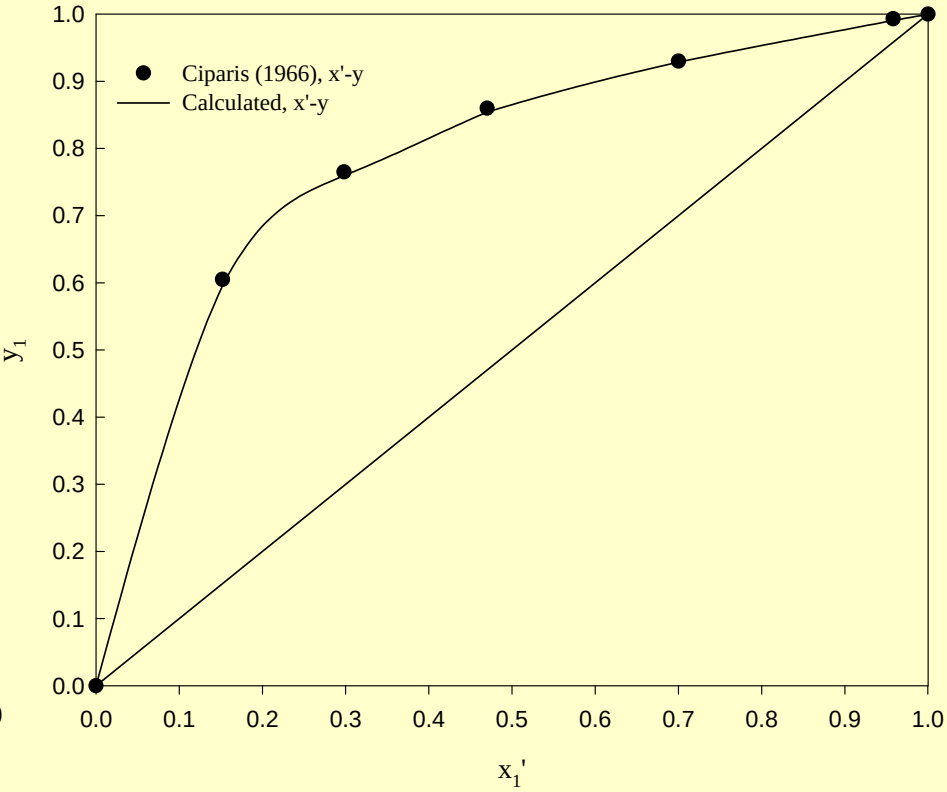

Fig.5-12 P-x'-y for MeOH(1)-H_2O(2)-LiCl(3) VLE at 298.15K.
m(LiCl)=1.0 mol/kg

Results : Isothermal VLE

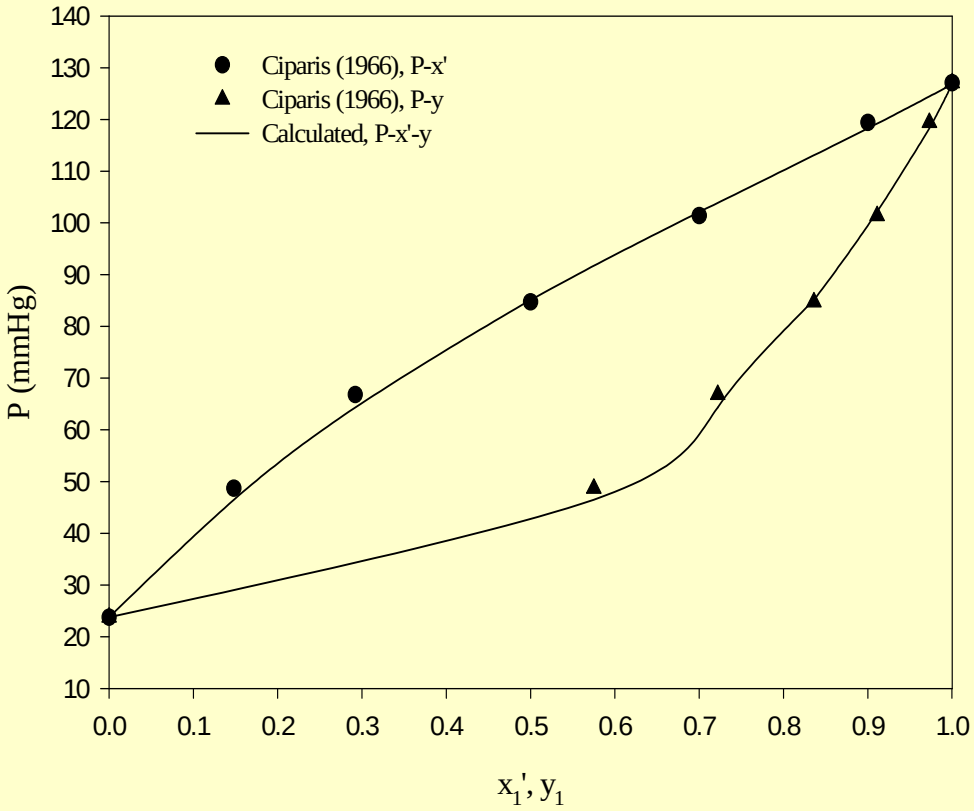

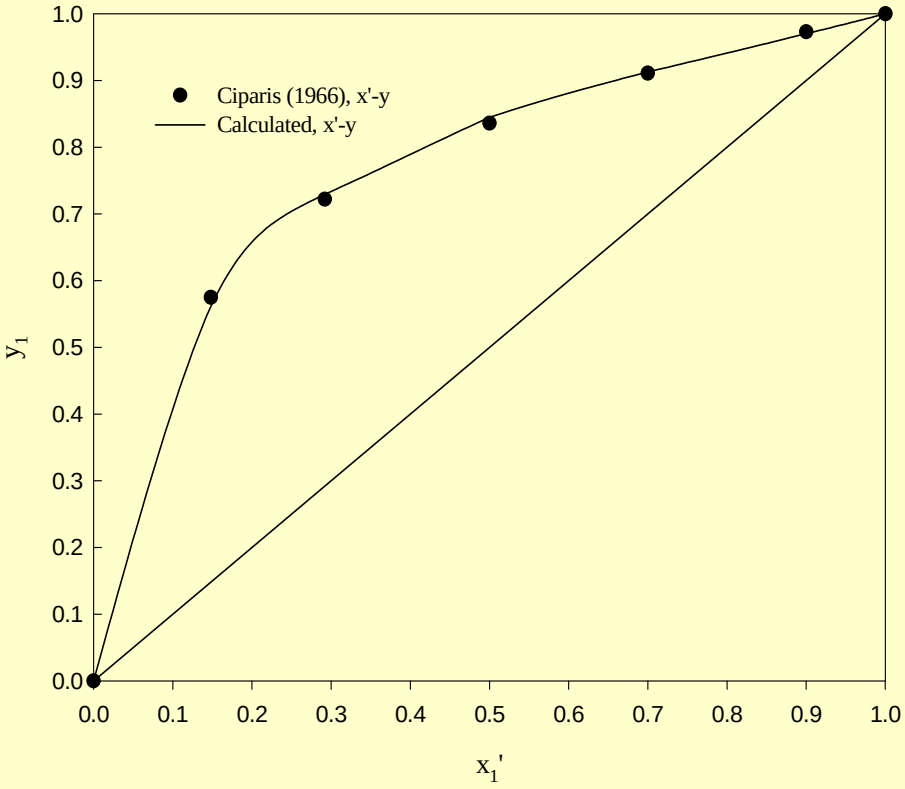

Fig.5-13 P-x'-y for MeOH(1)-H_2O(2)-NaBr(3) VLE at 298.15K. m(LiCl)=0.0 mol/kg.

Results : Isothermal VLE

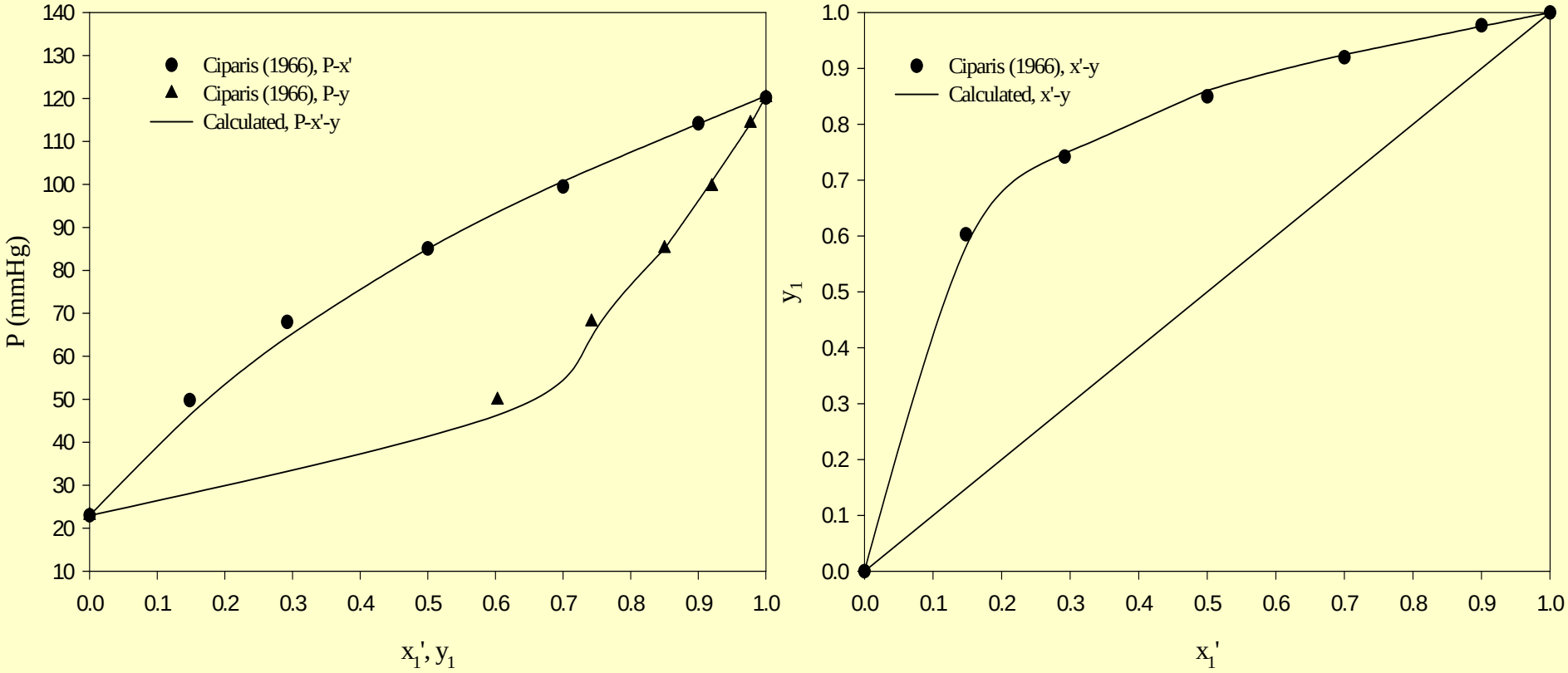

Fig.5-14 P-x'-y for MeOH(1)-H_2O(2)-NaBr(3) VLE at 298.15K.
m(LiCl)=1.0 mol/kg.

Results : Isothermal VLE

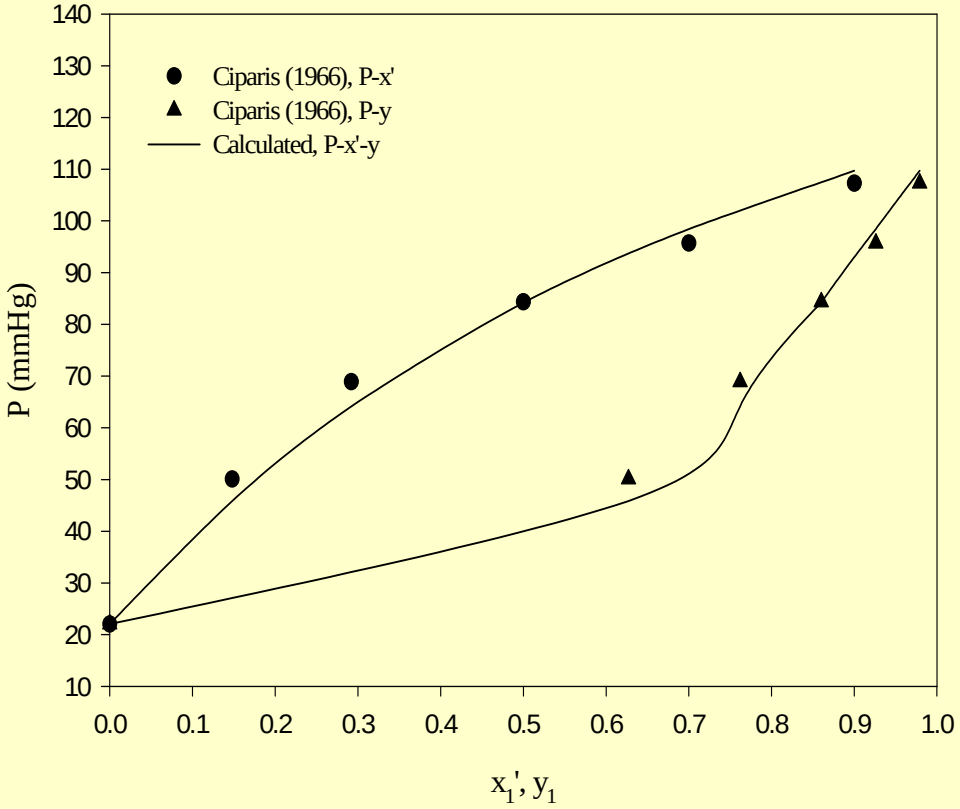

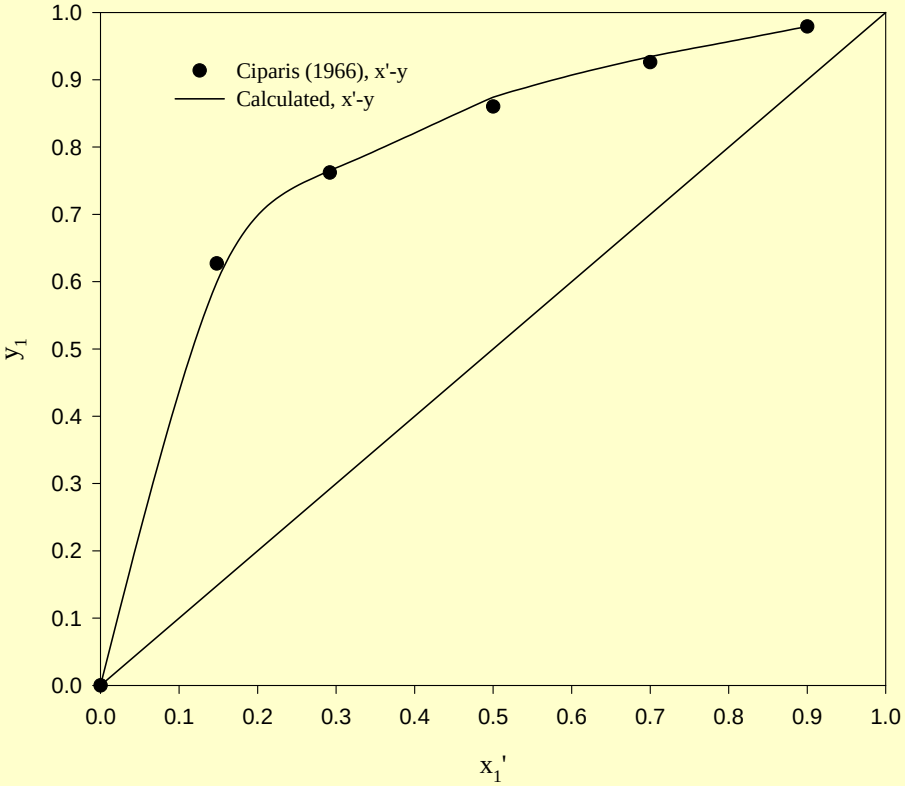

Fig.5-15 P-x'-y for MeOH(1)-H_2O(2)-NaBr(3) VLE at 298.15K.
m(LiCl)=2.0 mol/kg.

Results : Isothermal VLE

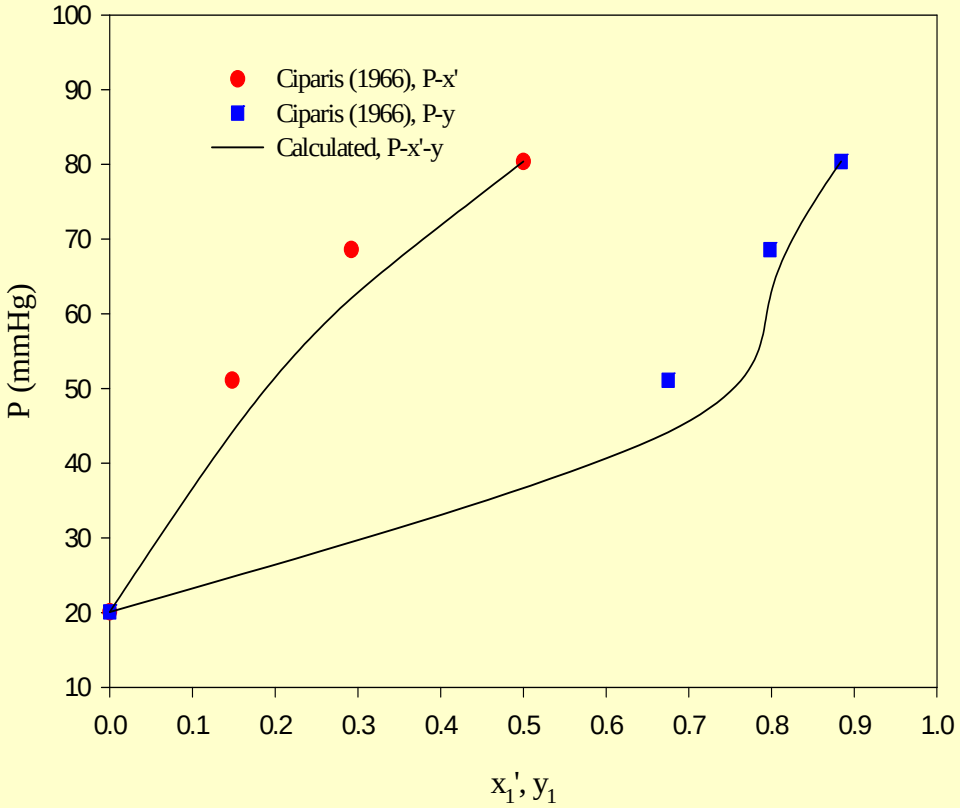

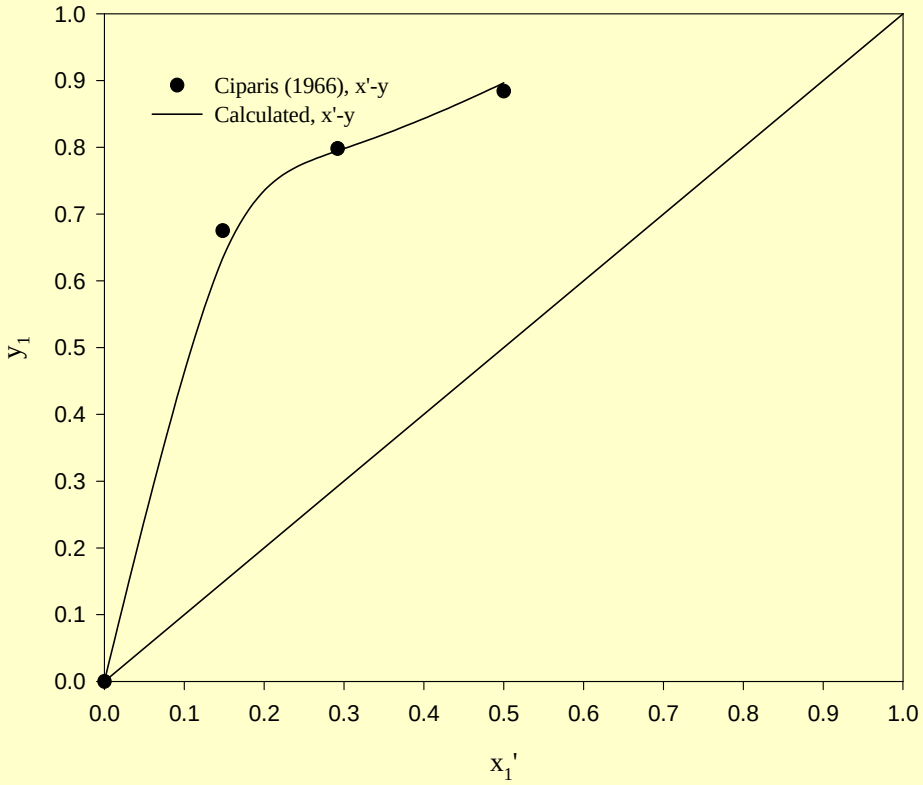

Fig.5-16 P-x'-y for MeOH(1)-H_2O(2)-NaBr(3) VLE at 298.15K.
m(LiCl)=4.0 mol/kg

Results : Isothermal VLE

Table 5-3. Comparison of RMS errors of Isothermal VLE for Ethanol(1)-Water(2)-Electrolyte(3) systems

		σ_y	σ_P/mmHg
$CaCl_2$		0.03	2.8
LiCl	(m=0.0)	0.01	0.8
	(m=0.5)	0.01	0.7
	(m=1.0)	0.01	0.3
	(m=4.0)	0.01	6.2
$MgSO_4$		0.02	1.4
Na_2SO_4		0.08	3.4
Average		0.02	2.2

Results : Isothermal VLE

Table 5-4. Comparison of RMS errors of Isothermal VLE for Methanol(1)-Water(2)-Electrolyte(3) systems

		σ_y	σ_P/mmHg
$CaCl_2$		0.01	3.7
LiCl		0.003	1.8
NaBr	(m=0.0)	0.005	1.0
	(m=1.0)	0.006	1.3
	(m=2.0)	0.009	2.4
	(m=4.0)	0.14	3.4
Average		0.03	2.3

Results : Isobaric VLE

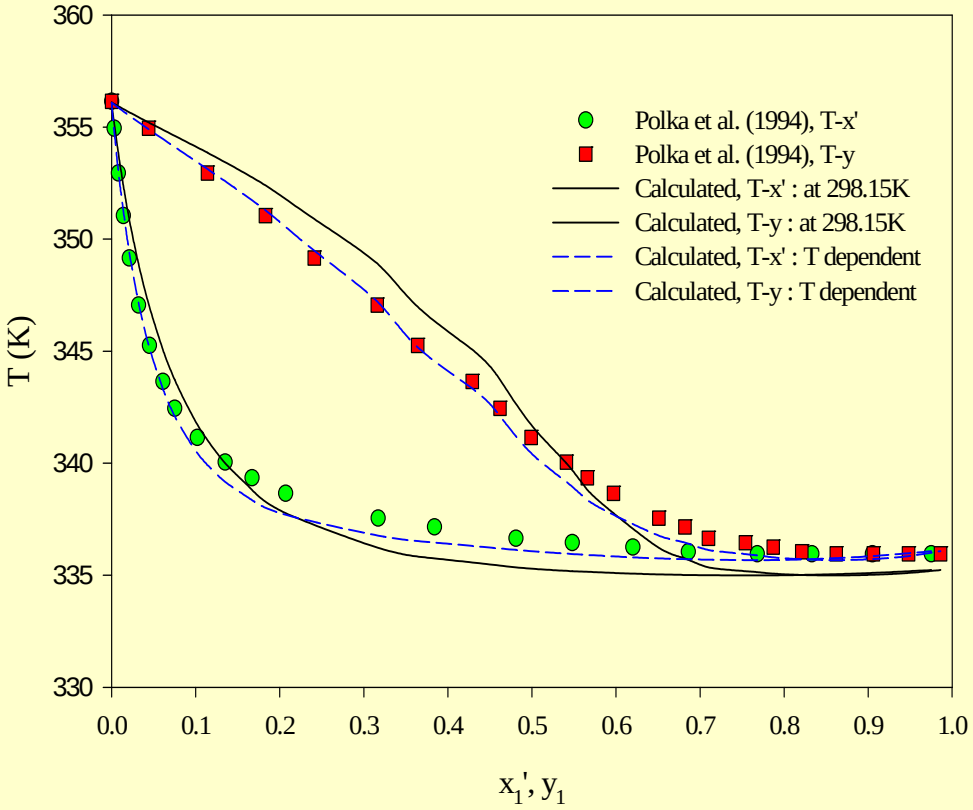

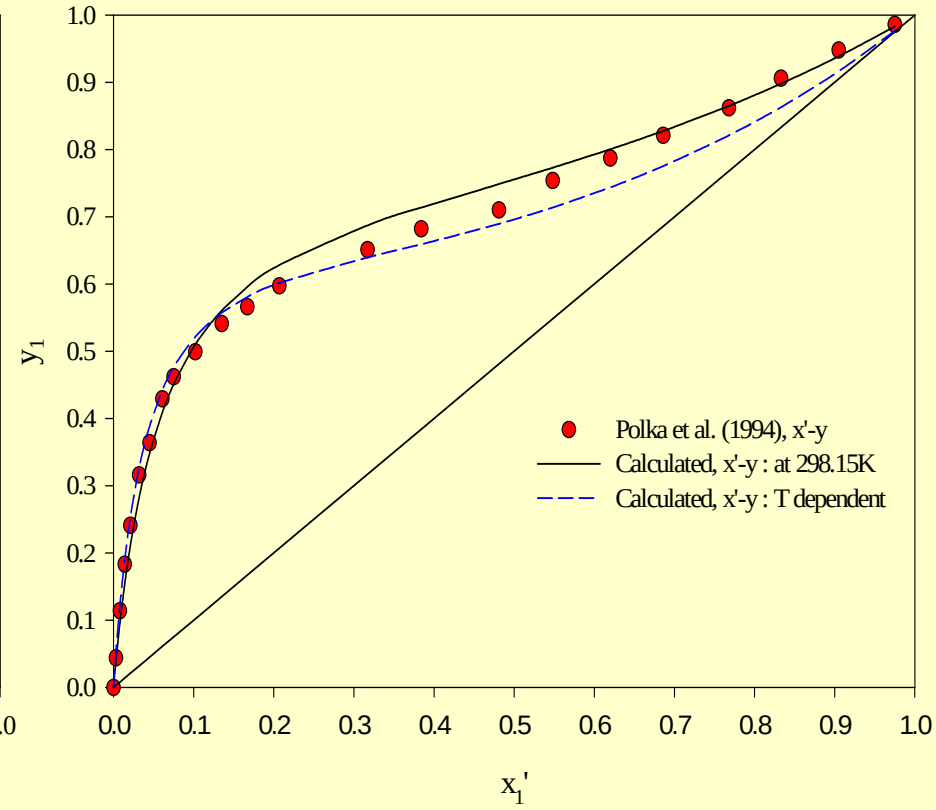

Fig.5-21 T-x'-y for EtOH(1)-H_2O(2)-$Ca(NO_3)_2$(3) VLE at 50.66kPa.
$m(Ca(NO_3)_2)$=1.038 mol/kg

Results : Isobaric VLE

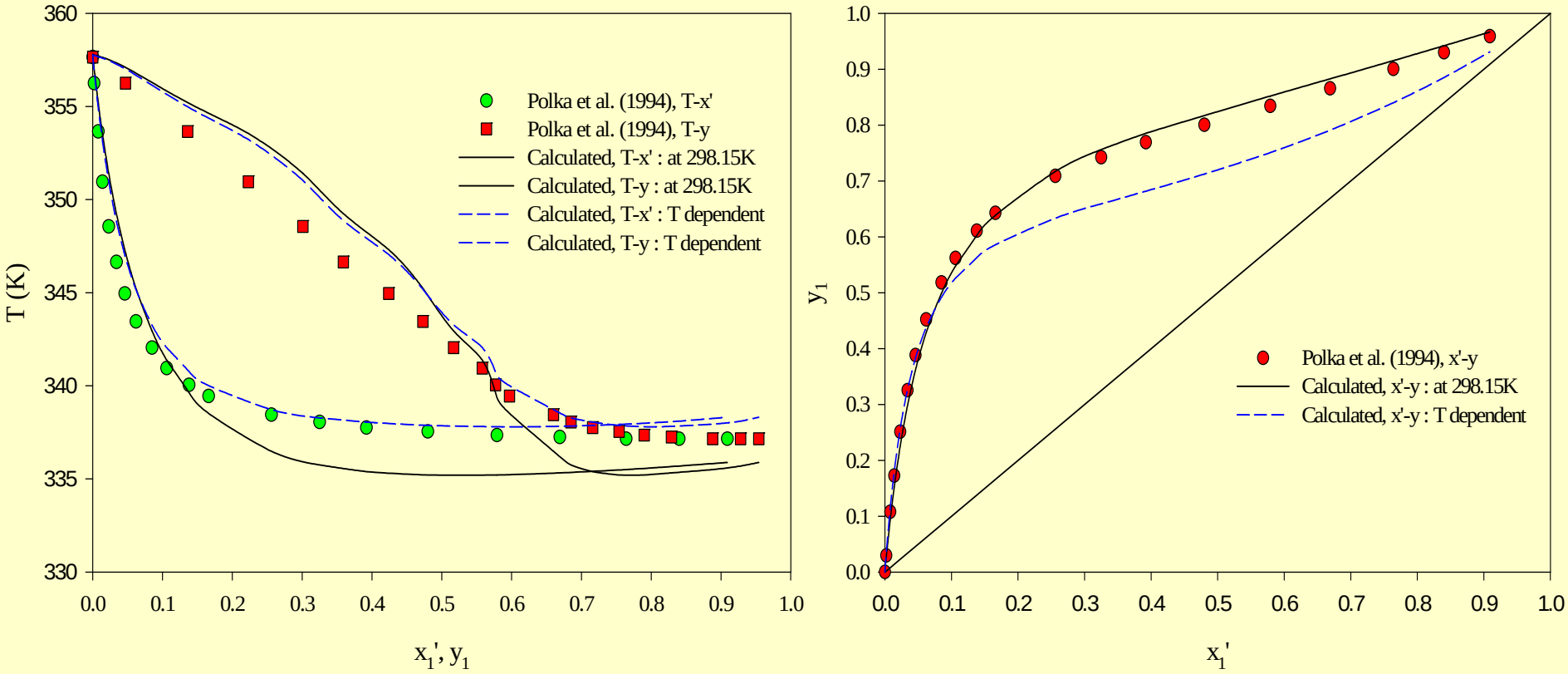

Fig.5-22 T-x'-y for EtOH(1)-H_2O(2)-$Ca(NO_3)_2$(3) VLE at 50.66kPa.
m($Ca(NO_3)_2$)=2.049 mol/kg

Results : Isobaric VLE

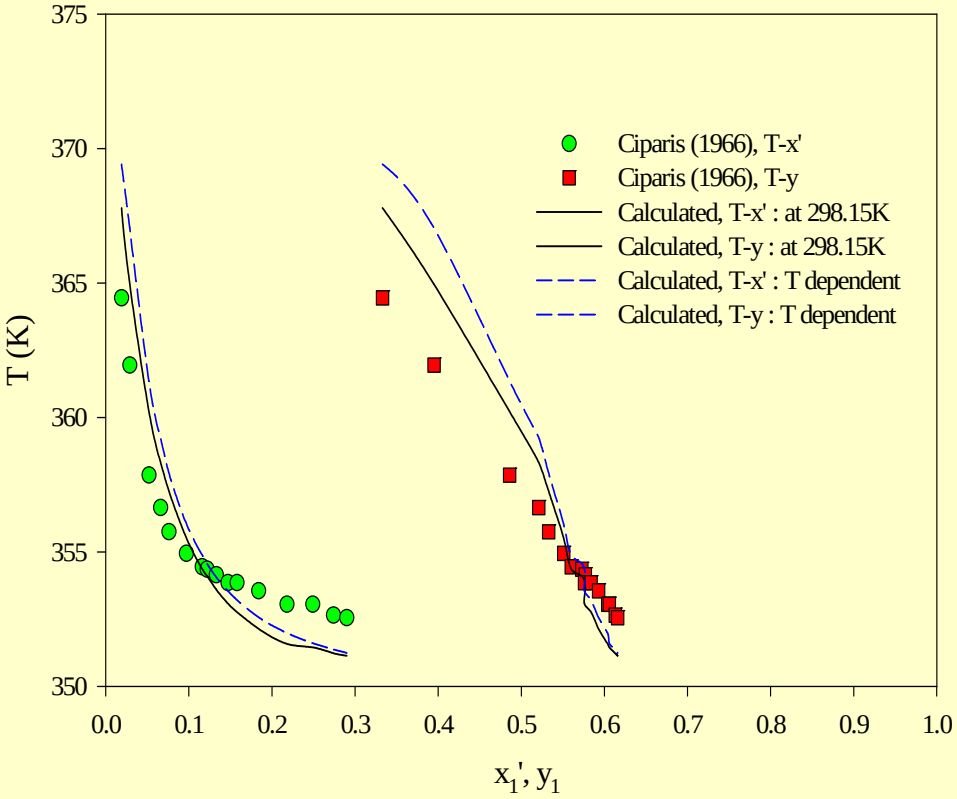

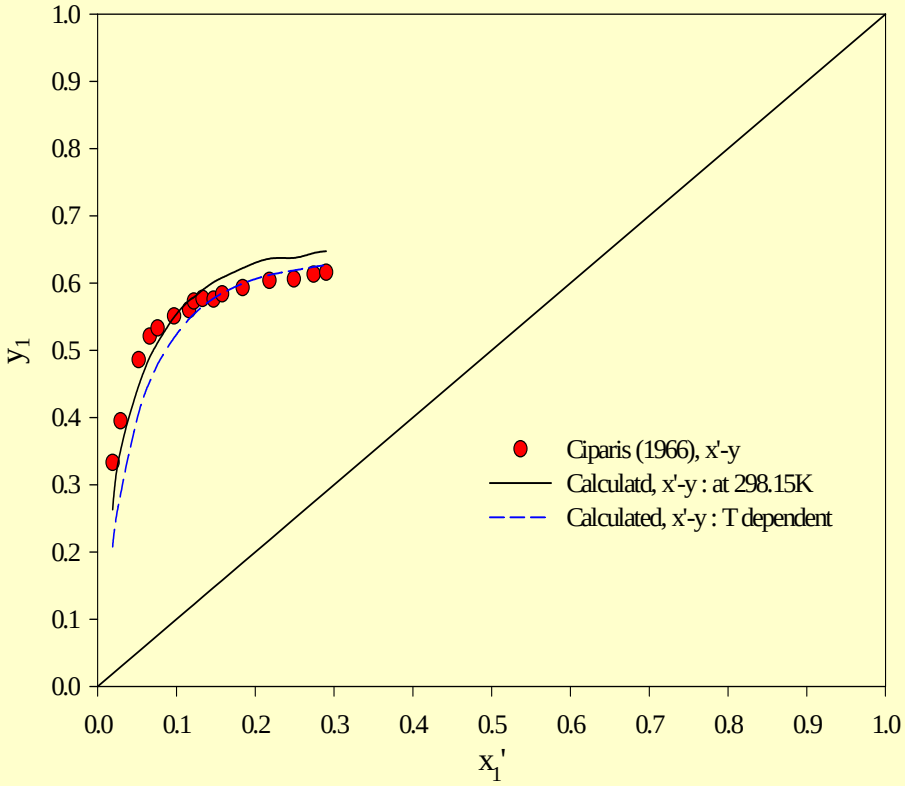

Fig.5-17 EtOH(1)-H_2O(2)-$BaCl_2$(3) VLE at 700mmHg.

Results : Isobaric VLE

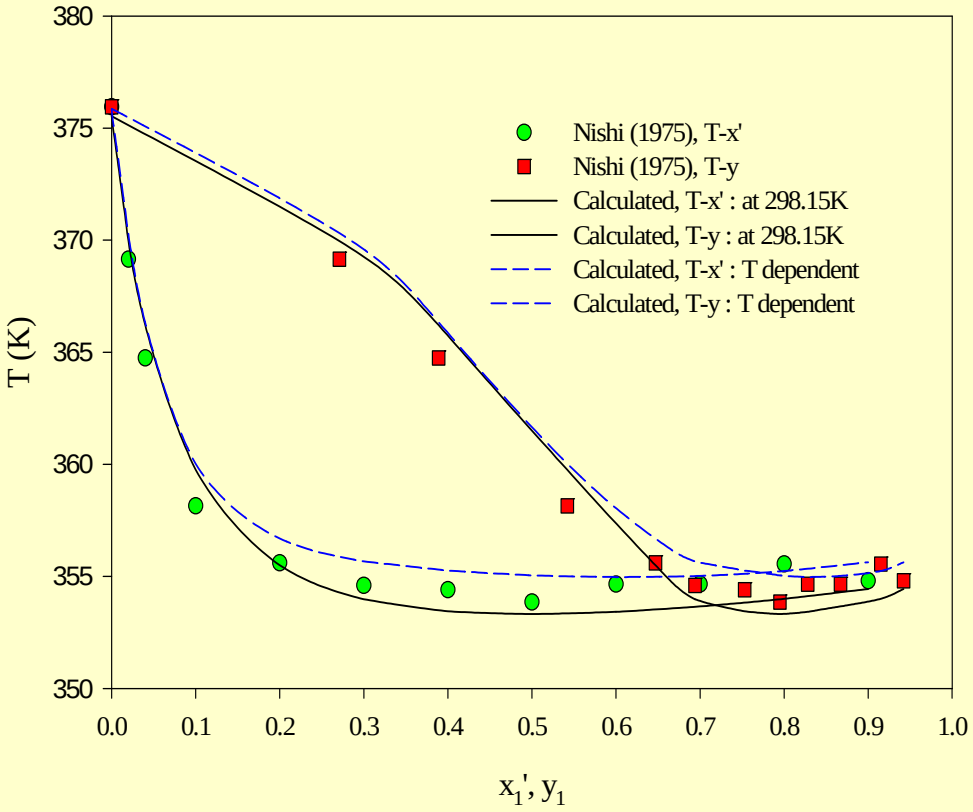

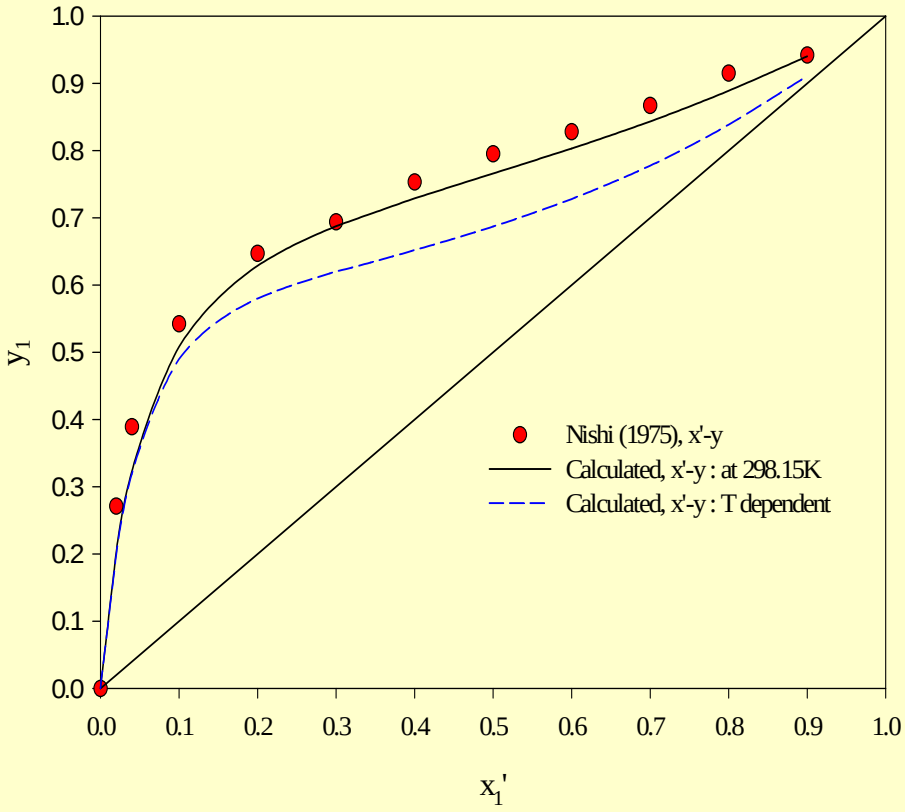

Fig.5-18 T-x'-y for EtOH(1)-H_2O(2)-$CaCl_2$(3) VLE at 1 atm.
m($CaCl_2$)=1.505 mol/kg

Results : Isobaric VLE

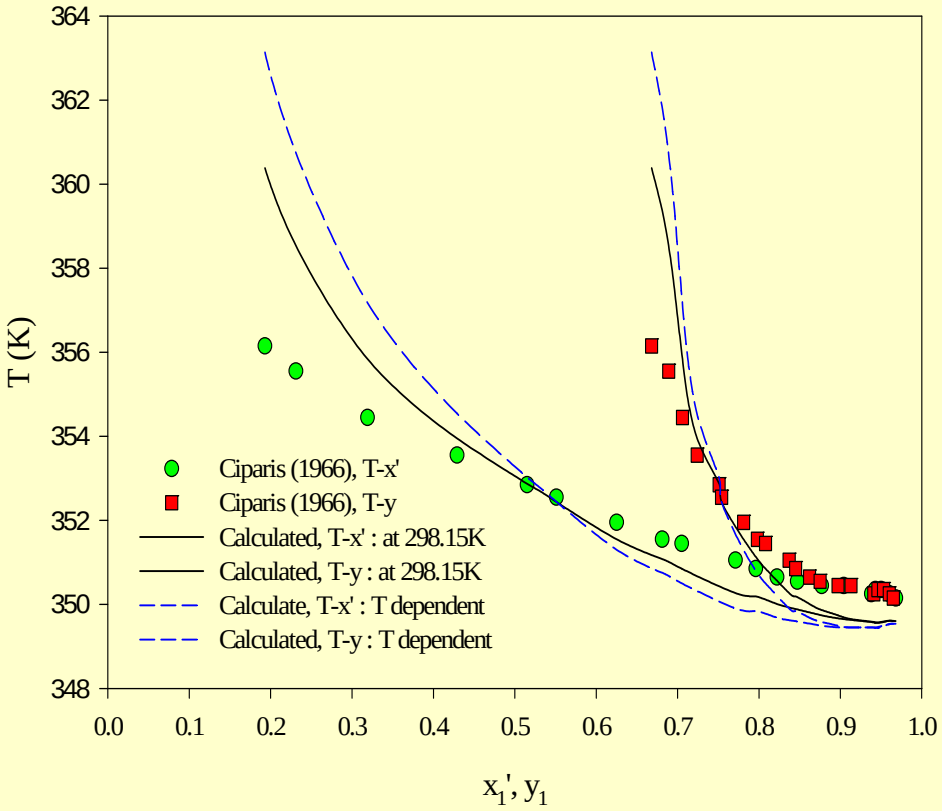

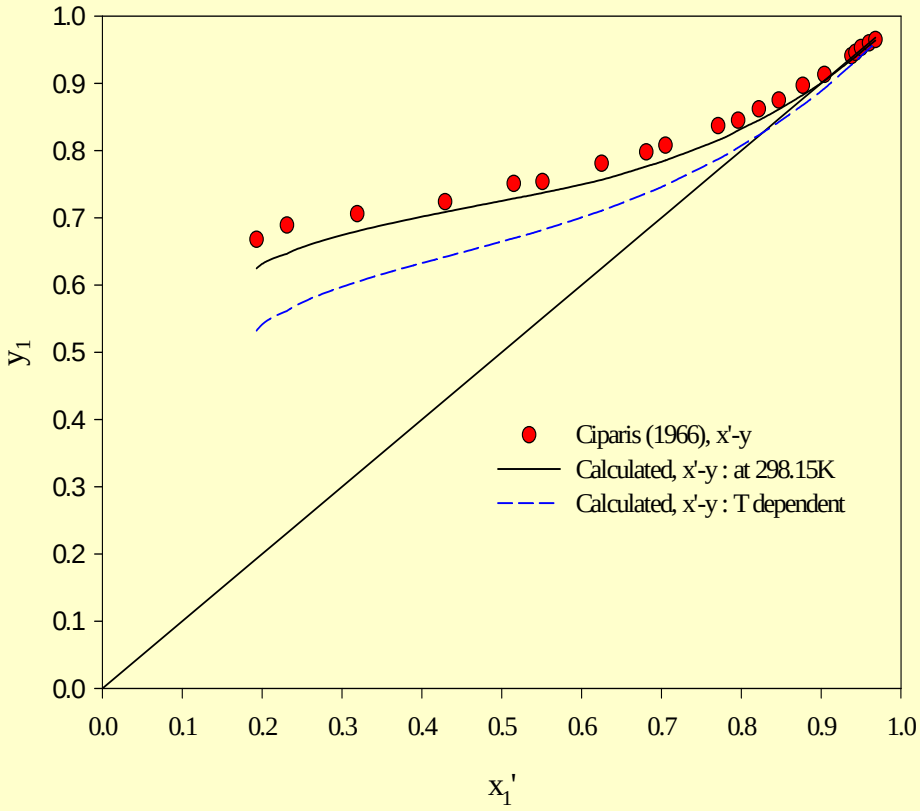

Fig.5-19 T-x'-y for EtOH(1)-H_2O(2)-KI(3) VLE at 700mmHg.

Results : Isobaric VLE

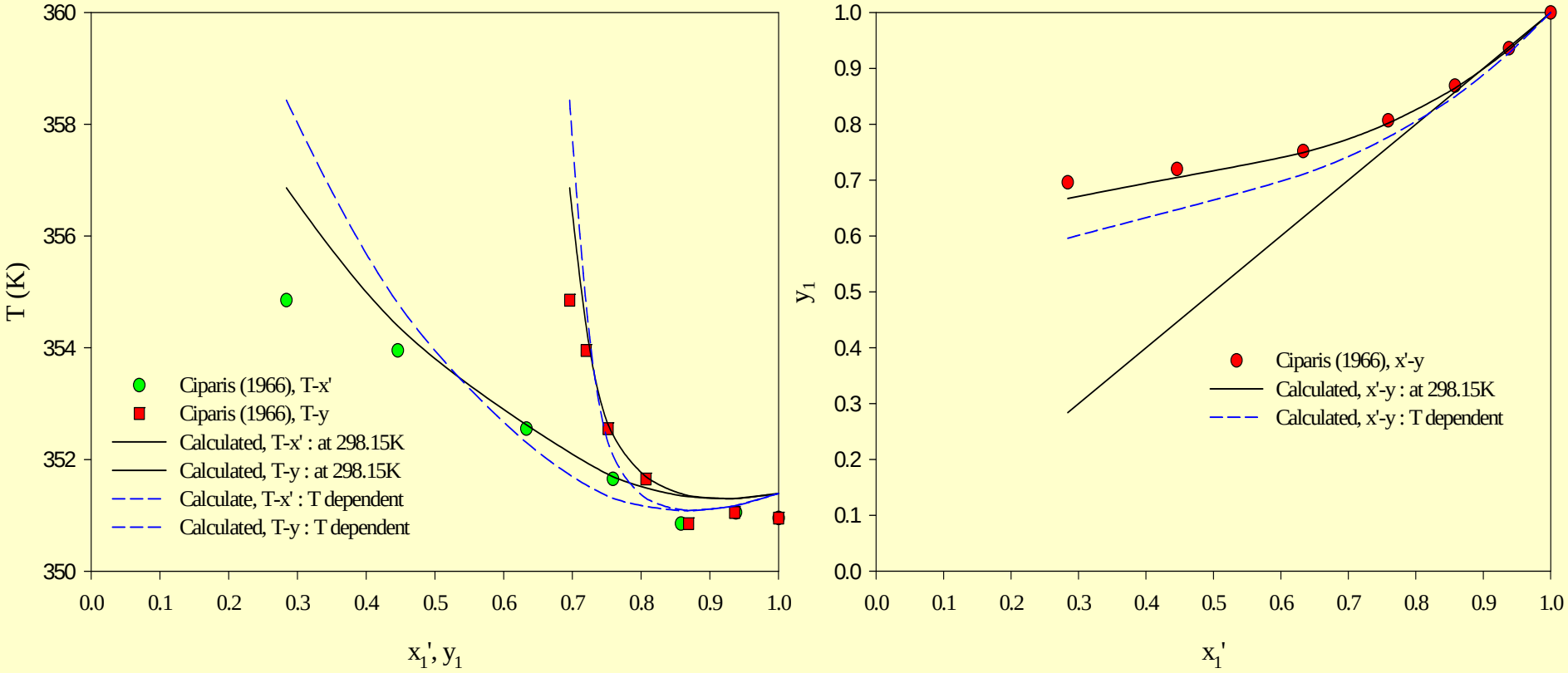

Fig.5-20 T-x'-y for EtOH(1)-H_2O(2)-NH_4Cl(3) VLE at 754mmHg.

Results : Isobaric VLE

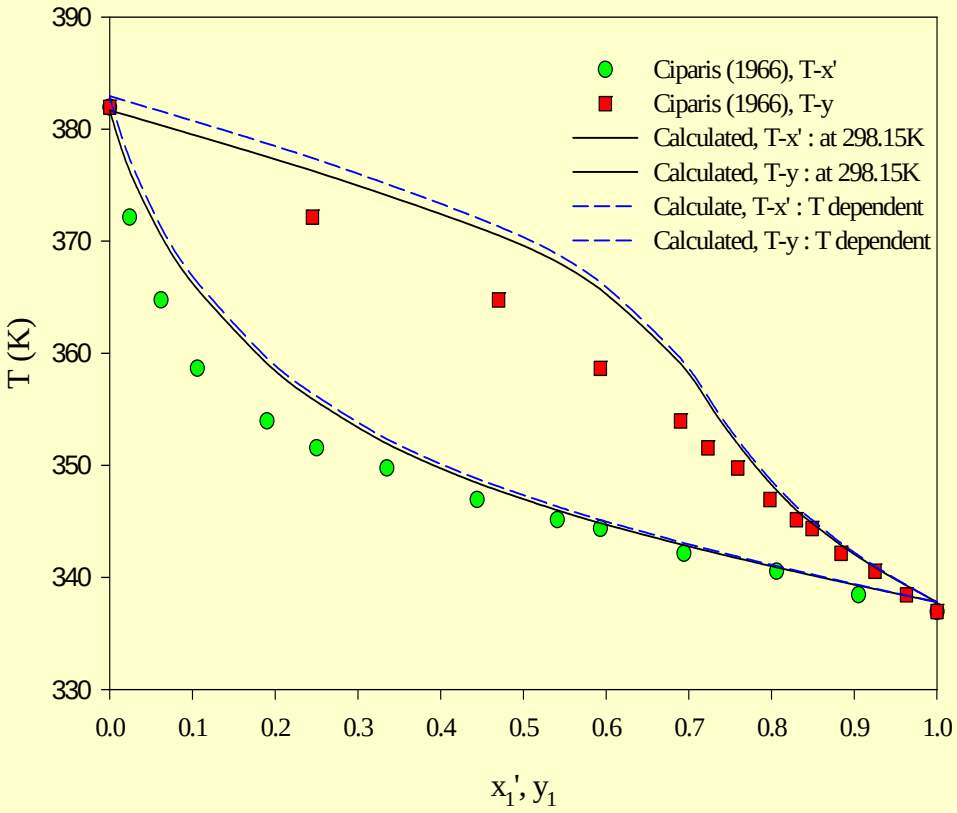

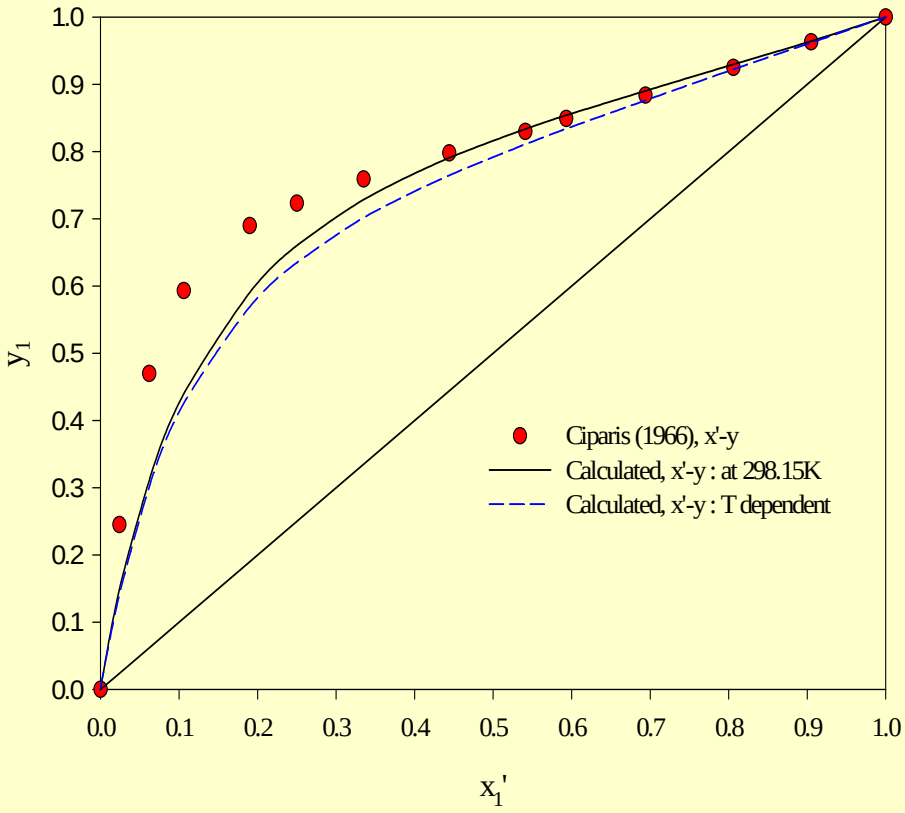

Fig.5-23 T-x'-y for MeOH(1)-H_2O(2)-KCl(3) VLE at 760mmHg.

Results : Isobaric VLE

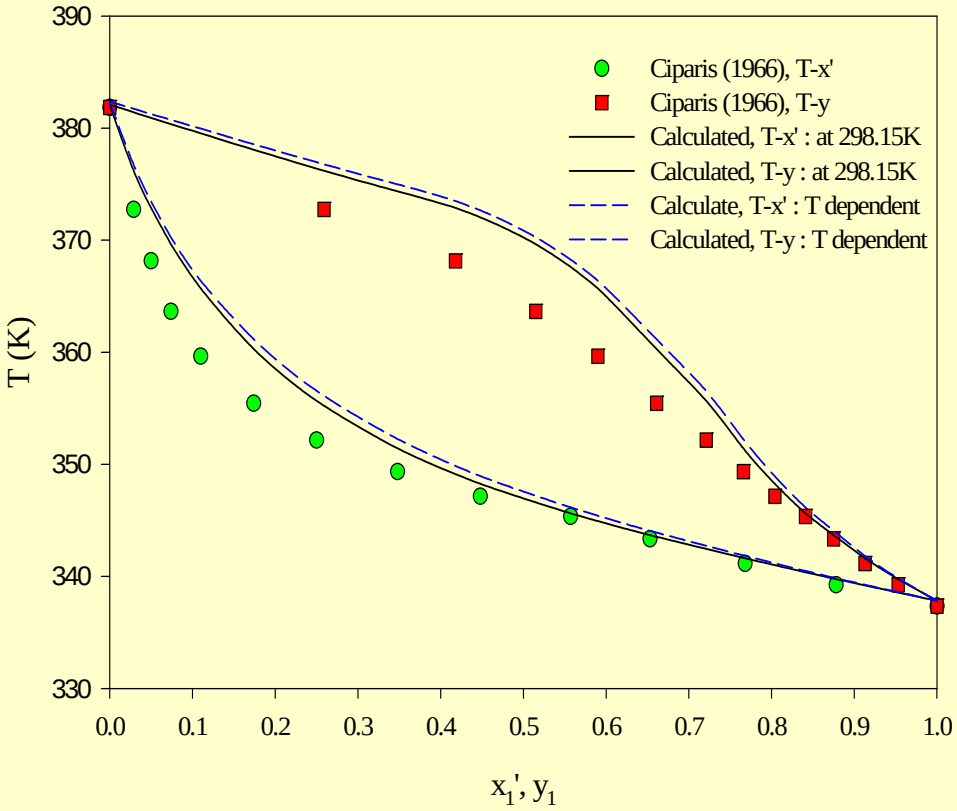

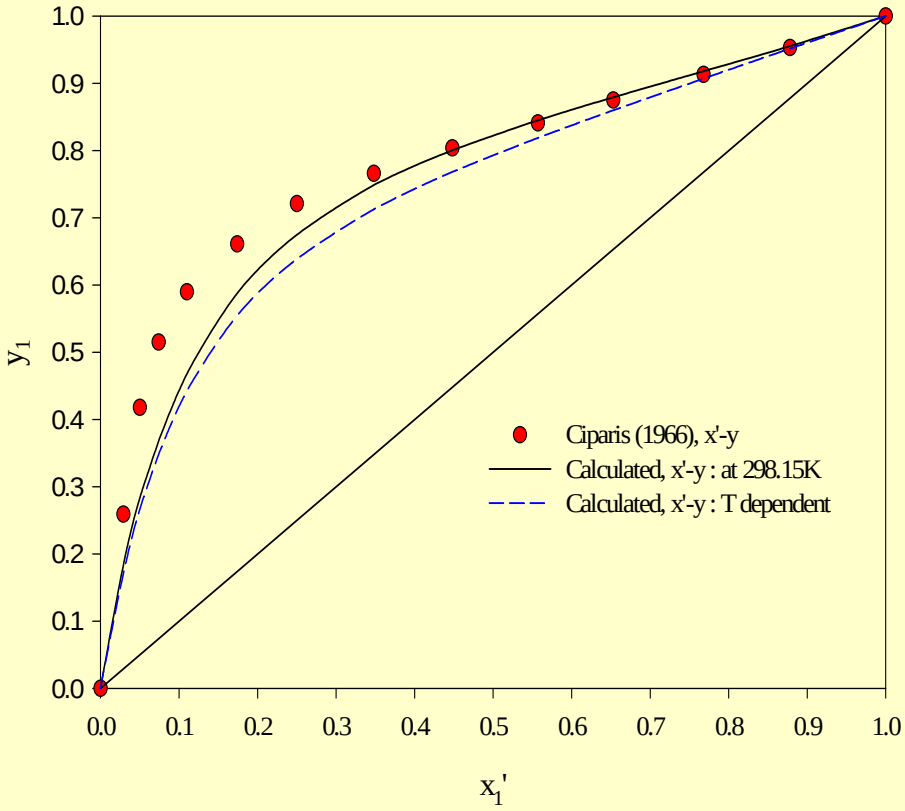

Fig.5-24 T-x'-y for MeOH(1)-H_2O(2)-NaCl(3) VLE at 762mmHg.

Results : Isobaric VLE

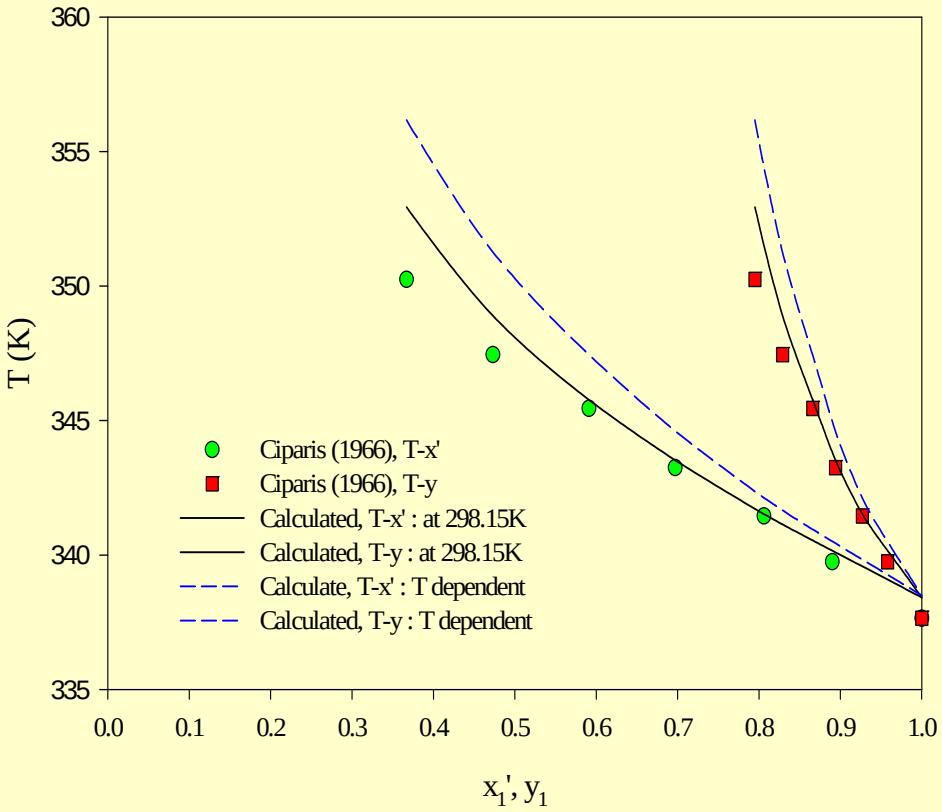

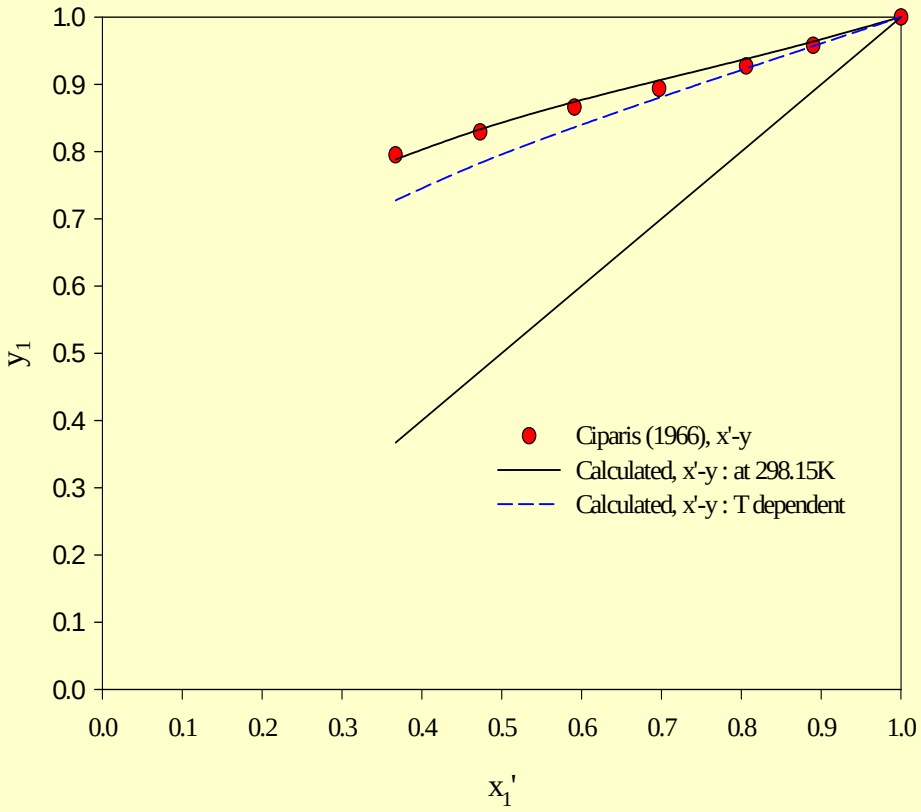

Fig.5-25 T-x'-y for MeOH(1)-H_2O(2)-NH_4Cl(3) VLE at 755mmHg.

Results : Isobaric VLE

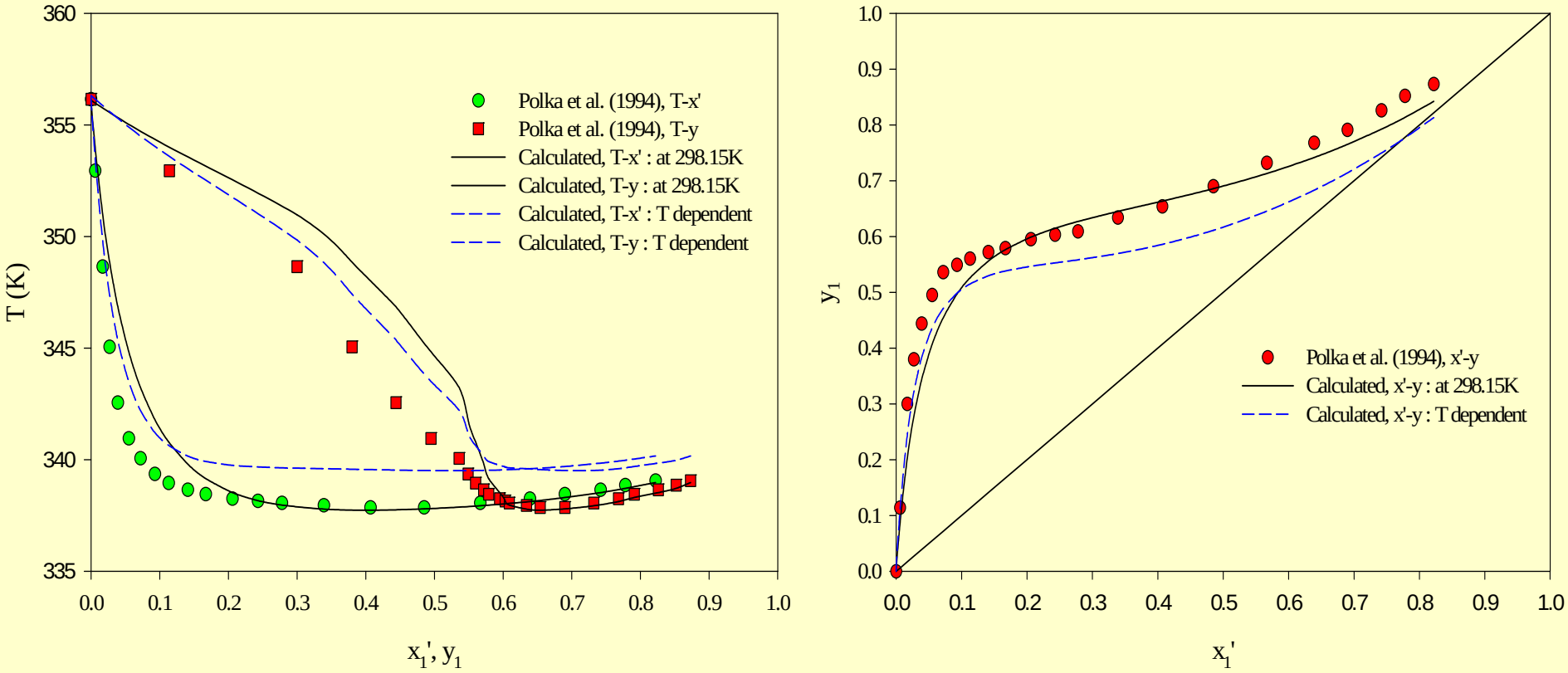

Fig.5-26 T-x'-y for Pr-2-OH(1)-H_2O(2)-$Ca(NO_3)_2$(3) VLE at 50.66kPa.
m($Ca(NO_3)_2$)=1.038 mol/kg

Results : Isobaric VLE

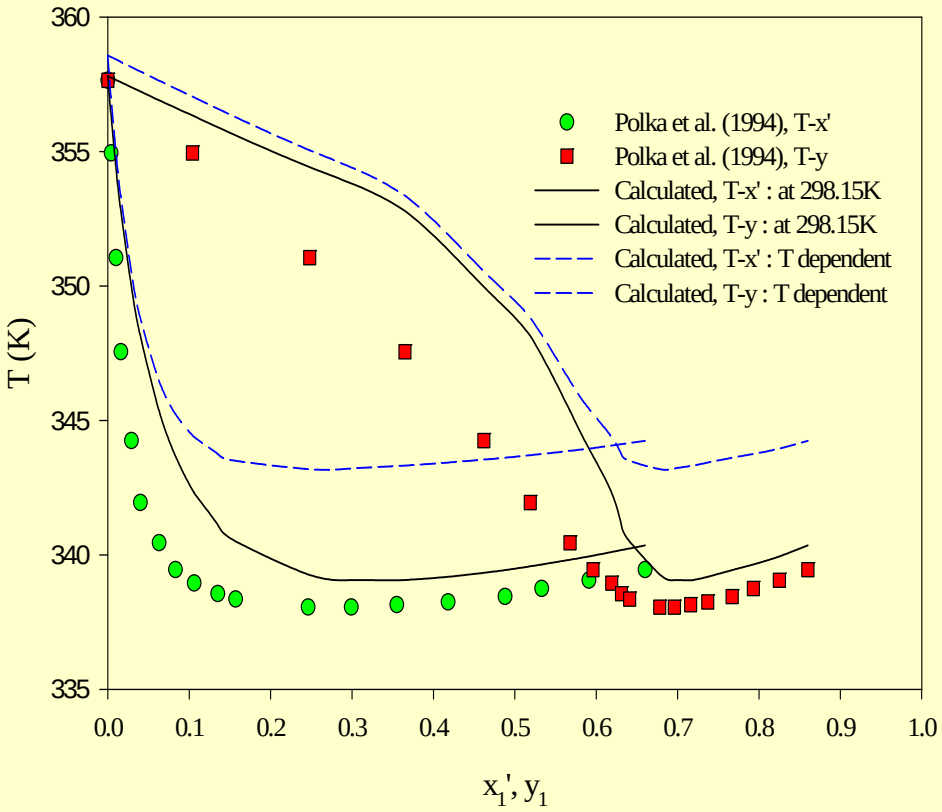

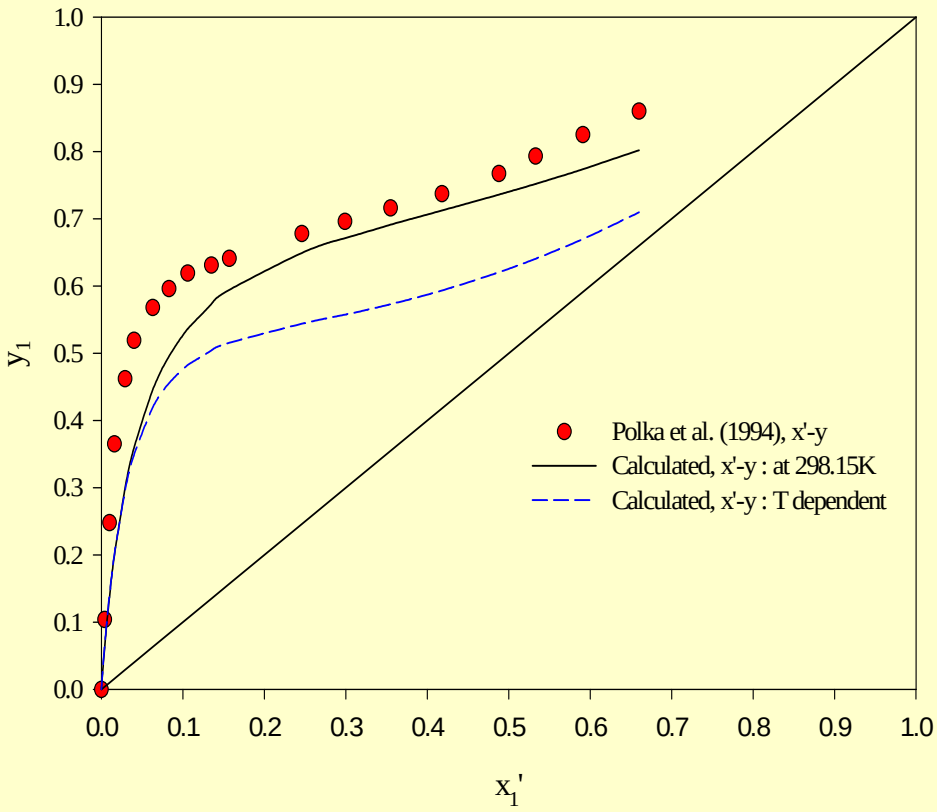

Fig.5-27 T-x'-y for Pr-2-OH(1)-H_2O(2)-$Ca(NO_3)_2$(3) VLE at 50.66kPa.
m($Ca(NO_3)_2$)=2.073 mol/kg

Results : Isobaric VLE

Table 5-5. Comparison of RMS errors of Isobaric VLE for Ethanol(1)-Water(2)-Electrolyte(3) systems

	Fixed		T dependent	
	σ_y	σ_T/K	σ_y	σ_T/K
BaCl2	0.07	1.9	0.06	1.9
$CaCl_2$	0.03	0.9	0.07	0.9
$Ca(NO_3)_2$ (m=1.308)	0.02	1.0	0.02	0.4
$Ca(NO_3)_2$ (m=2.049)	0.03	1.7	0.03	1.0
KCl (1)	0.06	2.5	0.07	2.6
KCl (2)	0.07	3.4	0.08	3.4
KI	0.02	0.9	0.05	1.4
KNO_3	0.14	5.9	0.16	5.5
NaCl (1)	0.06	2.7	0.08	3.1
NaCl (2)	0.06	2.9	0.08	3.4
NaI	0.02	0.5	0.06	0.6
$NaNO_3$	0.04	1.3	0.05	1.6
NH_4Cl	0.008	0.5	0.04	0.8
$SrBr_2$	0.02	0.8	0.05	0.8
$SrCl_2$	0.03	1.3	0.06	1.6
$Sr(NO_3)_2$	0.05	1.6	0.03	1.2
Average	0.04	1.9	0.06	1.9

Results : Isobaric VLE

Table 5-6. Comparison of RMS errors of Isobaric VLE for Methanol(1)-Water(2)-Electrolyte(3) systems

	Fixed		T dependent	
	σ_y	σ_T/K	σ_y	σ_T/K
KCl	0.05	2.7	0.06	3.1
NaCl	0.05	2.6	0.07	3.1
NH_4Cl	0.01	1.1	0.02	2.4
Average	0.04	2.1	0.05	2.9

Results : Isobaric VLE

Table 5-7. Comparison of RMS errors of Isobaric VLE for 1-Propanol(1)-Water(2)-Electrolyte(3) systems

	Fixed		T dependent	
	σ_y	σ_T/K	σ_y	σ_T/K
(x3=0.02)	0.03	0.8	0.07	1.3
(x3=0.04)	0.03	0.8	0.11	2.5
$Ca(NO_3)_2$ (x3=0.06)	0.02	0.3	0.08	1.8
(x3=0.08)	0.02	0.3	0.06	2.3
(x3=0.10)	0.01	0.5	0.01	1.2
KBr	0.03	2.3	0.10	4.4
KCl	0.03	0.9	0.07	2.2
NaBr	0.06	2.4	0.15	5.1
NaCl (1)	0.02	1.0	0.06	2.7
NaCl (2)	0.03	1.9	0.09	4.0
Average	0.03	1.1	0.08	2.8

Results : Isobaric VLE

Table 5-9. Comparison of RMS errors of Isobaric VLE for 2-Propanol(1)-Water(2)-Electrolyte(3) systems

	Fixed		T dependent	
	σ_y	σ_T/K	σ_y	σ_T/K
$Ca(NO_3)_2$ (m=1.308)	0.04	1.1	0.06	1.5
$Ca(NO_3)_2$ (m=2.073)	0.07	2.5	0.13	4.9
LiBr (1)	0.04	2.2	0.09	3.6
LiCl (2)	0.04	1.6	0.09	2.9
Average	0.05	1.9	0.09	3.2

Electrolyte Solution Based on Solvation

Previous Models

- G^E Model
  - Debye-Hückel (1923), Bromley (1973), Pitzer (1973)

    Meissner & Tester (1972), Chen et al. (1982)
- Primitive Model
  - Waisman et al. (1972), Blum (1975), Harvey et al. (1989), Taghikhani et al. (2000)
- Nonprimitive Model
  - Planche et al. (1981), Ball et al. (1985),

    Fürst et al. (1993), Zuo et al. (1998)
- Acceptable accuracy up to $\varepsilon = 6.0$ or less

Hydration Theory

G^E model

- **Ghosh and Patwardhan (1990)**
  - Based on lithium chrolide as a reference electrolyte
  - Hydration energy, function of the total moles of water hydrated per kg of solution
    - Fitted with expreimental ϕ, γ
  - Up to I=24 for 150 electrolyte solutions
- **Schoenert (1990, 1991,1993, 1994)**
  - Modified hydration model of Robinson and Stokes
  - Hydration of ions : ligand-binding equlibria
    - Transfer of water to the hydration spheres of ions
  - Up to m=1 for HCl,LiCl,NaCl,KCl,CsCl,NH_4Cl,NaBr

Hydration Model

SAFT Approach

- **Gil-Villegas et al. (2001)**
  - Ionic contribution : MSA
  - Monomer : perturbation expansion
  - Associaton : Solvent-solvent, solvent-ion, ion-ion pairing
  - Applied to the NaCl solution up to 10 m
- **Paricaud et al. (2001)**
  - Applied to the NaOH solution up to 22 m

In present work

- Solvation contribution from the Veytsman statistics Explicitly added to Lee et al. model
- Application to LiCl, LiBr, LiI and $LiClO_4$ solutions

Excess Gibbs Function

- **Long-range + Physical + Solvation**

$$G^E = G^E_{DH} + G^E_A + G^E_R + G^E_{HB}$$

  - **In high pressure limit, holes are vanished**

$$A^E(T, P=\infty, x_i) = A^E(T, low\ P, x_i) = G^E(T, low\ P, x_i)$$

  - **Physical interaction : Athermal + Residual**

    From Lee et al. model (1996)

  - **Solvation interaction**

    From a normalized Veytsman statistics (Park et al.,2001)

Activity Coefficient

- **For solvent in symmetric convention**

$$\ln\gamma_j = \ln\gamma_{DH,j} + \ln\gamma_{A,j} + \ln\gamma_{R,j} + \ln\gamma_{HB,j}$$

- **For solute in asymmetric convention**

$$\ln\gamma_j^* = \ln\gamma_j - \lim_{x_i \to 0} \ln\gamma_j$$

$$\ln\gamma_{\pm i}^* = \ln\gamma_{DH,\pm i}^* + \ln\gamma_{A,\pm i}^* + \ln\gamma_{R,\pm i}^* + \ln\gamma_{HB,\pm i}^*$$

Solvation Contribution

- **For solvent,**

$$\ln\gamma_{HB,k} = -\sum_{i}^{m} d_k^i \ln\frac{N_{i0}^k N_{i0}^0}{N_{i0} N_{i0}^{k,0}} - \sum_{j}^{n} a_k^j \ln\frac{N_{0j}^k N_{0j}^0}{N_{0j} N_{0j}^{k,0}}$$

- **For solute,**

$$\ln\gamma_{HB,\pm k}^{*} = -\frac{\nu_{+k}}{\nu_{\pm k}} \sum_{i}^{m} d_k^i \ln\frac{N_{i0}^0 N_{i0}^{\infty}}{N_{i0} N_{i0}^{0,\infty}} - \frac{\nu_{-k}}{\nu_{\pm k}} \sum_{j}^{n} a_k^j \ln\frac{N_{0j}^0 N_{0j}^{\infty}}{N_{0j} N_{0j}^{0,\infty}}$$

$$N_{i0}^{HB} = N_d^i - \sum_{j}^{n} N_{ij}^{HB}, \qquad N_{0j}^{HB} = N_a^j - \sum_{i}^{m} N_{ij}^{HB}$$

  - N_{ij}^{HB} **: the number of proton donor-acceptor pair for hydrogen bonding**

$$N_{ij}^{HB} N_r = \left(N_d^i - \sum_{j=1}^{n} N_{ij}^{HB} \right) \left(N_a^j - \sum_{i}^{m} N_{ij}^{HB} \right) \exp\left(-\beta A_{ij}^{HB}\right)$$

  - N_{ij}^{0} **with** $A_{ij}^{HB} = 0$

Parameters

- **For physical interaction**
  - **Size parameter of each ion and water, r_i**
  - **Energy parameters**

    Cation-water & anion-water, τ_{13}, τ_{23}, τ_{31}, τ_{32}
- **For solvation**
  - **Solvation number**
    - **Cation : donor number, *d***
    - **Anion : acceptor number, *a***
    - **Water : donor & acceptor number (*d*=2, *a*=1)**
  - **Solvation energy**
    - **Cation-water & anion-water, A_{13}^{HB} , A_{32}^{HB}**

Parameter Determinations

- **Size parameter**
  - **Cation : from crystalline ionic volume**
  - **Water : from Lee et al. model (2.5)**
- **Solvation number**
  - **From coordination numbers in hydration shells of ions (Krestov et al., 1994)**
- **Solvation energy of water : from Luck(1980)**

  (-10.55 kJ/mol)
- **Data for solute activity coefficients**
  - **Size parameter of each anion**
  - **Energy parameters for physical interaction**
  - **Solvation numbers & solvatoin energy parameters of cation- & anion-water**

Results

Table 1. Parameters for Lithium ionic Electrolyte Systems

	r_i	τ_{13} (or τ_{23})	d_{ii} (or a_{ii})	$\boldsymbol{A_{13}}$ (or $\boldsymbol{A_{32}}$) / kJ mol^{-1}
Li^+	0.1229	0.156	6	-15.61
Cl^-	0.615	0.143	5	-4.75
Br^-	1.145	1.167	8	-4.70
I^-	1.756	1.350	8	-4.45
ClO_4^-	1.845	1.052	8	-3.85

Results

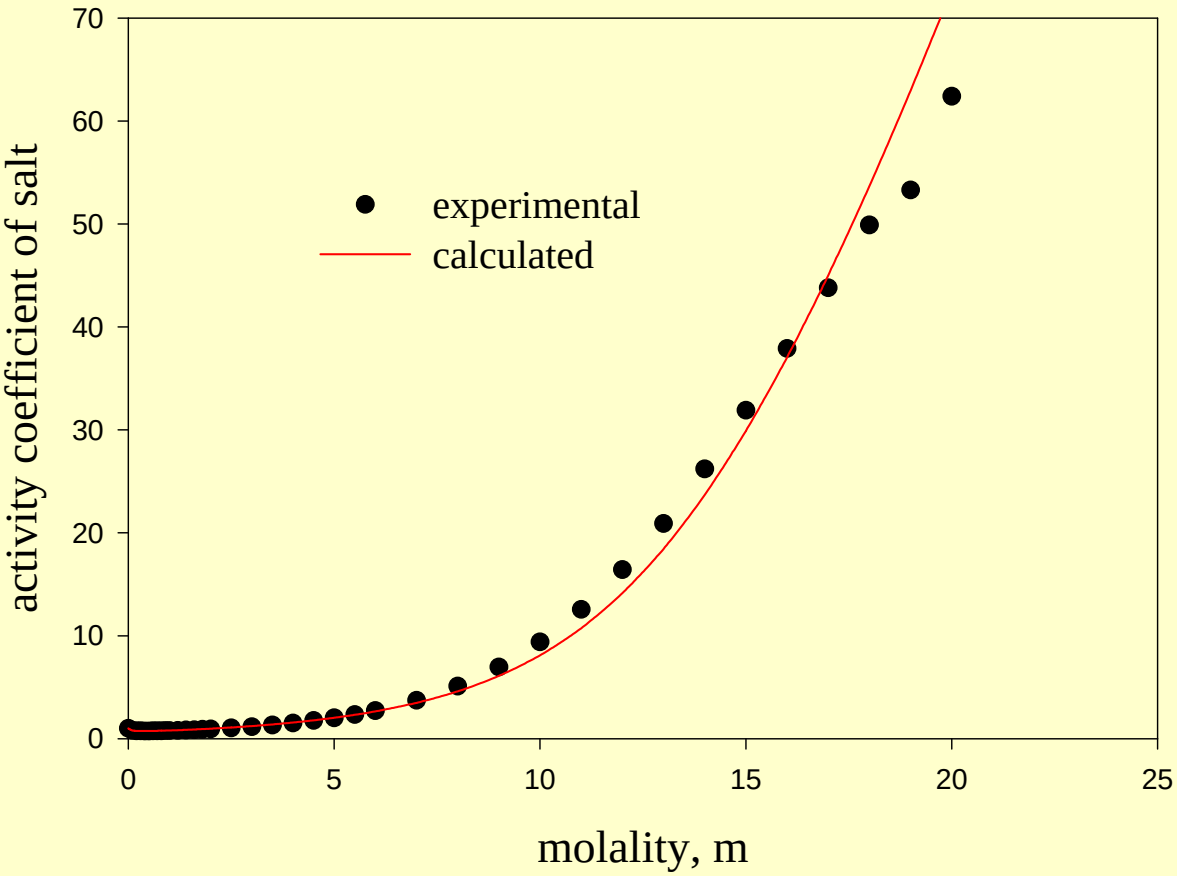

Fig.1 The activity coefficient of LiCl.

Results

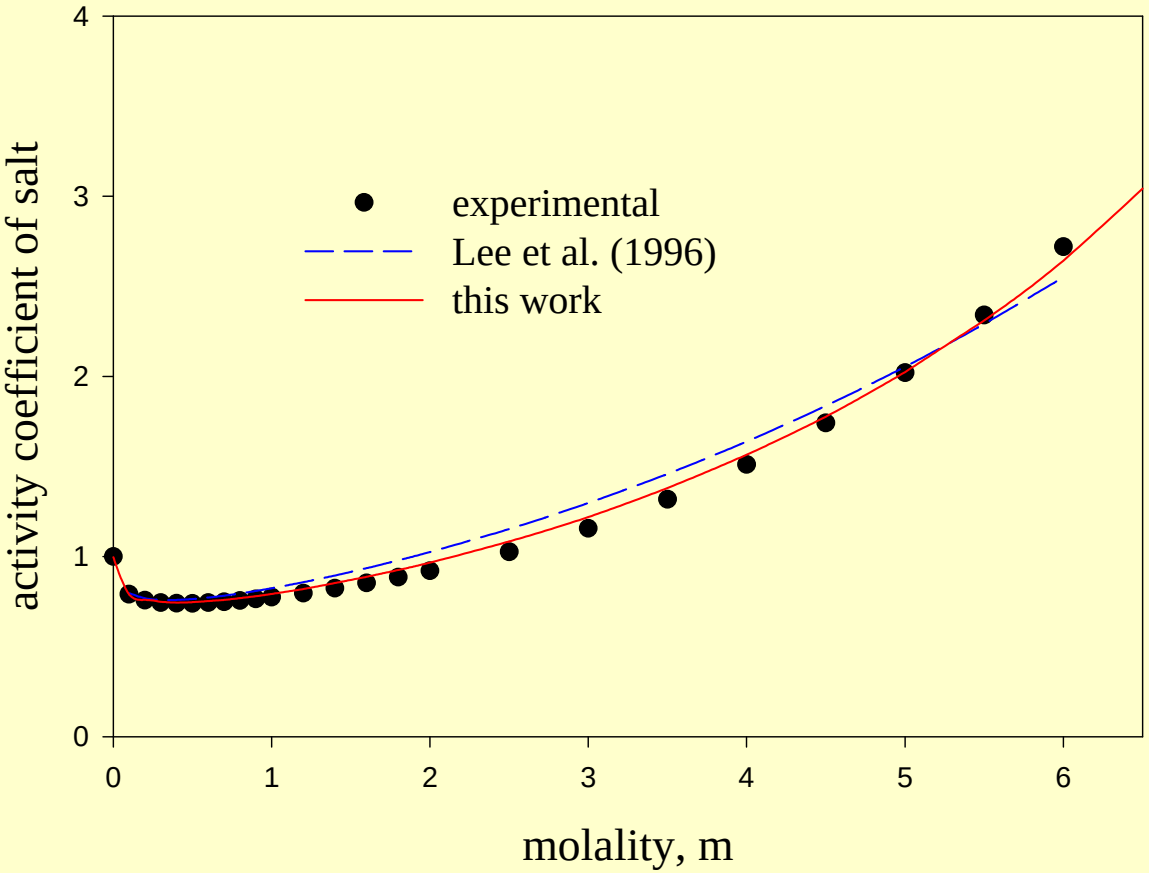

Fig.2 The activity coefficient of LiCl.

Results

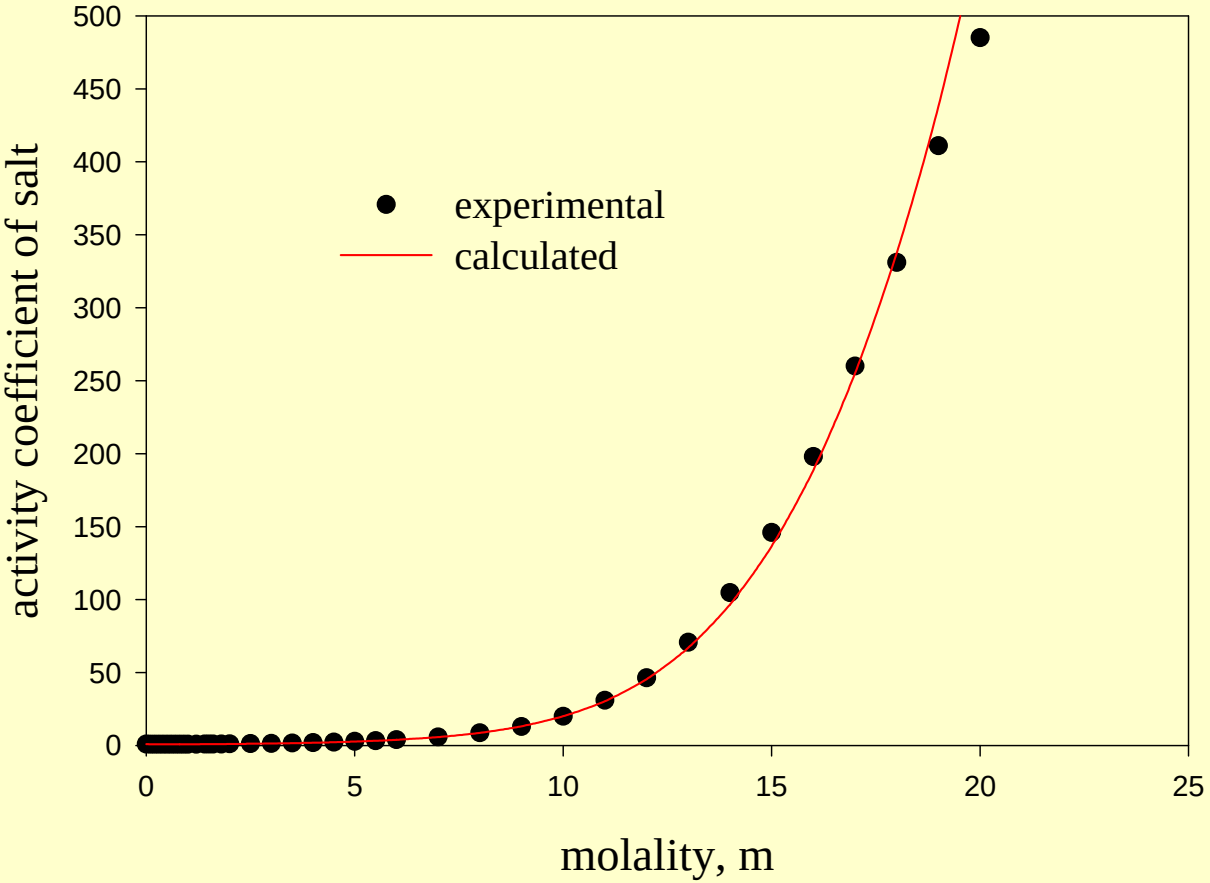

Fig.3 The activity coefficient of LiBr.

Results

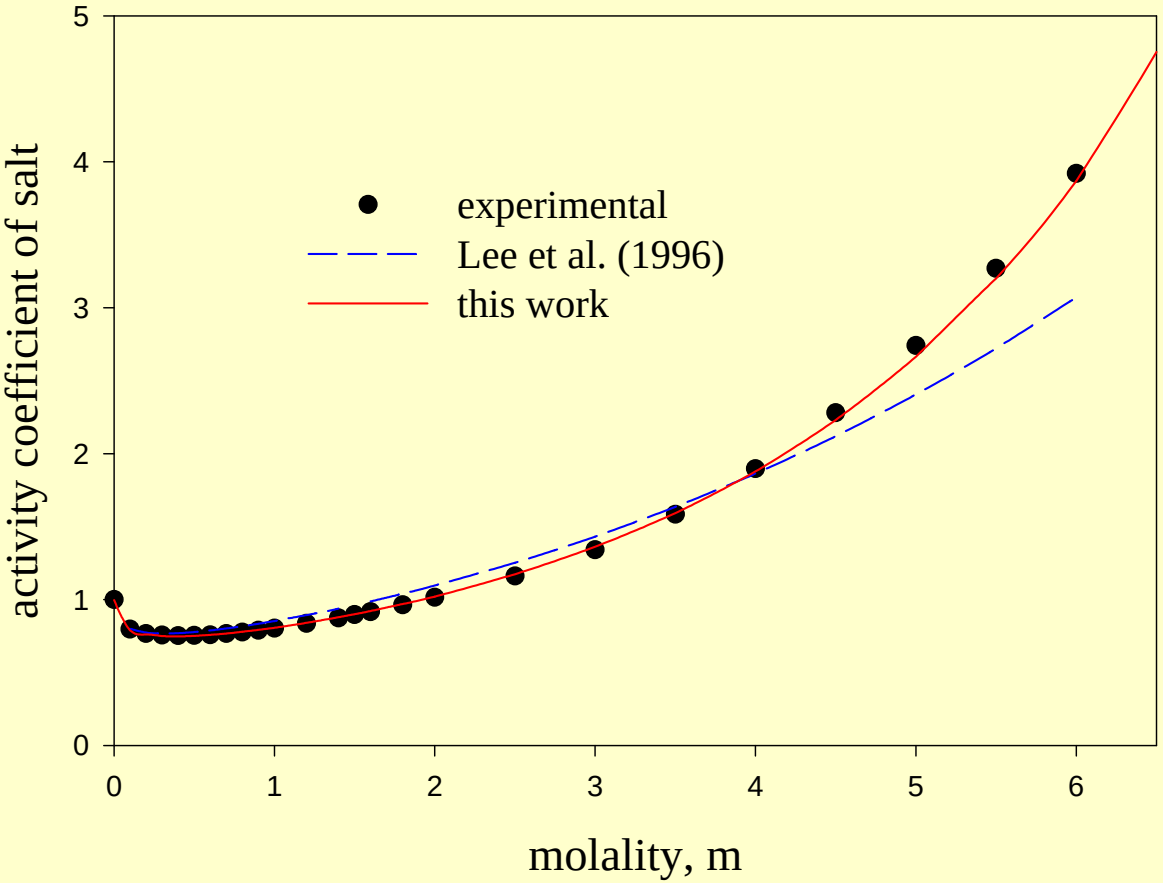

Fig.4 The activity coefficient of LiBr.

Results

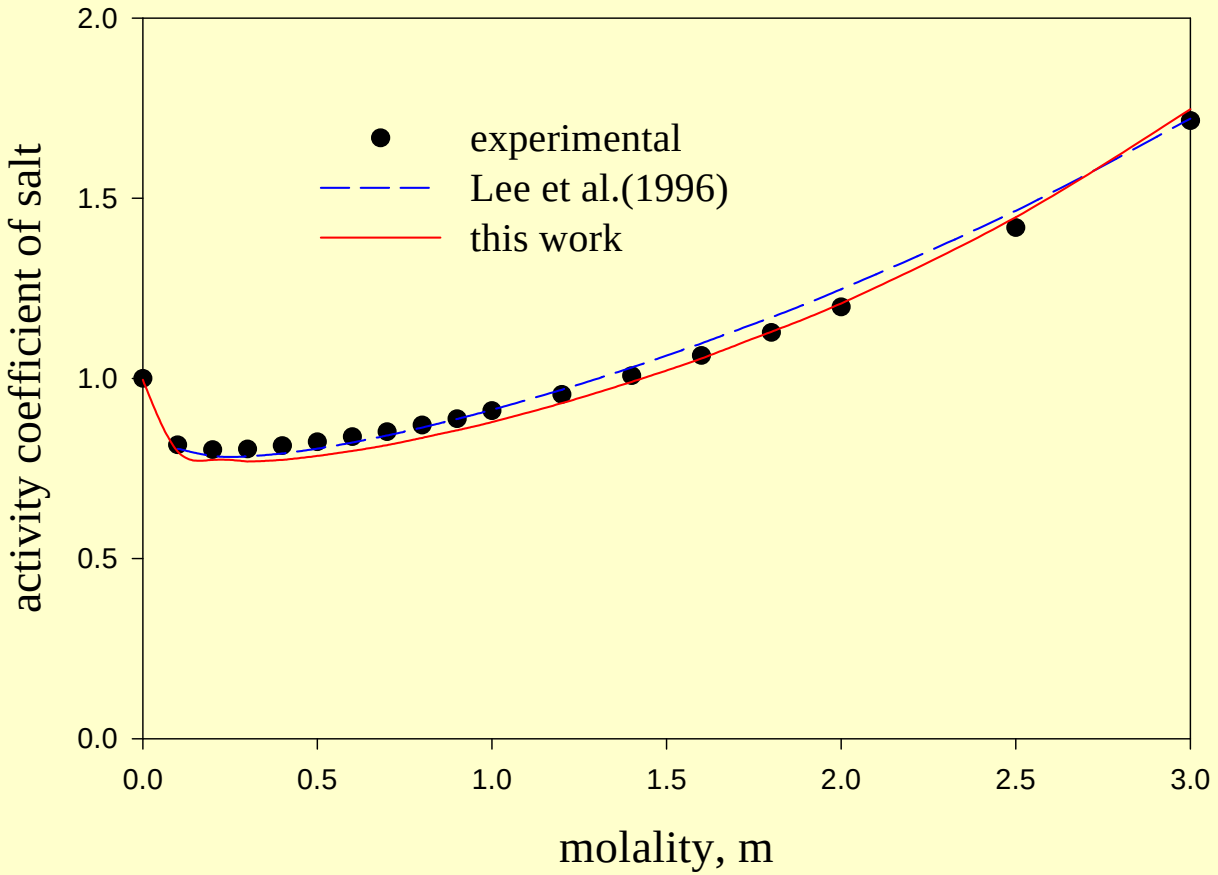

Fig.5 The activity coefficient of LiI.

Results

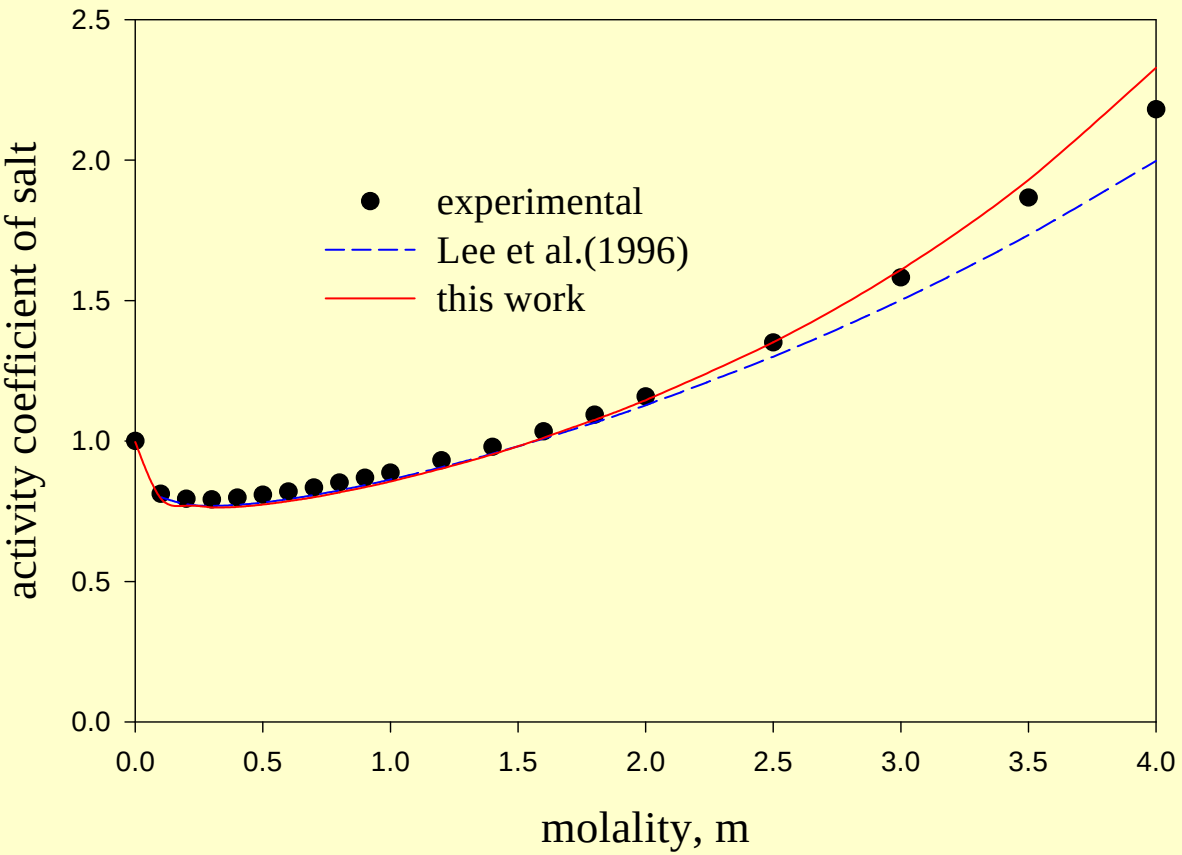

Fig.6 The activity coefficient of $LiClO_4$.

Conclusions

- Mass transfer mechanism in ammonia stripping process was analyzed for parallel and cross flow in shell side
- Measuring NH_3-H_2O-NaOH VLE data with a modified static method, we estimated the Henry's constant of ammonia in aqueous solution.
  - Due to the presence of air and the uncertainty in the amount of water present in vapor phase, it is difficult to measure the equilibrium data.
- Mass transfer coefficients of ammonia removal were correlated with the Henry's constant, and compared with those of oxygen removal of Sengupta et al. (1998)
  - Fitted parameter *a* : dependent to the removed species.

Conclusions

- **Lee et al. model was applied to the NH_3-H_2O-NaOH VLE assuming ammonia to be a solvent species. The calculated results show similar trend with the experimental data.**
- **Lee et al. model also was applicable to the salt-mixed solvent VLE systems with only solvent parameters fitted from solvent-solvent VLE data.**
- **Lee et al. model was extended to the high concentrated electrolyte solutions, explicitly including solvation from a normalized Veytsman statistics. The fitted results give a good agreement with experimental activity coefficients of LiCl, LiBr, LiI and $LiClO_4$ up to 20 molal concentrations.**